**Republic of Iraq**
**Ministry of Higher Education & Scientific Research**
**University of Babylon**
**College of Education for Pure Sciences**
**Department of Physics**

# Efficient of Graphine based Hybrid-nano composite for Dental Filler application

A Thesis

Submitted to the Council of the College of Education for Pure Sciences at University of Babylon in Partial Fulfillment of the Requirements for the Degree of Master in Education / Physics

by

**Mohanad Abdul Salam Husain Mousa**

B.Sc. in physics

(University of Baghdad, 2010)

Higher Diploma in material physics

(University of Babylon, 2017)

Supervised by

**Prof. Dr. Ehssan Dhiaa Jawad Al-Bermany**

**2022 A.D.** **1444A.H.**

***بسم الله الرحمن الرحيم***

**( لقد خلقنا الإنسان في أحسن تقويم )**

***صدق الله العلي العظيم***

**سورة التين ، ايه (4)**

# Dedication

*To My country with honor and dignity…*

*To the souls that will never leave us*

*My father who lights my way and my dear brother Oday*

*To the best woman in the universe, my mother*

*To my beloved wife*

*To my brothers and sister…*

*To my sons*

*To my close friends*

*To my teachers*

*and*

*Everyone who has helped me…*

*Mohamad*

# *Acknowledgements*

Thankfulness, praise be to Allah, the grace that befits his holy self, and peace and blessings be upon our Messenger, Muhammad Bin Abd Allah, May Allah's prayers and peace be upon him and his family and companions

After completing this work, it is my pleasure to extend my sincere thanks and appreciation to the owner of the generous hands, who contributed with his abundance of knowledge, his valuable time, and his sincere help in helping me to translate this research, Professor Dr. Ehssan Dhiaa Jawad Al-Bermany

Thanks to the Deanery of the College of Education for the Pure Sciences/ University of Babylon and the Department of Physics for offering me the opportunity to complete my research. I also would like to express my thanks to all the teachers, instructors, and students of the Department of Physics for their assistance .

Finally, many thanks go to those who supported me and alleviated the difficulties I have faced during my work and to everyone who helped me in one way or another during my preparation of this thesis. Especially my wife. I apologize to those I missed mentioning, and I wish success to all.

Mohanad

# Summary

Graphene-polymer nanocomposites significantly impact dental filler properties and antibacterial activity. Synthesis of graphene oxide (GO) and poly methyl methacrylate (PMMA) were used to reinforce two types of commercial hybrid/nano-dental fillings properties and their antibacterial activity.

The thesis is divided into four chapters; chapter one introduces the introduction, literature reviews and aims of the study, chapter two presents a brief introduction about the dental filler composites, physical concepts and calculations, chapter three reveals the experimental section and characterisations, and chapter four exhibited the results, discussions, and applications and presented the conclusions and future works.

Developed acoustic-solution-sonication-casting methods were applied to fabricate the new graphene-polymer-dental filler nanocomposites. The structure, morphology, rheological and mechanical properties, and antibacterial of the new fabricated filling-PMMA/ GO nanocomposites were investigated. Fourier transform infrared (FTIR) showed significant interaction between the filling and the additional materials. The X-ray diffraction (XRD) analysis revealed a considerable change in crystalline behaviour. Optical microscope (OM) with field emission scanning electron microscopy (FESEM) pictures demonstrated a considerable change in the morphology of the samples with a homogeneous and fine dispersion of the nanomaterials in the filler matrix.

Ultrasound mechanical properties measured the ultrasonic velocity, absorption coefficient, compressibility, bulk modulus, and other mechanical properties that notably enhanced after the contribution of GO

up to 325% of ultrasonic absorption coefficient in comparison with hybrid/nano-fillers. The inhibition zone improved in moth bacteria like Enterococcus faecalis and E. staph bacteria after the contribution of PMMA and GO nanosheets up to 46%.

Generally, nanofillers-PMMA/GO dental filler nanocomposites improved the inhabitance zone diameter of antibacterial that live in moth or tissue more than micro-hybrid-fillers-PMMA/GO dental filler nanocomposites.

# The Content

# List of Figures

# List of Tables

# List of Abbreviations

| Abbreviations | Full name Meanings |
|---|---|
| Bis-GMA | Bisphenol-A Glyceril Mathcrylate |
| DMF | Dimethylformamide |
| FT-IR | Fourier Transform Infrared spectroscopy |
| G | Grapheme |
| GO | Graphene oxide |
| GONS | Graphene oxide nanosheet |
| H1 | Dental filling hybrid |
| H2 | Dental filling hybrid + PMMA |
| H3 | Dental filling hybrid + PMMA+GO |
| MW | Molecular weights |
| N1 | Dental filling nano |
| N2 | Dental filling nano + PMMA |
| N3 | Dental filling nano + PMMA +GO |
| OM | Optical microscopy |
| PMMA | Poly(methyl methacrylate) |
| RGO | Reduce Graphene Oxide |
| SEM | Scanning Electron Microscopy |
| TEGDMA | Triethylene Glycol Dimethacrylate |
| UDMA | Urethane-Dimethacylate |
| D3MA | Decanediol methacrylate |
| UV | Ultraviolet Spectrum |
| XRD | The X-Ray Diffraction (XRD) |

# List of Symbols

| Symbol | Physical Meanings | Unites |
|---|---|---|
| **A** | Wave Amplitude after Absorption | none |
| $\mathbf{A_0}$ | Initially Amplitude of the Ultrasonic Waves | none |
| **D** | Relaxation Amplitude | $m^{-1}KHz^2$ |
| **ds** | The disc thickness | nm |
| $\mathbf{d_{1,2,3}}$ | The thickness of the samples | nm |
| **F** | Ultrasonic Frequency | Hz |
| **k** | Bulk Modulus | $g.m^2/ml.s^2$ |
| **M** | Mass | Kg |
| ***P*** | Density | g/ml |
| $\mathbf{t_s}$ | The solution flow time, | S |
| $\mathbf{t_o}$ | The water flow time | S |
| **V** | Ultrasonic Velocity | m.s |
| **W** | Weight of the Sample | G |
| **Z** | Specific Acoustic Impedance | g.m/ml.s |
| $\boldsymbol{\lambda}$ | The X-ray beam incident wavelength | M |
| $\boldsymbol{\eta_s}$ | Viscosity | $(N.s/m^2)$ |
| $\boldsymbol{\eta_o}$ | The viscosity of water | $(N.s/m^2)$ |
| $\boldsymbol{\theta}$ | The incident angle | degree |
| $\boldsymbol{\beta}$ | Compressibility | $ml.s^2/g.m^2$ |
| $\boldsymbol{\rho_o}$ | The density of water | $g.ml^{-1}$ |
| $\boldsymbol{\rho_s}$ | The density of the experimental liquid | $g.ml^{-1}$ |

| | | |
|---|---|---|
| $\alpha$ | The absorption coefficient of the medium | $m^{-1}$ |
| **τ** | The relaxation time | S |
| **μ** | The linear absorption coefficient | $cm^{-1}$ |
| $\mu_m$ | the mass absorption coefficient | $cm^2/gm$ |
| $\chi_{½}$ | The thickness of the half | cm |

# Chapter One

# Introduction and Literature Survey

## 1.1 General Introduction

Composite dental fillings have gone through many stages since their invention to the present day, punctuated by qualitative and revolutionary leaps in terms of materials. These materials included composition and the properties that must be possessed because it is a very complex compound [1]. The dental fillings' mechanical, thermal, biological, and other essential properties must be a specific requirement. For example, it must contain a high resistance to corrosion that resists acids and enzymes secreted inside the human mouth [2]. Meanwhile, it must withstand the large chewing force to grind and break food without disintegrating [3]. Additionally, it must resist the different temperatures of food and drinks entering the mouth and not be affected by temperature changes. Moreover, it must be biocompatible with body tissues, not decompose, not toxic substances inside the human mouth, and antibacterial, which must be a not safe environment for growing harmful bacteria [4].

This filling must possess many mechanical specifications to face several absolute complex requirements and problems [5].

Despite the tremendous technological development and the discovery of new materials with prestigious specifications so far, specialists in this field have not reached an ideal filling, which has a long life, cohesion strength and gets the average human lifespan of about 60 or 70 years [6]. Researchers and specialists in dental materials have faced many challenges in developing permanent dental fillings and overcoming all the difficulties to reach better dental fillings with ideal characteristics.

Polymers have been introduced as one of the essential parts to reduce these problems in the manufacture of dental fillings because of their properties such as mechanical properties and simple economic cost [7]. Among these

polymers, polymethyl methacrylate (PMMA) entered the science of dental materials and has proven its success over the past 70 years. PMMA has been used to manufacture resin for dentures, term fix materials, and cement for bones. These are pros for the face and other applications, in addition to its good mechanical-biological qualities, manufacturing simplicity, and low cost [8].

In order to address polymer problems, nanomaterials were incorporated into the components of the dental filling recently to overcome several issues. Many researchers have been headed in this direction and found a specific property produced by nanotechnology [9], as this technology produced new materials with nanoscale dimensions and excellent properties [10]. Among these nanomaterials, one of the most exciting materials that have been used recently in dentistry is graphene oxide nanosheets [10]. Graphene attracted tremendous scientific attention when Novoselov et al. made the initial discovery in 2004 [11]. Graphene has unique characteristics and a wide variety of potential uses. It is a single sheet of carbon hexagonal network of carbon atoms with only two dimensions and unusual properties such as the mechanical characteristics with a muscular tensile strength of 130 GPa and a high Young's modulus of 1 Tp. It is the most vital substance discovered to date, with a flexible membrane and the ability to change the carbon backbone, including the functionalization of Graphene [12].

In the dentistry area, graphene and graphene-derivatives nanomaterials are gaining popularity. Evaluating these materials as part of their continuous usage in dentistry is critical to ensure they generate excellent biocompatibility [13]. One advantage of graphene-based materials is re-engineered ability for specific physical and chemical characteristics. The large functional groups, mechanical and optical, nano-size sheets and

conductivity, and other unique features of graphene make it possible to either decrease or improve the material's properties, promising for several applications. GO was reported to exhibit a robust antibacterial activity [23].

The PMMA and GO are nominated as essential nanosheet additives for dental filling applications based on the above. The study aims to involve the PMMA to modify the structure of the filler. In contrast, GO nanosheets modify and reinforce the materials' structure to prepare new dental fillers. Furthermore, it enhances their properties in addition to investigating their effect on the rheological and mechanical properties of two commercial dental fillings, which contain materials with nanoscale dimensions and micro and macro dimensions (hybrid). Fourier transform infrared (FTIR) spectroscopy, X-ray diffraction (XRD) spectroscopy, optical microscopy (OM) pictures, and field emission scanning electron microscopy (FESEM) images were applied to characterize the structure of the new fabricated nano/hybrid dental filler-PMMA/ nanographene dental nanocomposites. In addition to rheological viscometer and ultrasound, mechanical and antibacterial activities were characterized.

## 1.2 Literature Survey

**Olteanu *et, al.* in (2015)** [15], studied brings essential knowledge about the interaction of human dental follicle stem cells with graphene-based nanomaterials. The researchers showed that a high concentration (40 g/mL) of N-doped Graphene reduces the cell viability and alters the mitochondria membrane potential and cytoskeleton actin filaments by mechanical effects. At low concentrations (4 g/mL), it exhibited a good safety profile and a high antioxidant. The good results of graphene oxide exhibited in terms of low levels of cytotoxicity and mitochondria-induced damage in human

dental follicle stem cells. In contrast with these two materials, the thermally reduced graphene oxide showed increased cytotoxicity.

**Elashnikov *et al.* in (2016)** [16] prepared polymethyl methacrylate (PMMA) nanofibers doped with silver nanoparticles (AgNPs) and meso tetraphenylporphyrin (TPP) by electrospinning under prolonged light irradiation, the AgNPs/TPP/PMMA nanofibers, displayed enhanced longevity and photothermal stability they performed antibacterial tests on E. faecalis and S. epidermidis and showed that the AgNPs/TPP/PMMA nanofibers exhibited significantly greater antibacterial activity then AgNPs/TPP/PMMA continuous thin films. Also, the team noted the effect of light-induced AgNPs release and the increased TPP stability, opening the way for designing a new generation of antibacterial materials with combined antibacterial activity.

**Wen *et al.* in (2016)** [17] studied graphene-based nanomaterials with the behaviour of human dental follicle stem cells (DFSCs). DFSCs are isolated from healthy removed teeth and seeded onto GO substrates before being examined for cytotoxicity, changes in the cellular and mitochondrial membranes, and induction of oxidative stress for each produced substrate. GO is considered to be an excellent filler for dental nanocomposites.

**Srivastava *et al.* in (2017)** [18] added fluorine to the compound resin (BisGMA) and produced a compound called a fluorine-containing bis GMA analogue (per FB-bis GMA). Where they wanted to reduce the shrinkage of the polymerization of the dental filling and increase its hatred of water, They studied the Rheological properties, polymerization shrinkage, hydrophobicity, and mechanical properties. The FTIR assays showed that a chemical reaction occurred between fluorine and bis GMA and that adding fluorine reduced polymerization shrinkage and increased hydrophobicity without affecting the mechanical properties of bis GMA.

**Han Xie *et al.* in (2017**) [19] studied Graphene and its derivatives are versatile materials that present unique characteristics such as large surface area and high mechanical properties. They could be transferred or deposited onto different substrates. As they discussed, functionalized and combined with several biomolecules and biomaterials, these carbonaceous materials hold great potential to design bio-composites with fine-tuned physicochemical and mechanical properties and to confer to existing biomaterials enhanced bioactivity and new capabilities.

**Alhareb *et al.* in (2017)** [20] added nitrile rubber/ceramic fillers to the PMMA denture base to improve the following properties: Impact strength, fracture toughness and hardness. Where nitrile butadiene rubber (NBR) with two ceramic fillers ($Al_2O_3$ and YSZ, respectively) have been studied, the mechanical properties of denture base are investigated. The examination was performed by Field Emission Scanning Electron Microscopy (FESEM) to determine the morphology of the fracture surface of specimens.

The results of the statistical analysis of 180 models divided into six groups for this study showed a significant improvement in impact strength (IS) and fractured toughness (KIC).

**Malik *et al.* (2018)** [21] described a new, simple, and cheap method to make large quantities of few layer Graphene (FLG), starting with commercially available multi-layer graphene (MLG) and also incorporating this Graphene into dental polymer composites. They demonstrated that the fabricated graphene-dental polymer composites have significantly enhanced mechanical properties compared to the plain dental-polymer material (control group). The mean compressive strength of the graphene-dental polymer showed a 27% increase, and the mean compressive modulus showed a 22% increase compared with the control group.

**Tahriri *et al.* (2019)** [22] studied Graphene, and its derivatives can be functionalized with several bioactive molecules, allowing them to be incorporated into and improve different scaffolds used in regenerative dentistry. In this study, they focused on the control of stem cells of dental origin.

The interactions between graphene-based nanomaterials and cells of the immune system, along with the antibacterial activity of graphene nanomaterials, are discussed. The researchers also showed that using Graphene with living tissues faces several challenges; the two main challenges in applying Graphene and its derivatives are the production parameters and in vivo toxicity, which needs to be evaluated precisely.

**Bacali *et al.* in (2019)** [23], a study evaluated the effect of adding graphene-Ag nanoparticles (G-AgNp) to a PMMA auto-polymerizing resin, with a focus on antibacterial activity, cytotoxicity, monomer release, and mechanical properties. They added different concentrations of graphene-Ag nanoparticles. The sample with 1wt% G-AgNp exhibited a good safety profile and antibacterial activity on all the tested strains. At the same time, the material with 2wt% G-AgNp showed a higher capacity to activate the mechanisms of antioxidant defence. Flexural strength was improved for both reinforced samples; they proved that PMMA resin with G-AgNp presents promising antibacterial activity associated with minimal toxicity to human cells in vitro and improved flexural properties, and they checked whether the PMMA loaded with graphene-silver nanoparticles constituted an improvement over current denture materials.

**Ioannidis *et al.* in (2019)** [24] investigated the antimicrobial efficacy of silver nanoparticles (AgNPs) synthesized on aqueous graphene oxide (GO) matrix (Ag-GO) with various irrigates and in vivo infected tooth modes.

Nutrient-stressed, multi-species biofilms were grown in the prepared root canals of single-rooted teeth. The dentine tubule surfaces were analyzed with confocal laser scanning microscopy (CLSM). They concluded that, within the limitations of this study, the microbial killing and biofilm disruption capacity of Ag-GO was successfully achieved using a novel ex vivo infected tooth model. Ultrasonic activation selectively enhanced the microbial killing and biofilm disruption of Ag-GO in lateral canals.

**Aunkor *et al.* in (2020)** [25] demonstrated that graphene oxide has antibacterial activity and good biocompatibility as they tested GO with different types of bacteria (Gram-positive and Gram-negative) and used a multidrug drug-resistant (MDR) hospital superbugs grown in solid agar-based nutrient plates with and without human serum through the utilization of agar healthy diffusion method, live/dead fluorescent staining and genotoxicity analysis.

**Dhulfiqar *et al.* in (2020**) [26] added nanographene and nano-silica to composite resin in precise weight ratios in dental fillers and investigated the relationship between topography and mechanical properties. They added the filler by LED curing for three periods (20-25-30). The mildew finished in magnitudes of 6x3mm. The researchers established that increased curing time is critical for optimizing the polymerization process; also, mechanical characteristics analysis revealed that nano silica has a lower compressive resistance than nano graphene. AFM measurements show that nanographene's surface is rougher than nano-silica.

**Bacali *et al.* (2021)** [27], using the Association of Graphene Silver Polymethyl Methacrylate (PMMA) with Photodynamic Therapy for Inactivation of Halitosis Responsible Bacteria in Denture Wearers. This study aimed to evaluate the possibility of inactivating bacteria associated

with halitosis in acrylic dentures. Graphene silver nanoparticles in 1 and 2wt% were added to a commercial acrylic resin powder. The addition of graphene silver nanoparticles to PMMA acrylic resins showed antimicrobial effects on halitosis-responsible bacteria. Extra-oral activation of a photosensitizing agent placed on denture base materials enhanced with graphene silver nanoparticles (1wt% and 2wt%) proved to increase the inhibition of bacteria associated with halitosis in acrylic denture wearers, especially when using laser light and higher nanoparticle concentrations (2 wt. %).

## 1-3 Aims of the Work

This study aims to investigate the following issue:

1- Impact of PMMA polymer and GO nanosheets on the two different commercial dental fillers.
2- Investigate the structure change of the two dental fillers after reinforcing with PMMA and GO nanosheets.
3- Investigate the two dental fillers' rheological and mechanical after reinforcing with PMMA and GO nanosheets.
4- The effectiveness of fabricated nano/hybrid dental filler-PMMA/ nanographene dental nanocomposites against the mouth and other antibacterial activity.

# Chapter Two

# Theoretical Part

## 2.1 Introduction

This chapter describes a general explanation of the theoretical parts of this study, such as physical concepts, optical and mechanical properties equations, mechanisms to kill bacteria, and scientific clarifications used to interpret the results.

## 2.2 Composite material phases

A compound is defined as a substance that arises from the union of two or more substances, each with different properties from the other, that combine to form a new meaning that differs from the properties of each of the common substances in its composition, with a cohesive structure resulting from the homogeneity of two different implications in terms of design. Resin by reducing particle size and improving the adhesion between the filler and the primer. The compound used in dental treatment is a complex material consisting of three primary phases: the organic phase (the base), the inorganic phase (the fillings), and the bonding substance [28].

### 2.2.1 Organic phase

The resin is the active component in the compound, as it is initially in the form of a liquid monomer, but it becomes a solid monomer by the reactions of the addition of roots, and this ability to transform from a paste to a solid is what made it use a filling material in dentistry.

The visceral compound materials at the beginning of their manufacture were based on methyl methacrylate, but in the mid-1960 it became based on an Aromatic Dimethacrylate System such as (Bis-GMA) monomer, which is one of the most common types of monomers produced from the reaction of (Bisphenol - A and Glycidyl Methacrylate). It is called as It has

a wide range of Bown's monomer relative to its discoverer, as it has a higher molecular weight than methyl methacrylate, which helps reduce the polymerization contraction, as it has a polymerization shrinkage value (7.5 vol%) compared to methyl methacrylate, which has a polymerization contraction (22 vol%), as well as the ability to cause bonding High cross-linked [29], there is another monomer used in some types of dental composites called Urethane Dimethacrylate region and symbolized by UDMA. It is characterized by high viscosity, high tensile strength, and chromatic stability. In a few products, (Bis-GMA) and (UDMA) are mixed [30]. Another uncommonly used monomer (Decanediol methacrylate) is cronym (D3MA).

Both Bis-GMA and UDMA are high viscosity liquids due to their high molecular weight. To solve this problem, monomers with low molecular weights are added during the manufacturing process to reduce and control viscosity, called Viscosity-Controllers (Bis-DMA, EGDMA, TEGDMA, MMA) [31]. To ensure longer life of the compound before use, i.e. to prevent the self-hardening process, polymerization inhibitors (Inhibitor) such as Hydroquinone at 0.1% or less are added.

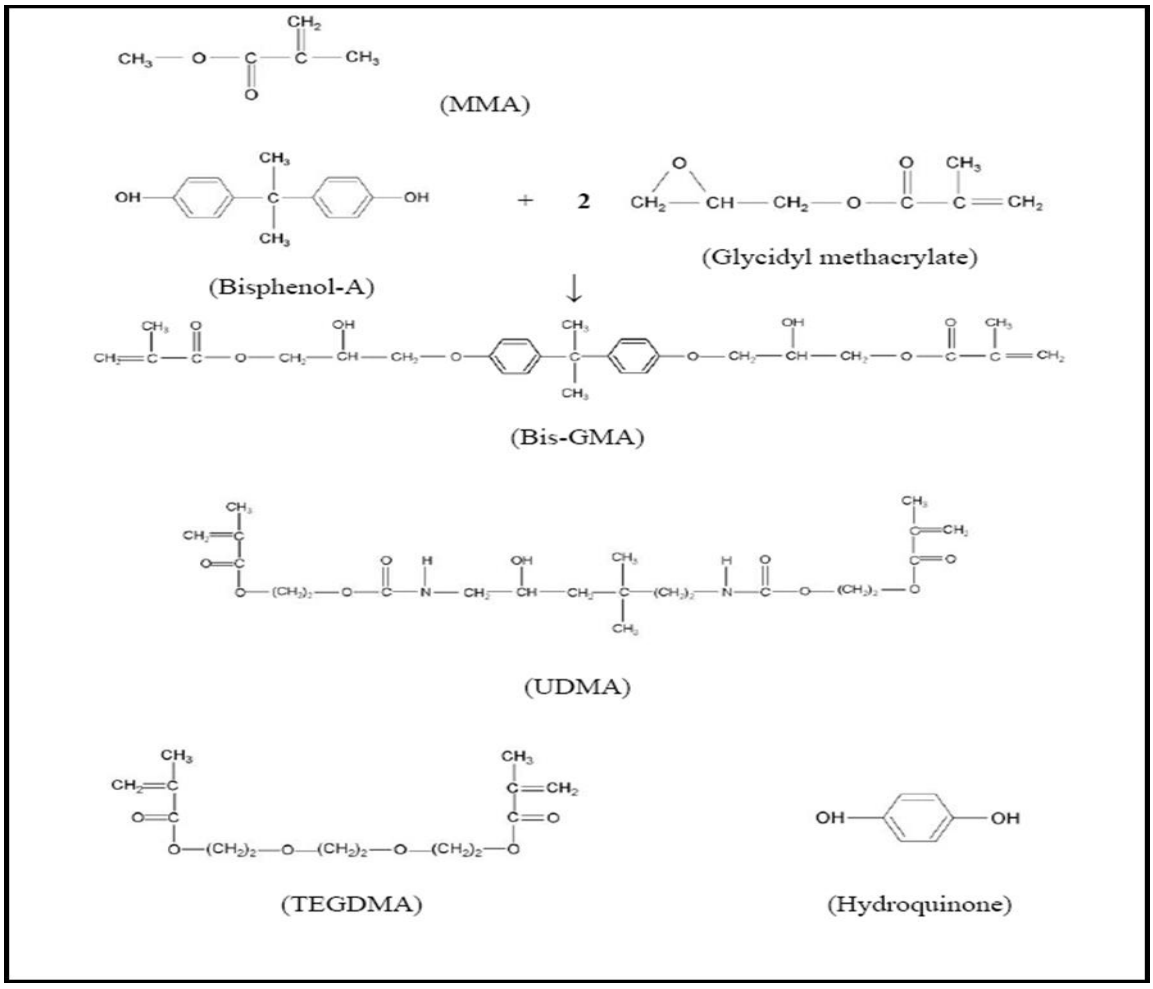


**Figure (2-1). Chemical composition of the primer used, dilute monomers, and polymerization inhibitors in dental composites** [32]**.**

### 2.2.2 Inorganic phase

The inorganic phase in the composite is based on different inorganic fillers materials. The reason for using different types of fillers is to obtain chemical and physical properties. The main objective of integrating a percentage of the filler particles with the resin matrix is to improve these properties, and these improvements started in 1950 when Quartz infills were produced and used with (MMA) to achieve several benefits [31][33]:

1- Using fillers improves mechanical properties such as hardness and compressive strength.

2- One of the characteristics of methyl methacrylate polymerization is that it produces a significant amount of polymerization shrinkage; however, the incorporation of filler particles into the polymerization process reduces this percentage significantly because a lower rate of resin is used, and the filler particles do not participate in the polymerization process.
3- Because the coefficient of thermal expansion of methacrylate monomer is high (80 ppm/C$^{o}$), using filler particles such as ceramic materials can significantly reduce the coefficient of thermal expansion. This is because ceramic materials' thermal expansion coefficient is similar (10 ppm/C$^{o}$) to the coefficient of thermal expansion of the tooth expansion.
4- The aesthetic features of the filling can be controlled by the fillers, such as maintaining the degree of opacity and transparency. The leading fillers used quartz, boron silicate, lithium-aluminium silicate, and in many compounds, part of the quartz is replaced by heavy metals such as barium, zinc, and aluminium [33].

### 2.2.3 Coupling Agent

To obtain a compound that has good mechanical properties, it is essential to have a strong bonding between the organic phase and the fillers. This bonding is accomplished during the manufacturing process by treating the surface of the fillers with a binder before mixing it with the substrate. One of the most common types of bonding materials in use is called silane, which is one of the organic silicon compounds. When silane is deposited on the fillers, the methoxy group reacts with the O-H group in the fillers. After mixing it with the base, the double carbon bond in the silene interacts with the base, and thus the bonding will be accomplished between the fillers

with the base. Figure (2-4) shows the typical structure of silane and its interaction with the substrate and fillers [32].

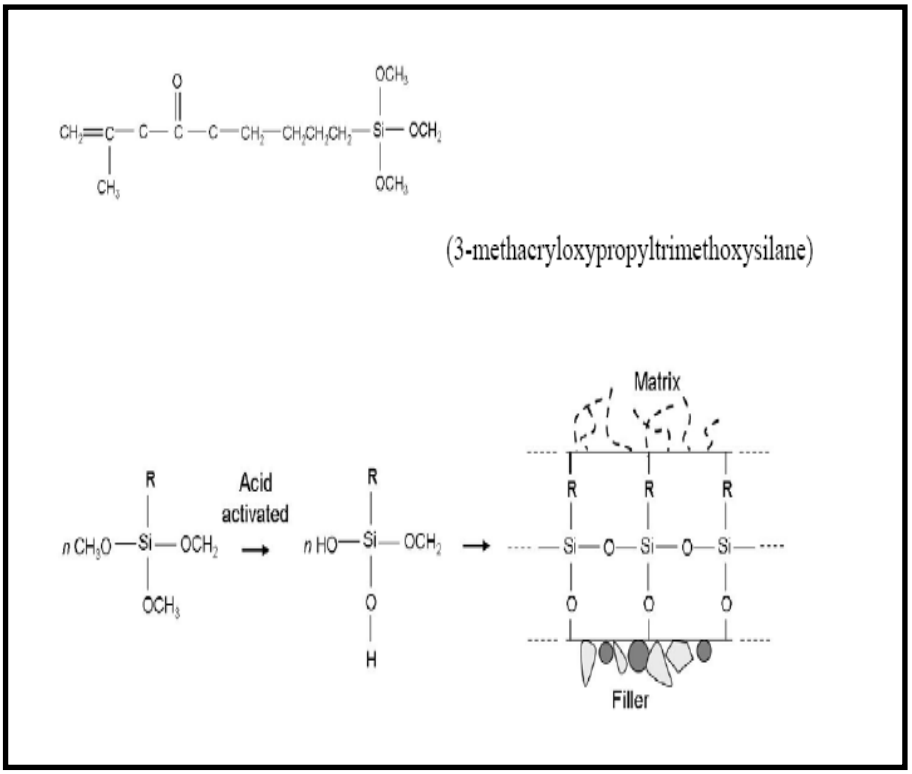


**Figure (2-2) Typical structure and the reaction of the silane binder.**

The dental compound consists of other materials added to it as inhibitors, such as Phenols, which are added to the resin by (200-1000 ppm) to preserve the fabric from self-polymerization during storage and also help not to polymerize the material in the room light when preparing to fill the gap [83], Ultraviolet absorbents such as 2-Hydroxy Benzophenones (0.1 w%-0.5 w%) are also added to help prevent discolouration due to oxidation. The initiating system varies according to the type of filler. Camphoroquinone is often used as a light initiator, added during the manufacturing process in an amount ranging (from 0.2-1%), as it is a source of free radicals needed for the polymerization process, as it absorbs blue light in the range of 400-500 (nm) [33]. Figure (2-5) shows Camphoroquinone.

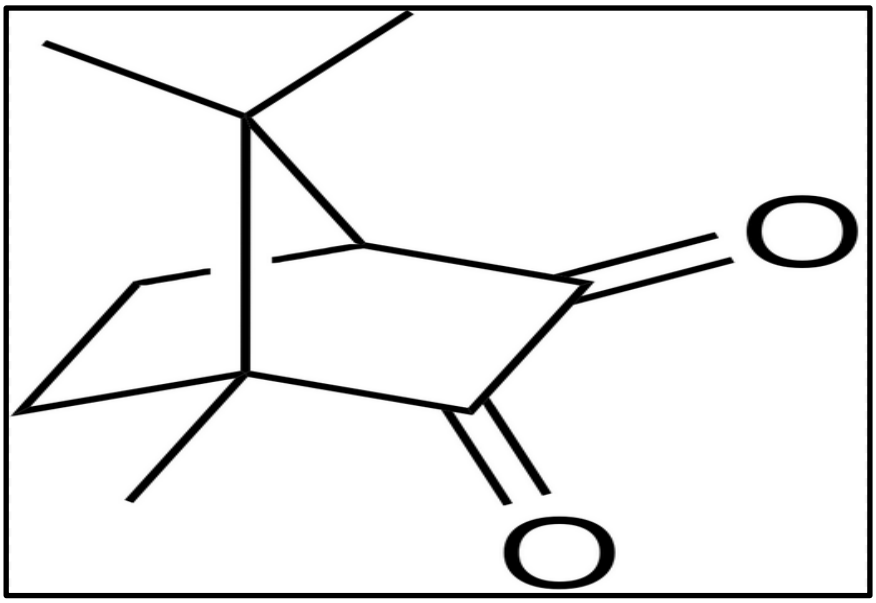


**Figure (2-3). The structure of a compound Camphoroquinone**[34]**.**

Finally, pigments are added at a rate ranging from (0.05%-0.001%) to obtain a colour gradation so that the colour of the filling matches the colour of the tooth, which is inorganic [34].

### 2.3 Types of dental filling

There are many types of dental fillings, and each style has advantages and disadvantages. The latest sort is the composite filling, but it always needs continuous development to obtain the best structural and mechanical properties.

There is a wide choice of materials which can be used for fillings. Many new medications are being introduced to the market and used on patients suffering. There is limited evidence that they are more effective or robust than existing materials. Some of these factors are the properties of filling material, the operator's skill and technique teeth, and the environment around the tooth. Types of tooth restorations may be classified as intracranial when placed within a cavity prepared in the crown of a tooth, or extra coronal, when the tooth, as in the case of a peak. At the moment,

dental amalgam, composite resins, glass ionomer cement, resin-modified glass ionomer types of cement, composers and cermet, cast gold, and other alloy inlays and porcelain are used to fix intracranial preparations[35].

1- **Dental amalgam**: is an alloy of mercury with silver and other metals such as tin and copper to give a set material that does not adhere to tooth tissue and is not tooth coloured. It has been available for over 100 years, but the original formulation of the material has been modified considerably; in particular, the addition of copper and zinc to the alloy powder has enhanced its physical properties. Concerns over the safety of amalgam appear to be unjustified.12 The Department of Health's Committee on Toxicity concluded that dental amalgam is free from the risk of systemic toxicity, and only a very few cases of hypersensitivity occur[36].
2- **Composite resin**: Several groups of composite materials that e classified based on their resin and filler components. All are tooth-coloured and are essentially a mixture of filler particles, consisting of various types of translucent glass embedded in a matrix of resin that binds the filler particles together. The original generation of materials set by a chemical reaction has been largely superseded by composites that are set by applying bright light. The use of composite materials has been supplemented with the pretreatment of tooth tissue with a mild acid, which is then coated with a thin resin wetting agent before placement. More recently, applying acids and other agents to dentine has been advocated to reduce leakage and improve retention. These dentine bonding agents are rapidly evolving[35].
3- **Glass ionomer**: types of cement are tooth colored and adhere chemically to tooth tissue. They are similar to composite resins,

consisting of embedded filler particles. However, their formulation and setting reactions differ[37].

4- **Resin-modified glass ionomer cement and composers:** Compounds and resin-modified glass ionomer cement new generations of materials are essentially glass ionomer types of cement. The `resin-modified materials are more akin to glass ionomer types of cement, whereas the compomers are more like composites. Again, these materials are tooth-coloured and are available in various formulations[38].

5- **Cast gold and other alloys:** Cast gold or alloy restorations are called inlays and are made outside the mouth in an indirect technique that requires laboratory facilities. The advantage of cast inlays is their strength in thin sections, but they are more expensive. They are cemented in place with either traditional dental cement or can be used with more modern bonding systems[39].

6- **Porcelain**: Porcelain inlays can now be cemented into the prepared cavity. There are different kinds of porcelain and other ways to make them, and all of them can be used with different cementing agents[40].

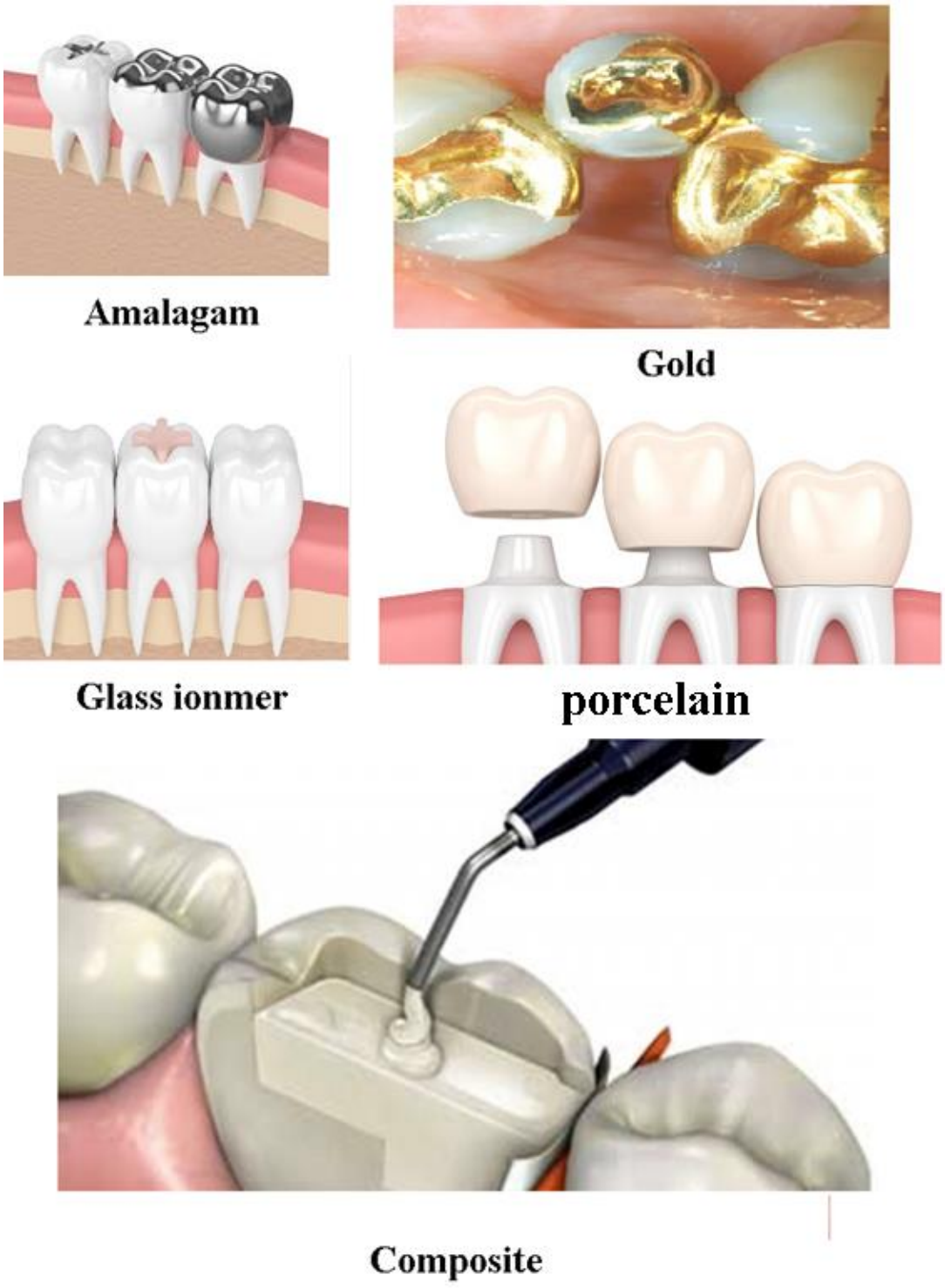


**Figure(2-4) Some of the types of dental fillings.**

## 2-4 The Nanotechnology in the Dental material

Nanotechnology has grown in popularity in recent years due to its capacity to enhance the performance of various systems. Many studies have focused on the medicinal uses of nanotechnology. Medical equipment has already been made smaller and stronger using this technology, making them better for individuals who rely on them to complete their jobs [41].

The purpose of creating nanoparticles is to develop materials with novel features, which include many properties. First: the distances between particles or groups of particles are small or nonexistent. This property makes nanomaterials extremely fine and robust, and it has a variety of additional properties. Second: the atoms on the particle's boundary are unsaturated, indicating that the particle is not saturated. Because of this unsaturation, nanoparticles are effective and require interaction with other nanoparticles or with other substances. For example, if an atom on the boundary of a particle has four bonds, two of these bonds are linked inside the particle while the other two bonds remain outside the body without bonding. As a result, nanoparticles are effective and require interaction with other nanoparticles or with other substances [42].

Richard Feynman, the creator of the nano-phenomenon, is credited with establishing the field of nanoscience in the 1950s [34]. According to the scientist Norio from the University of Tokyo, the term (Nanotechnology) means the process of separating or combining materials at the atomic or molecular level, one atom by another atom or one molecule by another molecule [43], during the year 2006, nanotechnology was introduced into a variety of life applications and took up a significant portion of the applied sciences, particularly in the fields of medicine, biology and pharmacology, as well as electronic materials and chemistry. Many industrial sciences use nanotechnologies, such as drug delivery, semiconductors, and dentistry

materials like fillings [44]. Nanoparticles are atomic assemblies ranging in size from five to a thousand atoms, which are far smaller than the dimensions of bacteria and living organisms. Nanoparticles are used in a variety of applications [45]. The use of nanotechnology in dentistry has provided both the dentist and the patient with a new and exciting viewpoint. Nanotechnology has helped to improve dental and oral hygiene by delivering drugs and diagnosing problems more effectively [46].

When it comes to dental applications, nanoparticles are preferred since they are affordable and possess unique dental features (Dentin). Nanotechnology will significantly impact science since its qualities will be improved. As a result, nanocomposites have become increasingly popular in dental restorations. Another key element that causes tooth damage and, as a result, results in a decrease in antibacterial activity, polymerization contraction, plaque collection and partial leakage, as well as the creation of cavities, has to do with tobacco use. The development of caries in the mouth has just been concluded by scientists, who have discovered that oral biofilms play a significant role [41].

On the other hand, nanotechnology improves mechanical properties. It gives them unique specifications, which are very required and necessary in dental fillings, as they face very harsh surrounding conditions in the human mouth, so the filling must have specifications close to the specifications of the natural tooth in terms of durability and resistance to corrosion and others. Also, it needs to have good rheological properties and the correct viscosity and density so that the dental filling doesn't shrink during polymerization, crack, or have other problems with its structure [47].

## 2.5 The Material used:

### 2-5-1 Nano Graphene

Graphene is a material composed of monoatomic carbon nanosheets that have a honeycomb-like structure. It comprises a single atomic layer of sp2 hybridized carbon atoms arranged in a hexagonal lattice to produce a hexagonal lattice [48].

Graphene has a solid structural that makes a thin slice of it one atom thicker (300) times more potent than steel with the same thickness (this is if we assume theoretically that iron can become with the same thickness), and this is what was shown by one of the tests conducted in (2009). This led to the classification of graphene as one of the most robust materials currently known [49].

Graphene exhibits unique and exciting physical and chemical properties. The mechanical properties of nano-graphene are unique, and it is the most transparent, hardest, thinnest, lightest and most conductive material in the world. Its derivatives include graphene oxide, graphene obtained by hydrogenation, and graphene derivatives with magnetic properties. Recently properties of graphene are more widely used than its derivatives, as it can be mixed with metal to prepare composite materials. It is considered an effective material in technology and significantly on the future technological revolution. It is now known that it exhibits the highest possible strength due to the immense strength between the carbon atom structures conferring the increased power to graphene. Overall, graphene is widely used in the preparation of new high-strength, high-performance composite materials increasingly used in defence, industry and other fields where graphene can be mixed with A variety of materials, including metal-metal compounds and polymers [50]

In 2004, two Russian scientists worked on extracting graphene, which is one of the forms of carbon (Allotropic) (graphite, diamond, fullerene, carbon tubes, graphene flakes). Ordinary adhesive tape by peeling off the graphite material known in pencils, although it is one of the forms of carbon, it has a two-dimensional hexagonal crystal structure like a slice of a beehive, as shown in Figure (2-1). In addition, it is an excellent conductor of electricity, much better than copper cells. Graphene is almost entirely transparent, allowing it to be used in manufacturing touch screens and photovoltaic cells. Graphene is used in many technological and medical applications such as biosensing, drug delivery, development of medical materials and devices, antiviral, antibacterial or antitumor therapy [51]. Graphene films can increase the differentiation of stem cells as these materials significantly improve dental products' physical and mechanical properties [52].

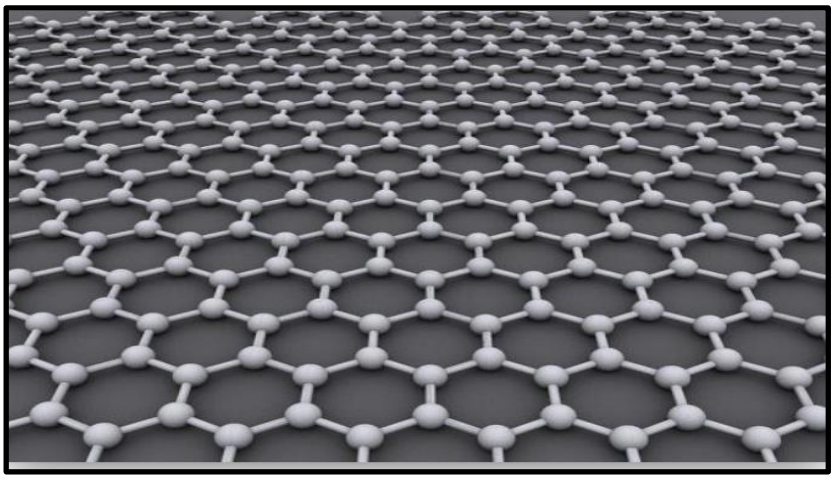

**Figure (2-5). The structure of two-dimensional graphene** [51]**.**

### 2-5-2 Poly methyl methacrylate (PMMA) polymer

Among the oldest and best-known polymers is Poly (methyl methacrylate), a kind of acrylic acid [53]. It is a significant and intriguing polymer because of its appealing physical and optical qualities, which are critical to its wide range of applications [54] PMMA is a non-biodegradable polymer that exhibits excellent transparency, mechanical strength, and chemical resistance while being lightweight [55] Good tensile strength and hardness, as well as high rigidity and transparency, are all characteristics of thermoplastic materials [54] Colorlessness, resistance to weathering corrosion, and solid insulating capabilities are all characteristics of this material [55].

In addition to brittleness and limited chemical resistance, Poly (methyl methacrylate) has a number of drawbacks that may be mitigated by chemical or physical modification. In each unit of PMMA, there are both hydrophobic (ethylene) and hydrophilic (carbonyl) groups present [54]. Poly (methyl methacrylate) is generated from the polymerisation of methyl methacrylate in the presence of other monomers [56]. PMMA is the most widely used polymer in the methacrylate family. It is widespread usage in a variety of industries [55], especially in the dental/medical fields for removable or implantable devices (e.g., denture base resin, provisional restorative materials, bone cement, facial pros-theses) due to its desirable mechanical/biological properties, easy fabrication, and economic cost [57]. A chemical structure of the repeating unit of PMMA polymer, as shown in Figure (2-2).

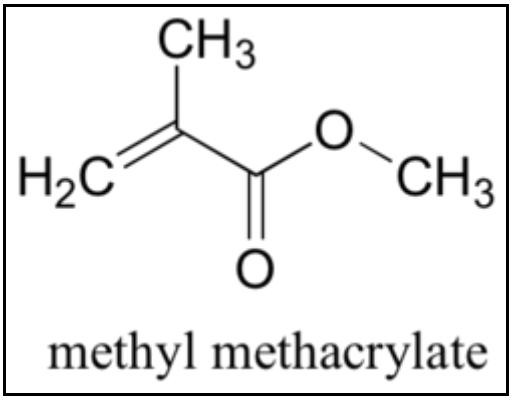


**Figure (2-6). A chemical Structure of the Repeating unit of PMMA Polymer** [58]**.**

**Table (2.1). The Most Important Properties of PMMA Polymer** [59][60]**.**

| Parameters | PMMA |
|---|---|
| **Chemical formula** | $CH_2=C(CH_3)COOCH_3$ |
| **Molecular Weight Mw (g/mol)** | Varies |
| **Refractive index** | 1.49 |
| **Solution PH** | 5.5 to 6.4 |
| **Density ($g/cm^3$)** | 1.2 $g/cm^3$ |
| **Glass transition temperature Tg ºC** | 106 ºC |
| **Melting point Tm ºC** | 213 ºC |

## 2.6 The Properties

### 2.6.1 Rheological Properties

#### 2.6.1.1 Density

Density is the result of the ratio between the mass of a solution and its volume [61] that was calculated using equation (2-1).

$$\boldsymbol{Density\ (\rho) = \frac{mass(m)}{volume(V)}} \qquad \textbf{(2-1)}$$

### 2.6.1.2 Viscosity

Viscosity is the resistance experienced by the particles of the liquid during the moving that depends on the nature of the material and its temperature. Equation (2) was employed to determine the viscosity of the test liquids ($\eta_s$) [62].

$$\boldsymbol{\eta s = \eta o\ (ts/to)(\rho s/\rho o)} \qquad \textbf{(2-2)}$$

$\eta_o$ means water viscosity, $t_o$ means water flow time, $\rho_o$ means water density, $t_s$ means experimental fluid flow time, and ρs means the density of the experimental fluid.

### 2.6.2 Mechanical properties

Ultrasound-based approaches are quick to implement. In most cases, a single measurement can be accomplished in minutes. Acoustic attenuation is exceptionally appealing for online characterization because of this property and the capacity to measure flowing systems. Ultrasonic thickness measuring is a frequently used technology in the industry, identification of flaws and a limited but growing scope of material characterization [63]. The critical element of ultrasonic is a piezoelectric transducer, commonly utilized for emission and reception. Ultrasonic research is likewise a burgeoning field, with efforts being made in a variety of ways. However, as it is commonly used, ultrasonic has several drawbacks or limits. The main one is the need for contact or fluid medium for ultrasound coupling to the tested part. Others include piezoelectric transducers' limited bandwidth and sensitivity to the phase of the ultrasonic wavefront across the transducer element, making an inspection of components with acute curvature problematic. Researchers have known for a long time that these constraints may be overcome by utilizing lasers and light to generate and detect ultrasound, a technique known as laser ultrasound [64].

### 2.6.2.1 Ultrasonic Velocity

The velocity of an ultrasonic wave propagating through a medium is affected by the material's physical qualities. Molecules in low-density mediums such as air and other gases can move long distances before influencing surrounding molecules. The velocity of an ultrasonic wave in these media is relatively low. In solids, molecules are restricted in their mobility, and ultrasound travels at a relatively high speed. Ultrasound velocities in liquids are halfway between those in gases and solids [65]. Because variations from the linear dependency of rate and compressibility on the mole fractions provide information about the physicochemical features of liquid mixtures, ultrasonic velocity measurements are used to analyze molecular interactions in pure liquids and binary/ternary mixtures. Molecular interaction studies have been made on liquid mixtures [66]. The speed of sound is a property of the medium in the linear propagation regime (minor perturbation or small wave amplitude). It is independent of wave amplitude and may be calculated using the medium's material and geometrical properties. The generalized concept of an effective elastic modulus (K) and an effective mass density can be used to account for wave type-specific differences, such as bulk compression, bulk shear, surface, or guided wave-specific differences. The effective elastic modulus is determined by the elastic and geometrical properties of the medium, which define the stiffness of a particular wave. The ultrasonic velocity (V) was calculated using the equation(2-3) [67]:

$$\mathbf{V = \frac{X}{t}} \qquad \textbf{(2-3)}$$

These symbols, x and t, represent the sample thickness and the duration of wave recording over the sample, respectively.

### 2.6.2.2 Absorption Coefficient of Ultrasonic Waves

The physical properties of natural materials produce an effect which further weakens the sound. This further weakening results from attenuation. Attenuation is a function of material properties, distance, and frequency. The attenuation is a combined effect of scattering and absorption. Scattering is the reflection of the sound in directions other than its original direction of propagation due to the inhomogeneous nature of materials. Such boundaries can be caused by voids, inclusions, and grain boundaries. Absorption is the conversion of sound energy to other forms of energy. In this way, the strength of an ultrasonic signal reduces as it propagates through a given material [68]. Consider a thin layer of the medium that is normal to the direction of propagation at a distance (x) from an origin and of a thickness (dx), where attenuation is uniform, the fractional loss of energy per unit path length from the layer should be constant[69].

Where (E) represents the wave's initial energy density and is the medium's absorption coefficient. Since intensity (I) is directly proportional to energy density (E), where:

$$\frac{dI}{I_{\circ}} = -2\alpha dt \qquad \textbf{(2-4)}$$

By integrating this equation and applying the boundary condition that $I=I_O$, for t=0, obtained:

$$I = I_{\circ} \exp(-2\alpha t) \qquad \textbf{(2-5)}$$

In addition, *I* am proportional to the square of the amplitude A. Ultrasonic attenuation is the rate at which a wave decays as it travels through a medium. An equation can be used to express the amplitude change of a decaying plane wave [70,71]:

$$A = A_0 \exp(-\alpha t) \qquad \textbf{(2-6)}$$

This can be given by equation (2-7).

$$\alpha = \frac{-\ln A / A_0}{t} \qquad \textbf{(2-7)}$$

Where ($A_0$) is the initial amplitude of the ultrasonic waves, (A) is the wave amplitude after absorption, and (t) is the thickness of the sample.

### 2.6.2.3 Relaxation in liquids

When subjected to applied stress, polymers can be distorted by either or both fundamentally different atomistic mechanisms. The lengths and angles of the chemical bonds that connect the atoms may distort, causing the particles to shift to new places with more internal energy. This is a minor movement that happens extremely rapidly [72]. This process occurs during a relaxation period known as (Relaxation Time) (τ), defined as the time it takes for excitation energy to become translational. Temperature and contaminants play a role. The dispersion of ultrasonic velocity in a binary mixture reveals information about the relaxation process's characteristic time, which causes distribution. The relaxation time (τ) can be calculated using the following equation**:** $\tau = \frac{4\eta_s}{3\rho v^2}$ **(2-8)**

Where $\eta_s$ is the viscosity, $\rho$ is the density, and $v$ is the ultrasonic velocity of the solution [73]. Using the following equation, we can calculate the amplitude of an ultrasonic wave in a relaxing mode after colliding with particles solution and discomfiture caused by this collision and then returning to the comfortable state, referred to as the relaxation amplitude [74].

$$D = \alpha / f^2 \qquad \textbf{(2-9)}$$

where f is the ultrasonic frequency.

### 2.6.2.4 Compressibility

Adiabatic compressibility exists when no heat is transferred into or out of the system, which is the fractional reduction in volume per unit increase in pressure. These changes are related to the compressibility of the medium, according to the thermodynamic equation:

$$\beta = \frac{1}{V}\left(\frac{\partial V}{\partial p}\right) \qquad \textbf{(2-10)}$$

Aside from that, it may be computed from the speed of sound (v) and density of the medium (ρ) by utilising the equation of Newton Laplace [75]

$$\beta = \frac{1}{Y} = (\rho\, v^2)^{-1} \qquad \textbf{(2-11)}$$

### 2.6.2.5 Bulk Modulus

A substance's Bulk modulus, which defines its resistance to uniform compression, is defined as the amount of pressure necessary to shrink the volume. It was computed using the Laplace equation, developed in the nineteenth century [76].

$$K = \frac{1}{\beta} = \rho\, v^2 \qquad \textbf{(2-12)}$$

### 2.6.2.6 Specific Acoustic Impedance

Acoustic impedance is essential in determining acoustic transmission and reflection at the interface between two materials with varying acoustic impedance. It can also be used to create ultrasonic transducers and analyze sound absorption in a medium. The equation shows the ultrasonic velocity and density product acoustic impedance, as shown below [77].

$$Z = \rho V \qquad \textbf{(2-13)}$$

### 2.6.3 The biological properties

Saliva is a complex mixture of fluids that surrounds the oral tissues and arises from the major and minor salivary glands and non-glandular sources such as crevicular fluids, oral microorganisms, and host cells. Saliva can be watery, thick, or sticky depending on its composition, and the number of proteins present in saliva will be determined primarily by its thickness, density, and viscosity. The salivary pH is nearly neutral, and temporal factors such as inorganic phosphates in saliva at rest and the carbonic acid-bicarbonate system in stimulated saliva keep it neutral. Among the various protective functions of saliva, including loosening and cleaning the oral cavity and enabling ion exchange, some salivary properties may contribute to protection against the caries process as dental caries is the dissolution of minerals that causes dental caries surface by organic acids formed from the bacterial fermentation of sugars. The ability of saliva to expel microorganisms, concentration, and maintain oral hygiene is affected by pH and other factors [78].

#### 2.6.3.1 The antibacterial

The number of bacteria in the mouth of a person is estimated at one billion, scientists have discovered more than 700 different types of bacteria in the human mouth [79], but it should be noted that most of these types are considered natural inhabitants, meaning that they do not cause any health problems in the mouth. Still, some are useful and preserve the teeth [80]. On the other hand, there are types of bacteria problems, such as gingivitis, ulcers, and tooth decay [81].

Tooth decay is caused by acid from bacteria dissolving the hard tissues of the teeth (enamel, dentin, and cementum) [82]. Acid is produced by bacteria when food or sugar remains on the tooth's surface [83]. These

restorative materials have seen widespread use over the past three decades, and their application ranges from anterior to posterior restorations [84]. Studies have unfortunately shown a high number of failures, with secondary caries as the primary cause. It was discovered that resin composites accumulated more dental plaque than enamel and conventional restorations. As a result, alterations that introduce antibacterial qualities are required to meet the requirement of increasing the service life of resin composite restorations [85].

The definition of an antimicrobial agent is a chemical compound capable of killing pathogenic microorganisms [86]. An antibacterial component can be added in resin composite materials, through modifications made to the filler particles [87]or the resin matrix [88]. The two kinds of bacteria used in this study:

1- **Enterococcus faecalis bacteria** (E.F.) is the essential type of the genus of Staphylococcus with clinical importance for humans, and this bacterium has attracted the attention of scientists because it spreads naturally in humans. Enterococcus faecalis is a gram-positive bacteria that, like all other streptococci, has an essential role in human disease. Infection rarely occurs but is usually pathogenic; These bacteria also live in the mouth and vagina [89].
2- **E. staph** infections Staphylococcus aureus, Staphylococcus aureus, or Staphylococcus aureus (Latin: Staphylococcus aureus) is a kind of gram-positive bacteria, which can typically be found living on the skin, in the nasal passage, or the breathing tracts. Staphylococcus aureus is the most common cause of staph infections [90].

### 2-6-3.2 Antimicrobial mechanism of GO

In general, the development of antimicrobial activity for graphene-based nanosheets (including graphite, graphite oxide, GO, and rGO) proceeds in three steps [14]:

1- Deposition of nanosheets on the bacterial surface.
2- Membrane disruption by sharp nanosheets.
3- The ensuing superoxide anion-independent oxidation.

The level of antibacterial activity can be synergistically enhanced by membrane stress and oxidative stress. The stresses induced by GO lead to a more potent antibacterial activity than rGO and graphite. Specifically, the antibacterial activity of GO arises from various physical or chemical interactions between GO and bacterial cells Figure (2-2). During the physical interaction, the sharp edges of the GO nanosheets damage the cell membrane [91]

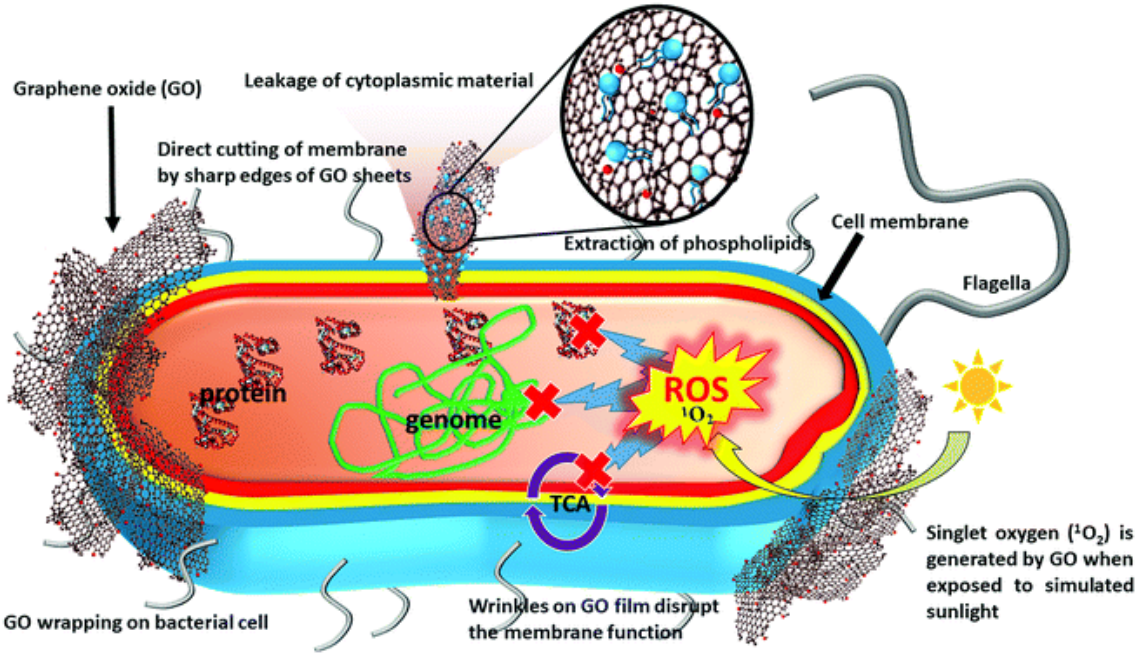


**Figure (2-7). Antimicrobial activity mechanism of GO through various physical and chemical interactions; including bacterial cell damage by the sharp nano-wall/ edge of GO, extraction of phospholipids, wrapping of a bacterial cell by large-**

**surface-area GO, ROS generation for disruption of genomic DNA, proteins and cellular metabolism (represented by TCA), and wrinkles in the GO film for membrane disruption** [92]

Hydrazine-reduced GO nanosheets possessing sharper edges can effectively mediate charge transfer between bacterial cells and thus show a higher antibacterial activity [91] because the damage to the cell membrane is caused by direct contact of GO with the cell, Gram-negative bacteria with an outer membrane are more resistant to such damage than Gram-positive bacteria. Molecular dynamics simulation on graphene nanosheets revealed that the nanosheets penetrate cell membranes spontaneously within a few nanoseconds when they align vertically at a distance of 3.5–4.7 nm from the membrane surface. This insertion occurs in three modes [93]:

1- In swing mode, the nanosheets contact the membrane surface multiple times.
2- The insertion mode, in which the membrane traps nanosheets by van der Waals forces and hydrophobic interactions, followed by membrane cutting.
3- The extraction mode leads to deformation and loss of membrane integrity.

On the other hand, the chemical damage is initiated by the formation of Reactive Oxygen Species (ROS) and/or charge transfer, subsequently resulting in oxidative stress [93]. The stress on the membrane can induce fragmentation of genomic DNA and cell death [94].

### 2.6.3.3 Factors affecting the antibacterial nature of GO

GO has different antibacterial mechanisms, including mechanical cutting of cell membrane, wrapping of the cell, ROS generation, and extraction of

cellular materials. Several intrinsic characteristics of GO nanomaterials, such as conductivity, catalytic activity, and level of interaction with biomolecules, are highly dependent on their morphological, physical, and chemical properties, including lateral size, purity, structural defects, charge, functional groups, degree of oxidation, and hydrophilicity. Therefore, all these factors contribute to the overall antibacterial activity of GO [95], as shown in Figures (2-3).

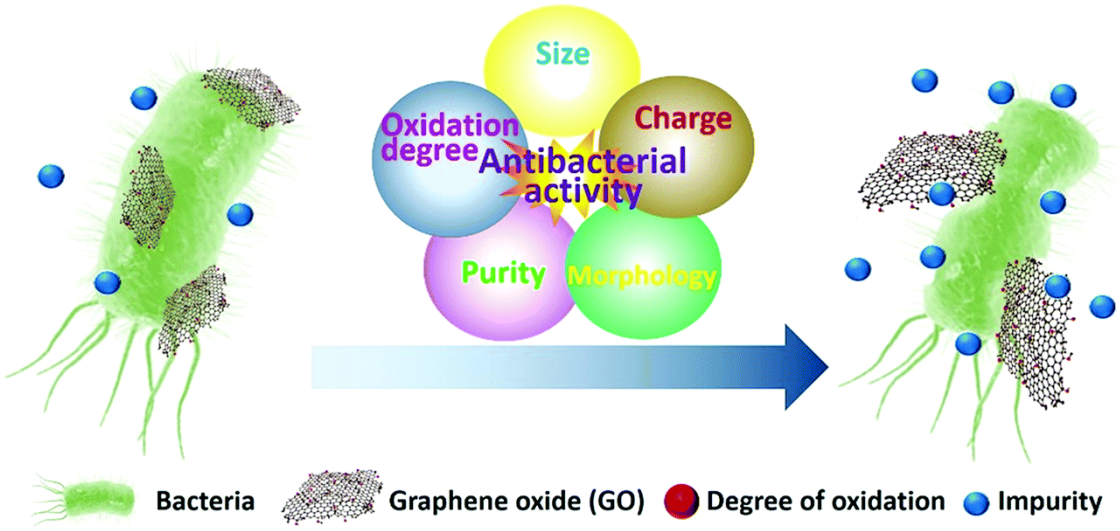


**Figure (2-8). Factors affecting the antibacterial properties of GO** [92]**.**

### 2.6.3.4 GO as an antimicrobial agent

The interaction between graphene-based nanomaterials and microorganisms has brought interest as a recently important topic. Oxygen atoms make GO superior to pristine for various applications [92]. The antibacterial activity of graphene-based nanomaterials was first reported by Fan *et al*. [96], where the GO nanosheets exhibit no significant cytotoxicity to adenocarcinoma human alveolar basal epithelial cells (A549) at a low concentration of 20 μg $mL^{-1}$ [96]. The viability of bacteria in the presence of GO-based nanomaterials is determined by the nature of GO, incubation time, and nanomaterial concentration [97][94][98][99]. Chen et al. [99]

found that bacterial inactivation typically occurs in the first hour of incubation, and the rate of cell death increases with increasing GO concentrations [99]. The in vitro and in vivo studies by Zhao et al. [97] showed that GO Inhibits the growth of Klebsiella pneumonia, thereby increasing the survival rate of mammalian lung cells; reducing tissue damage; decreasing inflammation of various organs; and decreasing the mortality rate of mice [97]. The studies suggest that GO can be a promising nanomaterial against multidrug-resistant (MDR) pathogens.

However, a bacterial infection could recur after the treatment with GO, compared to the mock-treated mice, suggesting different antimicrobial activities of graphene materials between in vitro and in vivo cases. Therefore, an in-depth understanding of the antibacterial mechanism and various environmental conditions affecting the antibacterial properties and cytotoxicity toward mammalian cells is needed to derive more effective antibacterial GO-therapeutics [92].

1- The size: The antibacterial ability of GO Nanosheets are specifically related to the effectiveness of cell adhesion, cell intake, and cell damage caused by the interaction between GO and cell. The lateral size of GO Highly influences bacteria. The GO nanosheets with a slight lateral size exhibit antimicrobial effects mainly through oxidative stress, which is related to the defect density of the nanosheets, whereas GO Nanosheets with a sizeable lateral size exhibit antimicrobial effects through the cell entrapment mechanism. Therefore, small-lateral-sized GO has higher antibacterial activity, specifically in surface coating, whereas large-lateral-sized GO has high antibacterial activity in the form of suspension [100].
2- The morphology: morphological effects are associated with GO Nanomaterial and bacterial cells. The physical structure and

nanoscale geometry of GO Affect its interaction with bacteria. GO Films with surface wrinkles show excellent antibacterial properties due to their corrugated nature at the nanometric level [101]. The wrinkled GO Surfaces are more effective than planar surfaces in terms of inducing the interaction with cell materials and driving the alteration of cell alignment, orientation, and morphology [102].

3- Aggregation: The interaction between GO and bacteria significantly depends on GO Concentration, charge, dispensability, and aggregative state in different solutions (deionized water, phosphate-buffered saline, NaCl, $MgCl_2$, and $CaCl_2$ solutions), lead to varying antibacterial effects. The GO at low concentrations (<6 μg $mL^{-1}$) exhibits substantial antibacterial effects in all solutions. The non-aggregated GO Mechanically disrupts the bacterial membrane, resulting in the leakage of intracellular materials and eventually cell death [103].

## 2.7 Characterizations

### 2.7.1 Fourier Transforms Infrared (FT-IR) Spectroscopy

Fourier Transforms Infrared (FT-IR) is chemical investigative spectroscopy. This instrument measures the infrared intensity of the light wavenumber. IR light is composed of wavenumbers that are split into three regions: far-infrared, mid-infrared, and near-infrared, with wavelengths ranging from (4 to 400 $cm^{-1}$), (400 to 4,000 $cm^{-1}$), and lastly (4,000 to 14000 $cm^{-1}$), according to the wavelengths [104], The permissibility of this technique is dependent on the ability to detect the vibration of a chemical functional group in a sample. When infrared light interacts with the matter, the chemical bonds in the matter will be stretched to their maximum length. It is in this case that the infrared radiation is absorbed by a chemical

functional group in a specified wavenumber range, which is independent of the rest of the molecule's structure [104]. More complicated molecules contain more than one bond, which allows for the possibility of multiple sorts of vibrations. Vibrations may be divided into two basic categories: bending and stretching vibrations.

## 1. Bending Vibrations

When a bond angle is changed between two bonds in a common atom, this is referred to as deformation vibrations. A movement in the atoms group that is concerned with the residue of a molecule that occurs without any movement in another group of atoms is also referred to as bending vibrations or deformation vibrations [105]**.** Bending vibration may be classified into two categories, as seen in Figure (2-6).

**a) Out of Plane Bending Vibrations.**

**b) In-Plane Bending Vibrations.**

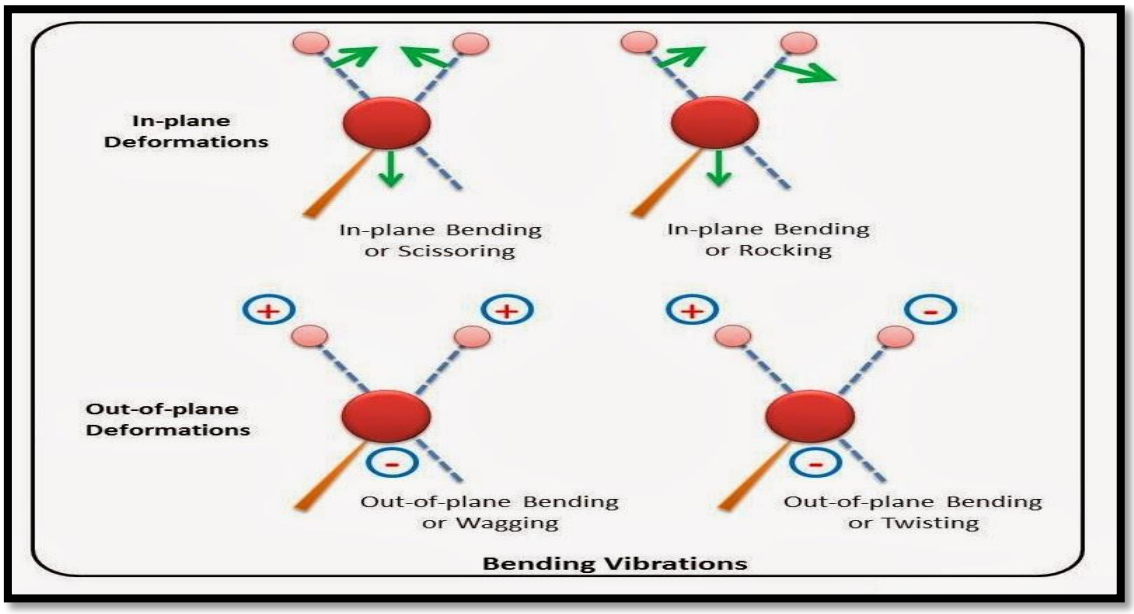


**Figure (2-9).Types of Bending Vibrations** [105]**.**

**2-Stretching Vibrations.**

The stretching vibrations took place on the bond length, which might increase or decrease at regular rests as the bond length varied. Vibrational stretching can be divided into two categories: symmetrical stretching and asymmetrical vibrations [106], as demonstrated in Figure (2-7).

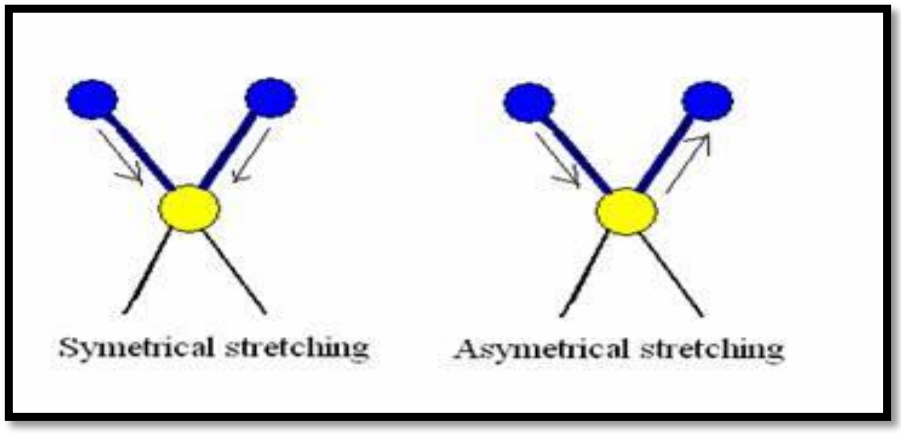


**Figure (2-10).Stretching Vibrations of Different Types** [106]**.**

The concept of this approach is that molecular bonds vibrate at different frequencies. FT-IR spectroscopy is a potent instrument for detecting types of chemical bonds in a molecule by producing an infrared absorption spectrum as a molecular "fingerprint." Depending on the elements and the type of connection, molecular bonds vibrate at different frequencies. Because FT-IR offers information on a material's chemical bonding or molecular structure without destroying it, it can be used to identify unknown materials, detect organic and inorganic additives at a low level, and assess chemical structure change and solvent residue [106], as shown in Figure (2-8).

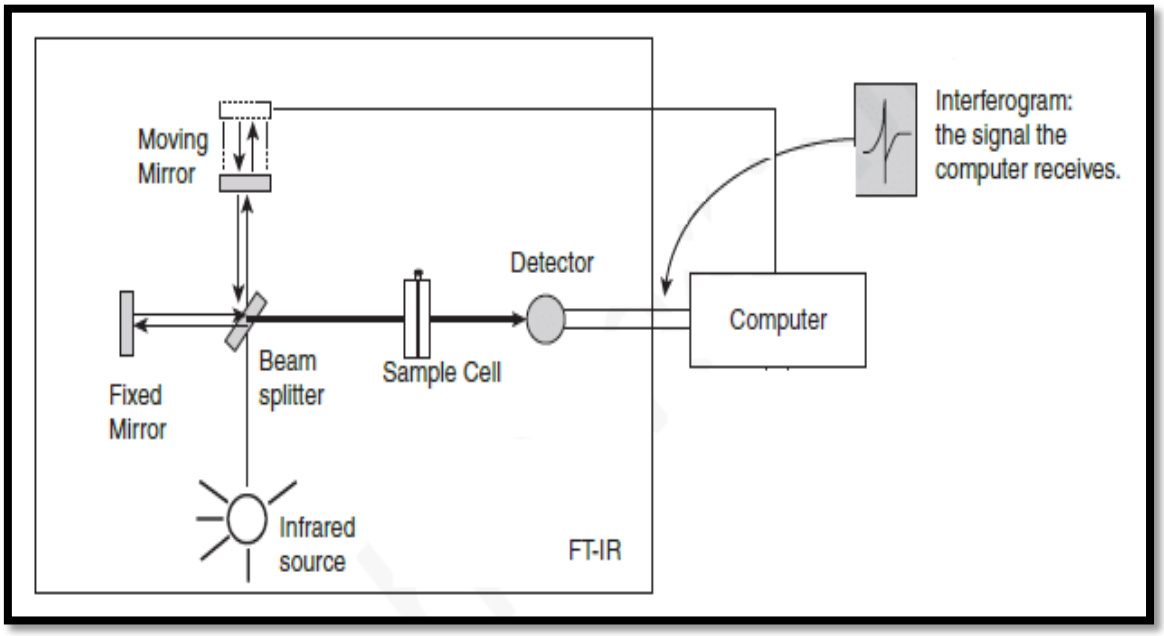


**Figure (2-11). Schematic Illustration of the FTIR System** [104]

### 2.7.2 X-Ray Diffraction (XRD):

X-ray diffraction (XRD) is a powerful instrument for researching electrode materials, particularly cathode materials, to confirm the crystallographic structure, the size of crystallites, and the desired specimen orientation. X-ray radiation is produced by a high-energy electron beam when anode materials such as copper are irradiated [107]. The wavelength range is 0.01-10 nm, and the order of planar crystals in the atom spacing (d) equals the number of atom arrays in the wavelength range [108]. After the dispersion patterns of the material have been analysed, X-rays that can be naturally dispersed from each collection of crystal lattice planes at a specific angle may be utilized to validate the crystal structure after it has been determined what the structure of the crystal is [109]. Bragg's law (equation 2.1) is widely applied to illustrate circumstances of diffraction from planes with spacing (d) see Figure (2-9) to build a link between wavelength and spacing of crystal [110].

$$n\lambda = 2d\sin\theta \quad (2\text{-}1)$$

In such case, n indicates An number that describes the degree of diffraction, where represents the wavelength of the X-ray beam incident on the crystal lattice, d denotes the spacing of the crystal lattice and denotes the angle of the incident X-ray beam [111].

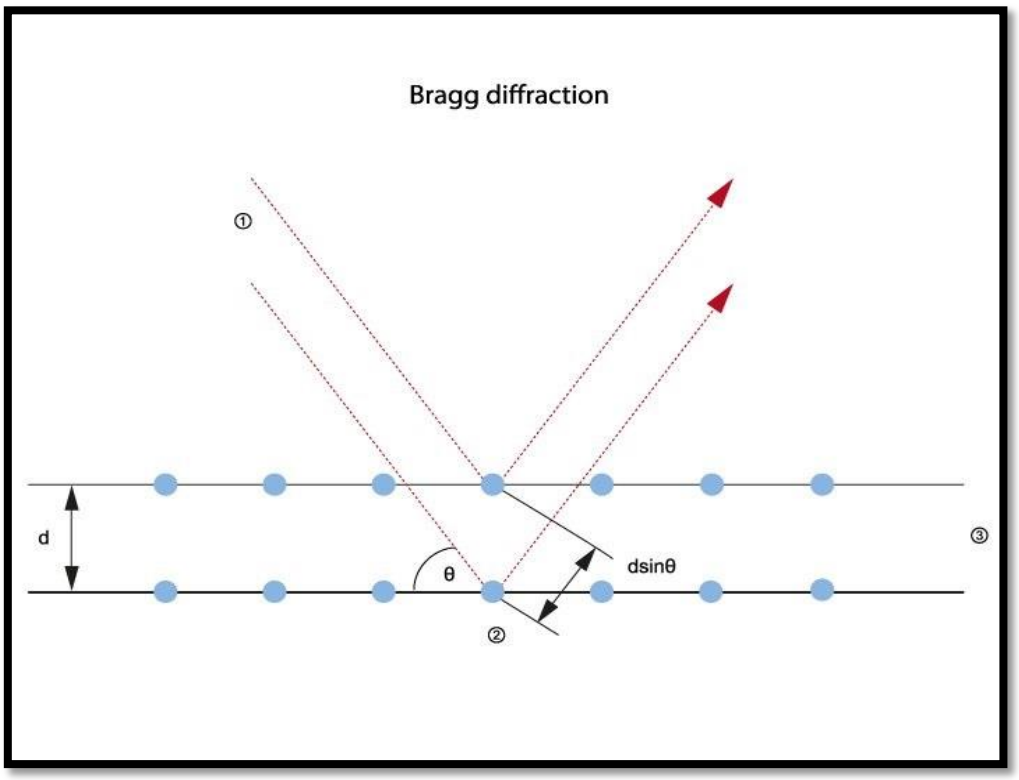


**Figure (2-12). Bragg's Diffraction** [112]**.**

In the meanwhile, the Scherrer formula employed to determine the size of the crystallites (D)[113]:

$$D = K\lambda/\beta cos\,(\theta)\ldots\ldots\ldots\ldots\ldots \quad (2\text{-}2)$$

For the average crystallite (0.9) and the whole width of materials, the form factors are (K) and ($\beta$), respectively.

### 2.7.3 Scanning electron microscope (SEM)

In many sectors throughout the world, the scanning electron microscope (SEM) is a critical research and production tool that is widely used in both study and manufacturing. The requirement of inspecting and gathering information on samples whose structural integrity is failing is the source of the instrument's attractiveness. The scanning electron microscope (SEM) offers a higher degree of resolution for examination and inspection than current optical microscopy methods. Furthermore, unlike the optical microscope, the scanning electron microscope (SEM) offers a variety of analytical modes, each of which delivers unique information on the physical, chemical, and electrical characteristics of a specific specimen, device, or circuit. As a result of recent advancements that remove or at the very least limit sample deterioration and contamination while permitting continuous nondestructive in-process inspection, the scanning electron microscope (SEM) is seeing growing usage in research and production quality control applications [114].

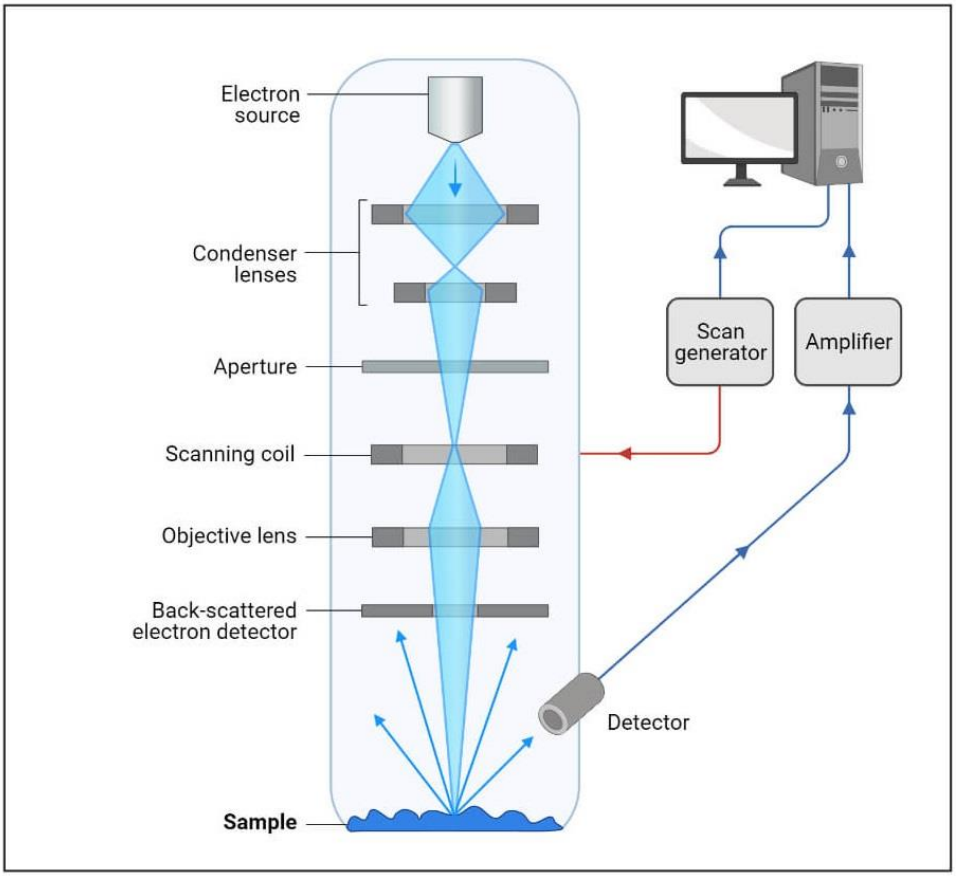


**Figure (2-13). Ray Diagram for a system of SEM** [115].

### 2.7.4 Optical microscopy (OM)

Optical microscopy is a technique employed to closely view a sample through the magnification of a lens with visible light. This is the traditional form of microscopy, which was first invented before the 18th century and is still in use now. An optical microscope, also sometimes known as a light microscope, uses one or a series of lenses to magnify images of small samples with visible light. The lenses are placed between the sample and the viewer's eye to magnify the image so that it can be examined in greater detail.

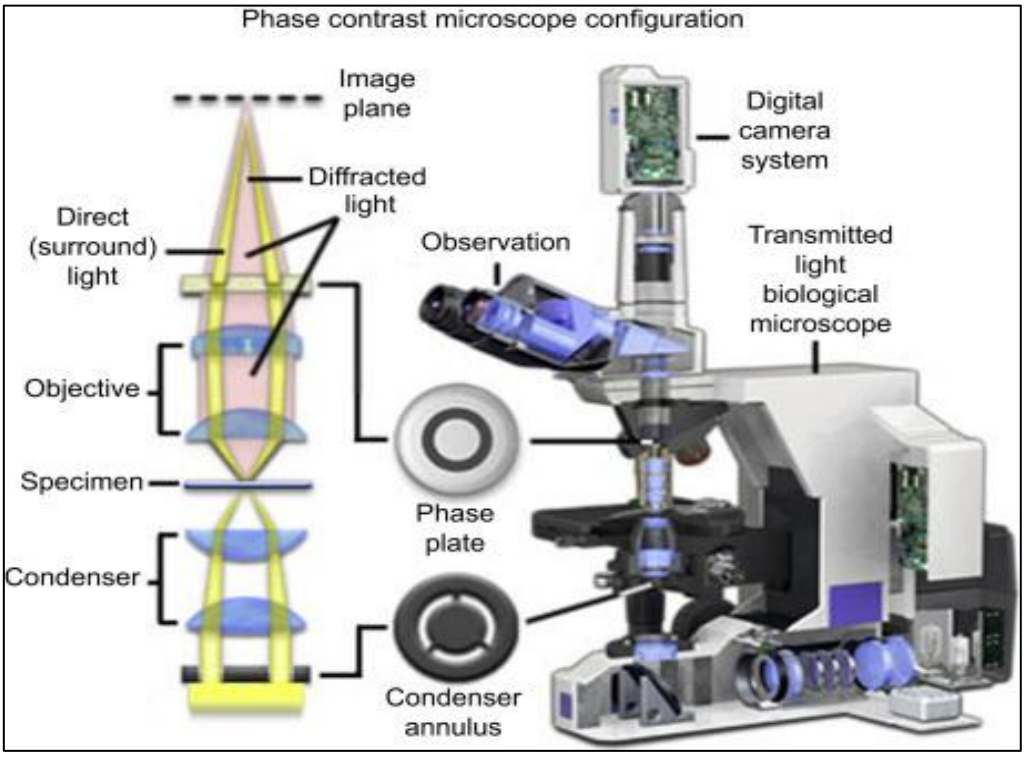


**Figure (2-14). Optical Microscope** [116] **.**

# Chapter Three

# Experimental Part

### 3.1 Introduction:

This chapter provided an overview of the used materials, methods, equipment's, instruments and antibacterial that were used in the preparation and measurement procedures, as well as the steps of sample preparation and testing measurement that were covered.

### 3.2 The Utilized Materials

a) **BEAUTIFIL II** is the hybrid filling contained a macro-micro particle that formed from (Bisphenol A-glycidyl methacrylate) (Bis-GMA). It is a resin commonly used in dental composite by the ratio (1-10%), Triethylenglycol dimethacrylate (1-5%), Aluminofluoro-borosilicate glass (60-70 %), $Al_2O_3$ (1-5%) and DL-camphor quinone that manufacture by Shofu Inc. Company and made in Japan.

b) **ENHANCE** is nano-hybrid universal contain Bis-GMA and barium glass, nanosize silica (10-50 nm), and prepolymer. It was supplied from Sincera Technology Company that was made in china.

c) **Poly methyl methacrylate (PMMA)** with molecular weight (18000-20000 g/mol), melting point 213 ºC, and 99 percent purity produced by Tuttlingen Company in China.

d) **Graphene Oxide (GO)** was synthesis by our group using modified Hummer methods [117] flowing the procedure in our previous publication with pH around 5.7, see the support information for full characterizations of GO nanosheets [118].

e) **Dimethylformamide (DMF) (**$C_3H_7NO$) with molecular weight (73.09 g/mol), minimum assay 99% manufactured by Thomas Baker (MIDC), Chemical Zone, India.

### 3-3 Fabricated of filler-polymer-based graphene nanocomposites

Developed aquatic dissolving-sonication-casting methods were applied to fabricate new modified dentil filler-polymer-based graphene oxide nanocomposites. Six samples were prepared from both fillers and each filler has three samples. Briefly, nano-filling and hybrid-filling were fully dissolved separately with a ratio of 100 wt. % in Dimethylformamide (DMF) by using a magnetic stirrer for three hours, firstly.

Secondly, PMMA dissolved in DMF using a magnetic stirrer for three hours at 80 ± 2 ºC, then it was added to each modified the fillers samples separately to prepare filler-PMMA samples that were mixed for 3h at a ratio of 75:25 wt. % of nano-filler: PMMA and hybrid filler: PMMA, to prepper the second samples of both fillers.

Thirdly, GO was loaded to modify and reinforce the filler- PMMA matrix structure with a ratio of 75:24:1 wt. % of filler: PMMA: GO The mixers of nano/ hybrid filler-PMMA/GO nanocomposites were mixed using a magnetic stirrer for 60 minutes and then sonicated for ten minutes using a sonication bath. This procedure was repeated for 48 hours until got a homogeneous mixture of the nano/ hybrid filler-PMMA/GO dental nanocomposite.

Finally, the samples were washed with tepid distilled water for removing any potentially harmful substances and then cast in a petri dish to dry at a temperature of 40 ° C for one week. The fabricated samples were pure nano/hybrid filling, nano/hybrid filling-PMMA, and nano/hybrid filling-PMMA/GO nanocomposites, as summarized in Table (3-1) and diagram in Figure (3-1).

**Table (3-1). Summarized the Synthesis of the filler samples and nanocomposites.**

| Sample ID | Filler type | Concentration wt. % | | | Dried method |
|---|---|---|---|---|---|
| | | Filler | PMMA | GO | |
| **N1** | Nano | 100 | 0 | 0 | 40 ± 3 ºC under air |
| **N2** | Nano | 75 | 25 | 0 | |
| **N3** | Nano | 75 | 24 | 1 | |
| **H1** | Hybrid | 100 | 0 | 0 | |
| **H2** | Hybrid | 75 | 25 | 0 | |
| **H3** | Hybrid | 75 | 24 | 1 | |

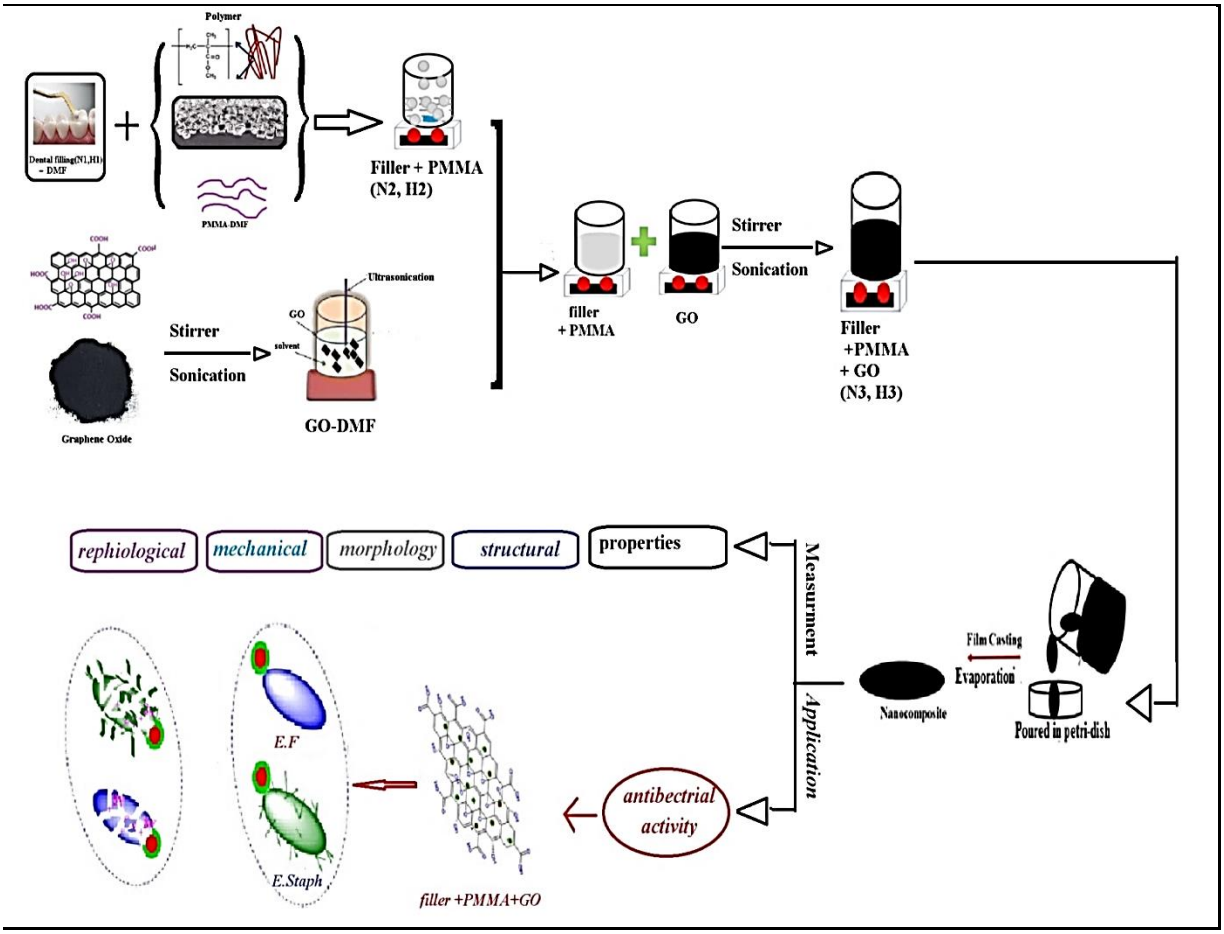


**Figure (3-1). Described the synthesis for the filler samples with nanocomposites.**

## 3.4 Characterizations

### 3.4.1 Structure Characterization

FTIR spectra were recorded by FTIR (Bruker Company, German origin, type vertex 70). FTIR was implemented at the University of Babylon /College of Education for Pure Sciences/Department of Physics. In this study, the considered wavenumber range is (400-4000) $cm^{-1}$ .

### 3.4.1.1 XRD Spectrum

All crystal structures of the polymeric preparations were characterized using an XRD (6000) diffraction device in the University of Technology. Manufacturing and Country/ Tescan, France - Model/Xpert. An X-ray diffraction instrument was used to examine the crystal structures of the nanocomposites. X-ray diffraction (XRD) data were collected of (2θ) from ($0^o$ - $80^o$). It has the following characteristics, wavelength: 0.154 m, voltage: 40.0 (kilovolts), current: 30.0 (mA), high power: 3 (kilovolts), target: copper, measurement temperature: 25 °C and the type of X-ray generation tube (copper, Bα).

### 3.4.2 Morphology Characterization

### 3.4.2.1 Optical Microscope (OM)

The change of surface morphology dental filling samples and nanocomposites is observed applying the optical microscope. The use of OM was provided by Olympus (Top View, type Nikon-73346). It is implemented at the University of Babylon /College of Education for Pure Sciences/ Department of Physics.

### 3.4.2.2 Scanning Electron Microscope (SEM)

SEM is an electron microscope that uses a high-energy electron beam to photograph the surface of a sample in a raster scanning pattern. After sample preparation, the portion of each sample was cut out with dimensions (5 mm × 10 mm) and inserted into an SEM sample holder for examination. The surface morphology of the dental filling (N1, N2, N3, H1, H2 and H3) using Model/Mira-3 - Details/1.2 nm at 30 kV; 2.3 nm at 3 kV - Manufacturing and Country/Tescan، France.

### 3.4.3 Rheological Properties

#### 3.4.3.1 Density and viscosity

The factory's sensitive balance was built by a meter Switzerland Company and the density was measured using a density bottle with a capacity (25 ml) and the sensitive balance of the factory (0.0001). An Ostwald's viscometer calibrated with doubly distilled water was used to measure the viscosity of the aqueous solutions. The experimental liquid and the Ostwald's Viscometer were immersed in a temperature-controlled water bath. The time of flow was measured using an electronic stopwatch.

The timer used was the type of Her Wins Swiss (Swiss) made to measure the flow time of dental filling, nanocomposite solutions, and distilled water in a capillary tube with accuracy the amount of (± 0.0001 sec).

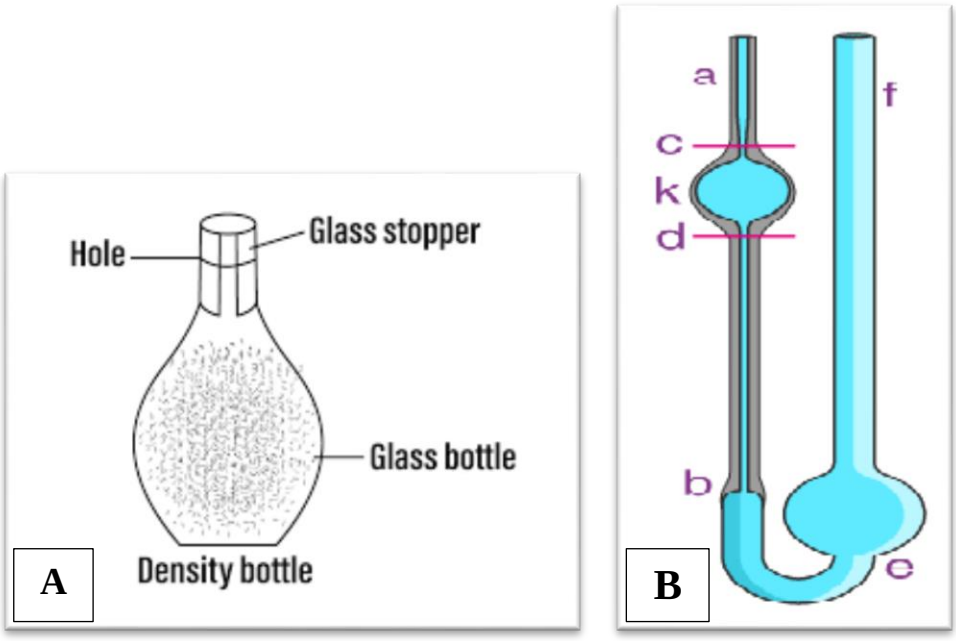


**Figure (3-2). (A) Density bottle, (B) Ostwald's viscometer.**

### 3.4.4 Mechanical Properties

Pulse technique of sender-receiver type (SV-DH-7A/SVX-7) velocity of the sound instrument – Korea) was used to do ultrasonic measurements. The tests were carried out at a frequency of 30, 40, and 50 Hz. The receiver quartz crystal was installed on a digital variable scale of slow motion, allowing it to be relocated parallel to the sender while the samples were placed between the sender and the receiver, as two traces of a cathode ray oscilloscope, the sender and receiver pulses (waves) were shifted. The digital delay time (t) of receiver pulses was measured concerning the sample thickness (x). The amplitude of the incident ultrasonic wave ($A_0$) is represented by the pulse height on an oscilloscope (CH1), and the amplitude of the receiver ultrasonic wave (A) is represented by the pulse height on an oscilloscope (CH2).

## 3.5 Antibacterial activity

### 3.5.1 Media preparation

#### 3.5.1.1 Nutrient Broth

Nutrient Broth was used for the general cultivation of less fastidious microorganisms. It was prepared by dissolving 13 gm in 1000 mL of distilled water , and the heat was used , if necessary , to dissolve the medium completely . Dispense as desired and sterilize by autoclaving at 121 ° C for 15 minutes [119].

#### 3.5.1.2 Mueller Hinton Agar

Mueller Hinton agar was used to the determination of susceptibility of microorganisms to antimicrobial agents. It was prepared by dissolving

38 gm in 1000 mL distilled water. The heat was increased to boiling to dissolve the medium completely. The medium was sterilized by autoclaving at 121 ° C for 15 minutes, and then cooled to 45 ° C and then poured into sterilized Petri dishes (9-10 cm). The bacteria were swabbed uniformly across the culture plate [120].

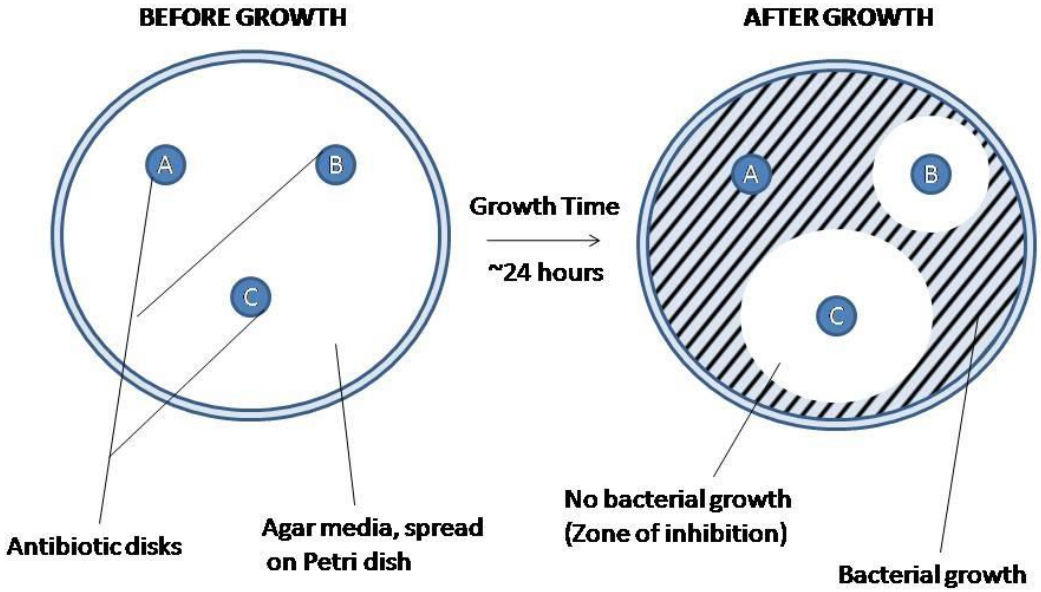


**Figure (3-3). The disk-diffusion agar method tests the effectiveness of antibiotics on a specific microorganism.**

### 3.5.2 Agar well diffusion method

Mueller Hinton agar plate surface was inoculated by spreading a volume of the microbial inoculum over the entire agar surface. Then, a hole with a diameter of 6 to 8 mm was punched aseptically using a sterile tip. If the samples were effective against the bacteria at a certain concentration, then no colonies would grow and the concentration in agar was greater than or equal to the effective concentration. This region is called the inhibition zone. The size of inhibition zone measures the efficiency of a sample. A more effective sample produces a larger clear area around the

disk. All tests were done under a laminar flow hood. Finally, all Petri dishes At the end of the incubation period, the diameters of inhibition zones formed around disks were determined and presented in mm The agar plates were then incubated under suitable conditions for 24-48 hrs. The antibacterial agent diffused in the agar medium and inhibited the growth of the microbial strain tested [121].

### 3.5.3 Maintenance of Bacterial cell

Enterococcus faecalis and E. Staph were obtained from Al-Ameen Center for Research and Biotechnology and maintained in Nutrient broth medium. Cells were subculture twice a week and incubated at 37 °C.

### 3.5.4 Inoculum Standardization

A McFarland 0.5 turbidity standard was prepared adding 99.5 mL of 1 % sulfuric acid to 0.5 mL of 1.175 % barium chloride solution. This solution was dispensed into tubes comparable to those used for inoculum preparation. The tubes were sealed and stored under dark conditions room temperature. The McFarland standard provided turbidity comparable to that of a bacterial suspension containing 1.5 x 10 cells / uL. The turbidity of the prepared bacterial suspensions was compared by observing the black lines through the suspension [122].

# Chapter Four

# Results and conclusion

## 4.1 Introduction

This chapter presents the findings and discusses the effects of (GO) nanosheets and polymethyl methacrylate (PMMA) on antibacterial activity, as well as some of the morphology, structural, and mechanical properties of nano/hybrid dental filler nanocomposites.

## 4.2 Structure and Morphology Properties

### 4.2.1 FT-IR Measurement

Figure (4-1) illustrates the Fourier Transform-IR spectrum for GO, PMMA, nano, and hybrid dental fillers and the nanocomposite samples in the range between 500 to 4000 $cm^{-1}$. The spectrum of graphene oxide (GO) that have peaks wavenumbers at 3214 $cm^{-1}$ of O-H (free water) stretching, 1738 $cm^{-1}$ of carbonyl C=O stretching, 1621 $cm^{-1}$ of C=C stretching, 1365 $cm^{-1}$ of C-H bending, 1222 $cm^{-1}$ of C-H stretching, 1055 $cm^{-1}$ of epoxy C−O−C stretching and 980 $cm^{-1}$ of C-O stretching functional groups in agreement with the literature [118]. The curve of polymer PMMA exhibited peaks at (2951, 1724, 1673, 1435, and 1145) $cm^{-1}$ related to C-H medium stretching of the methyl and methylene group, the stretching vibrations of C=O strong stretching of the ester group, and bond vibrations of (C=C), The carbon-carbon single bond (C-C) has low absorption, and (C-O) related to alkyl aryl ether group [123].

The nano dental filler pure at curve (N1) exhibited a small feature of the peak at (1720) $cm^{-1}$ associated with C=O stretching vibrations and a peak (1051) $cm^{-1}$ related to the strong stretching vibrations of (C-O), whereas new peaks presented in the N2 after the addition of the PMMA that showed a small peak at (2946) $cm^{-1}$ related to (C-H) stretching, in addition to shifting in the other peaks from 1720 to 1717 $cm^{-1}$ and (1051 to 1052) $cm^{-1}$. The contribution of GO in the nano-PMMA dental filler matrix (N3)

presented a new peak at (3413) $cm^{-1}$ corresponding to intermolecular strong bond (O-H) stretching, moreover, it presented a shifting in other some of the peaks such as from 2946 to 2941, 1717 to 1713, and 1052 to 1054 $cm^{-1}$.

The hybrid dental filler curve pure (H1) exhibited a small feature of the peak at (2934, 1713, 1452, 1161, 940) $cm^{-1}$ related to C-H medium stretching of the methyl and methylene group, the stretching vibrations of C=O strong stretching of the ester group, and the carbon-carbon single bond (C-C) has a medium absorption, (C-O) related to alkyl aryl ether group and (C=C) related to strong bending, respectively. The curve (H2) exhibited shifting in the peaks, such as (2934 to 2937), (1713 to 1722), (1452 to 1433), (1161 to 1144), and (940 to 960) $cm^{-1}$. Whereas, the contribution of GO in the hybrid-PMMA dental filler matrix in the curve (H3) when loading of GO in hybrid dental-PMMA matrix resulted in a new O-H peak at 3373, in addition, it presented a shifting in other some the peaks such as (2937 to 2958), (1722 to 1713), (1433 to 1434), (1144 to 1133) and (960 to 968) $cm^{-1}$.

The strong interfacial interaction was responsible for the presence of the new peaks, shifting, and changes in intensity peaks of the FTIR spectrum for both fillers after the addition of polymer, and GO refers to bonding these materials with a stronger hydrogen bond with dental fillers [118,123].

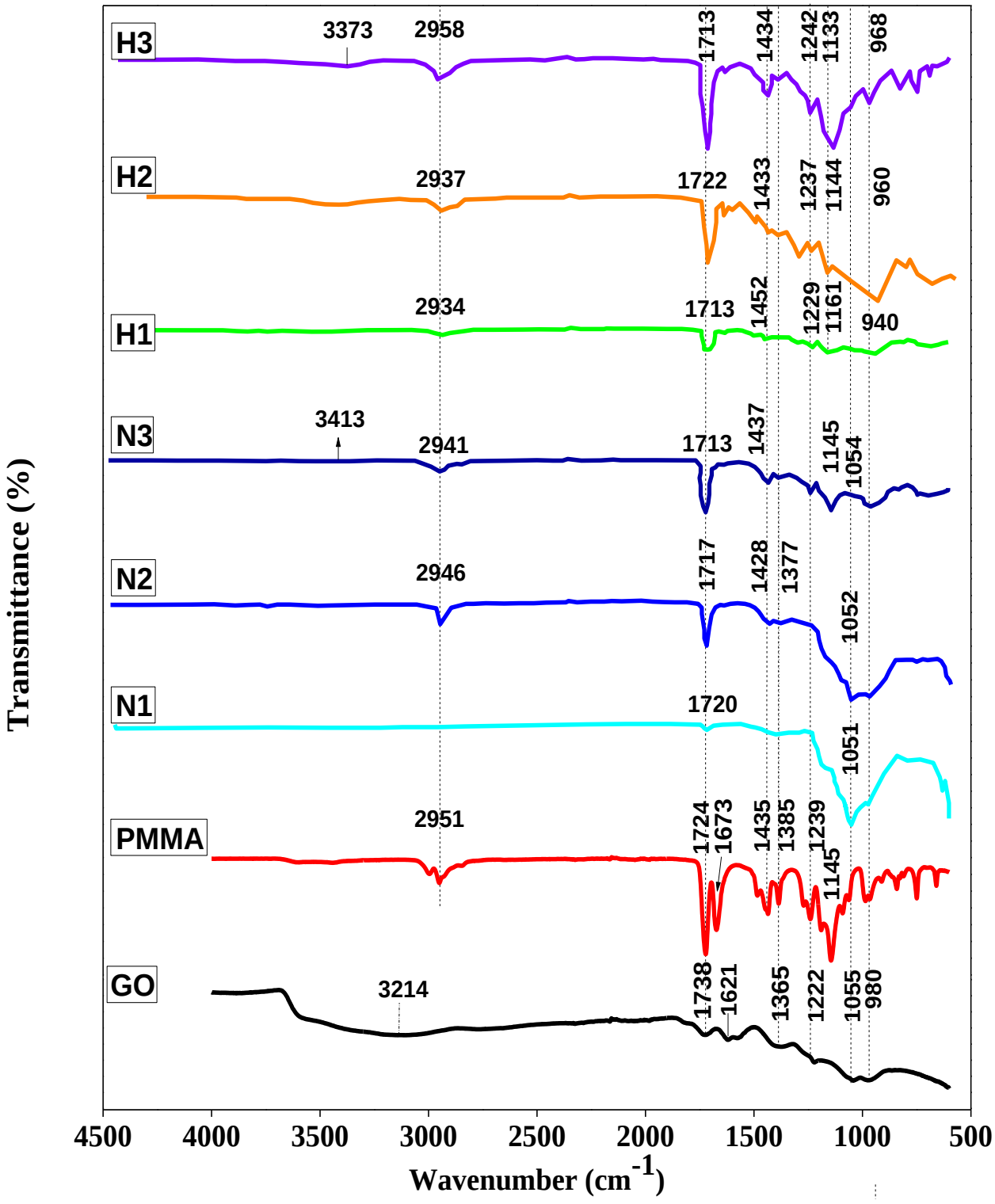


**Figure (4-1). FT-IR spectrum for GO, PMMA, N1, N2, N3, H1, H2, and H3.**

### 4.2.2 X-Ray Diffraction Measurement

Figure (4-2) (A, B) illustrates the XRD spectrum of the graphene oxide (GO), in addition to poly(methyl methacrylate) (PMMA). GO exhibits a peak at $2\theta = 11.1^{o}$ with (002) diffractions that is with 0.79 nm interlayer spacing, which was measured by the Bragg equation and agreed with the literature [123–126], while exhibiting three broad peaks at $2\theta = 14.2^{o}$, $29.92^{o}$ and $41.35^{o}$. These peaks are corresponding to the miller indices (111), (112), and (220), respectively, which related to the PMMA, and matched other findings [123,124,127,128].

Figure 2 (C) explains the XRD spectra of the pure nano filling (N1), nano filling-PMMA (N2) and Nano filling-PMMA/GO (N3).From this Figure, N1 observed peak at $2\theta = 20^{o}$ corresponding to the DL-Camphor quinone, which is one of the contents of Bis-GMA in nano filling [129], and peaks at $2\theta = 24.84^{o}$, $25.88^{o}$, $26.92^{o}$, $28.84^{o}$, $31.64^{o}$, $32.72^{o}$ and $42.72^{o}$ related to the $Al_2O_3$, which is another component of the of Bis-GMA in nano filling that corresponding to the miller indices (012), (115), (213), (117), (222) and (113), respectively. These results of the diffraction pattern match the combined (JCPDS) patterns of $\delta$-$Al_2O_3$ (JCPDS 00-016-0394) and agreed with another researcher's findings [130]. PMMA observed a significant change in XRD spectra of nanofillers (N2) in compression with (N1), which presented three abroad peaks areas started from $14^{o}$ to $22^{o}$, $25^{o}$ to $36^{o,}$ and $40^{o}$ to $47^{o}$, where the majority of the N1 peaks were found to be overlapping with the PMMA peaks, which displayed additional wide peaks as a result of the contribution of the PMMA. A change in the size of the peak might be a reference to an increase in the distance between interplanar crystals [127], and it was noted that the volume expansion in the macro [123].

GO revealed a significant impact in the XRD of N3 that presented two abroad peaks than N2, it was located between $8^o$ - $36^o$ and $38^o$ to $48^o$. Consequently, the XRD diffraction of GO may overlap with PMMA, or also the low loading ratio, full desperation, and orientation of GO nanosheets in the matrix could cause this disappearance, these cases make it is difficult to present the XRD patterns in agreement with the several works of literature that reported the same behviour [128,131].

Figure (2) (D) explains the XRD pattern of the pure hybrid filling (H1), hybrid filling with PMMA (H2), and hybrid filling with PMMA and GO (H3) nanocomposite. From this Figure, it is obtained that the H1 observed peaks at $2\theta = 20.12^o$, corresponding to the DL-camphor, which is one of the contents of Bis-GMA in the hybrid filling, and peaks at $2\theta = 25^o$, $25.92^o$, $26.96^o$, $28.84^o$, $31.6^o$, $32.84^o$ and $42.72^o$ related to the $Al_2O_3$, which one of the of Bis-GMA in hybrid filling components, these peaks corresponding to the miller indices (012), (115), (213), (117), (222) and (113), respectively. The recorded diffraction pattern matches with the combined JCPDS patterns of δ-Al2O3 (JCPDS 00-016-0394, which agree with the results of researchers [132,133].

From this Figure, loaded the PMMA in the hybrid filler in the H2 observed significant change by presenting two broad peaks between $18^o$ to $36^o$ and $38^o$ to $48^o$ matching the second and third PMMA peaks, whereas the H1 peaks were overlapped in these two broad peaks. H3 presented a strong impact of GO that lead to shifting in first abroad peak from $18^o$ to $36^o$ of H2 to $15^o$ to $39^o$, also it was noted to become bigger and wider compared with H2 peak. From the spectra of H3, the contribution of GO, all peaks were discovered to be placed in the wide-high intensity pattern of PMMA polymer, which ranged from $15^o$ to $40^o$. XRD patterns of GO are difficult to present in the samples in agreement with other literature that reported the

same behavior of GO because the peaks at graphene oxide and hybrid filling possibly overlap with PMMA abroad peaks. Additionally, the filled dispersion at GO nano-sheets for the mixture makes it hard to introduce [128,131]. These changes in the XRD behviour support the FTIR results that showed significant and strong interfacial interaction after the loaded of the PMMA and GO.

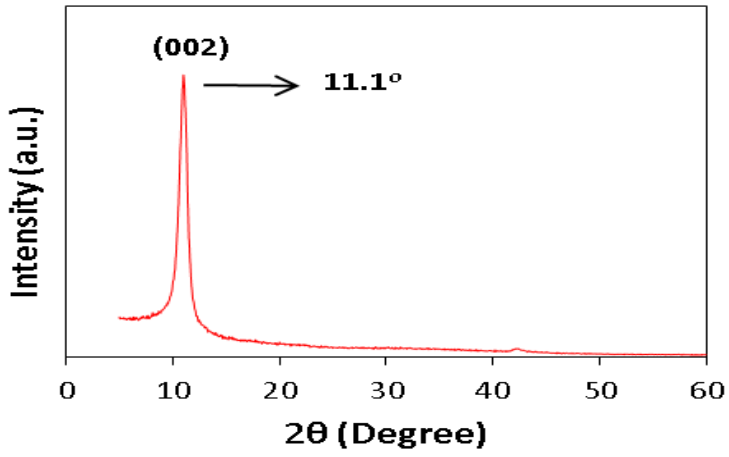


(A)

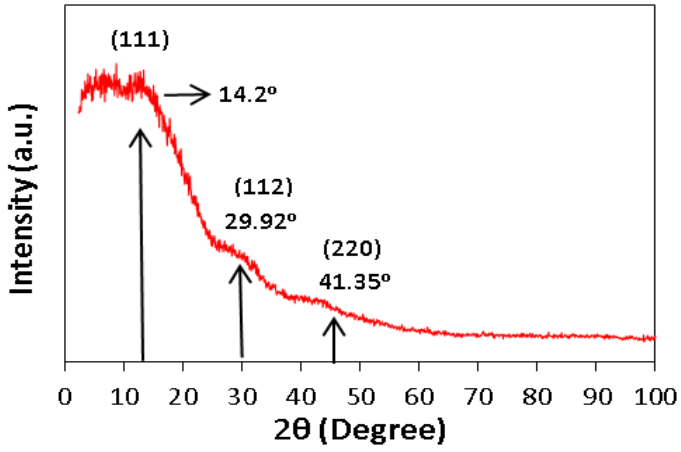


(B)

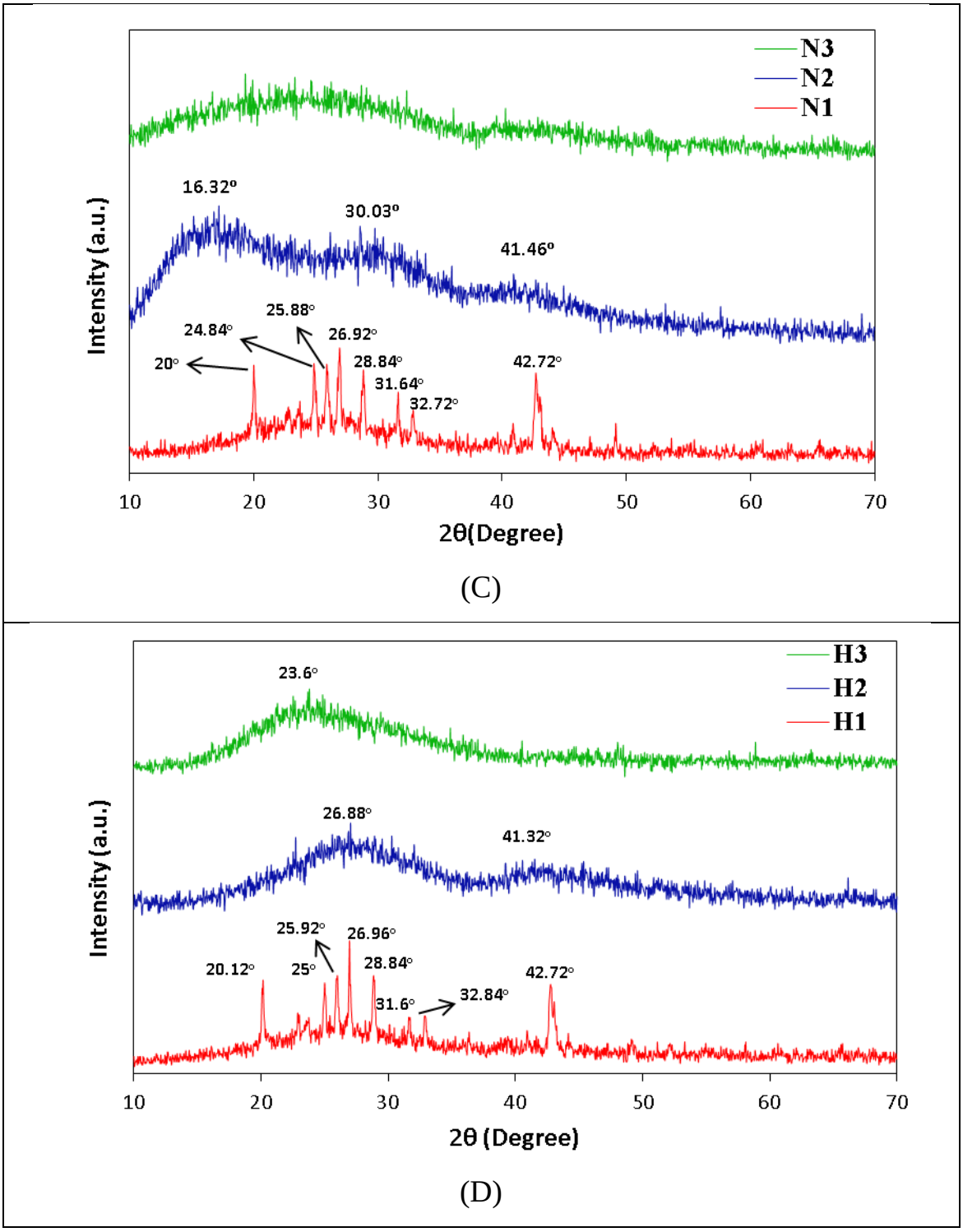


**Figure (4-2). XRD pattern of the (A) GO, (B) PMMA, (C) nano-filling, and (D) hybrid-filling.**

### 4.2.3 Optical Microscope

Figure (4-3) depicts the optical microscope images for the surface of the nano and hybrid dental filling, and their samples (N1, N2, N3, H1, H2, and H3). These images demonstrated the fine homogeneity of dissolved dental samples for the N1 and H1. The addition of the PMMA in N2 and H2 exhibited changes in the surface of the samples that exhibited some spherical particles related to PMMA. The addition of GO showed the good and fine distribution of GO in the N3 and H3 dental filling whereas, some nanomaterials were aggregated but that did not affect the optical transparency of the samples, this change in the surface of the nanomaterials was related to the bonded among the dental fillers, PMMA and GO nanosheets with strongest hydrogen bonds as showing in the FTIR results.

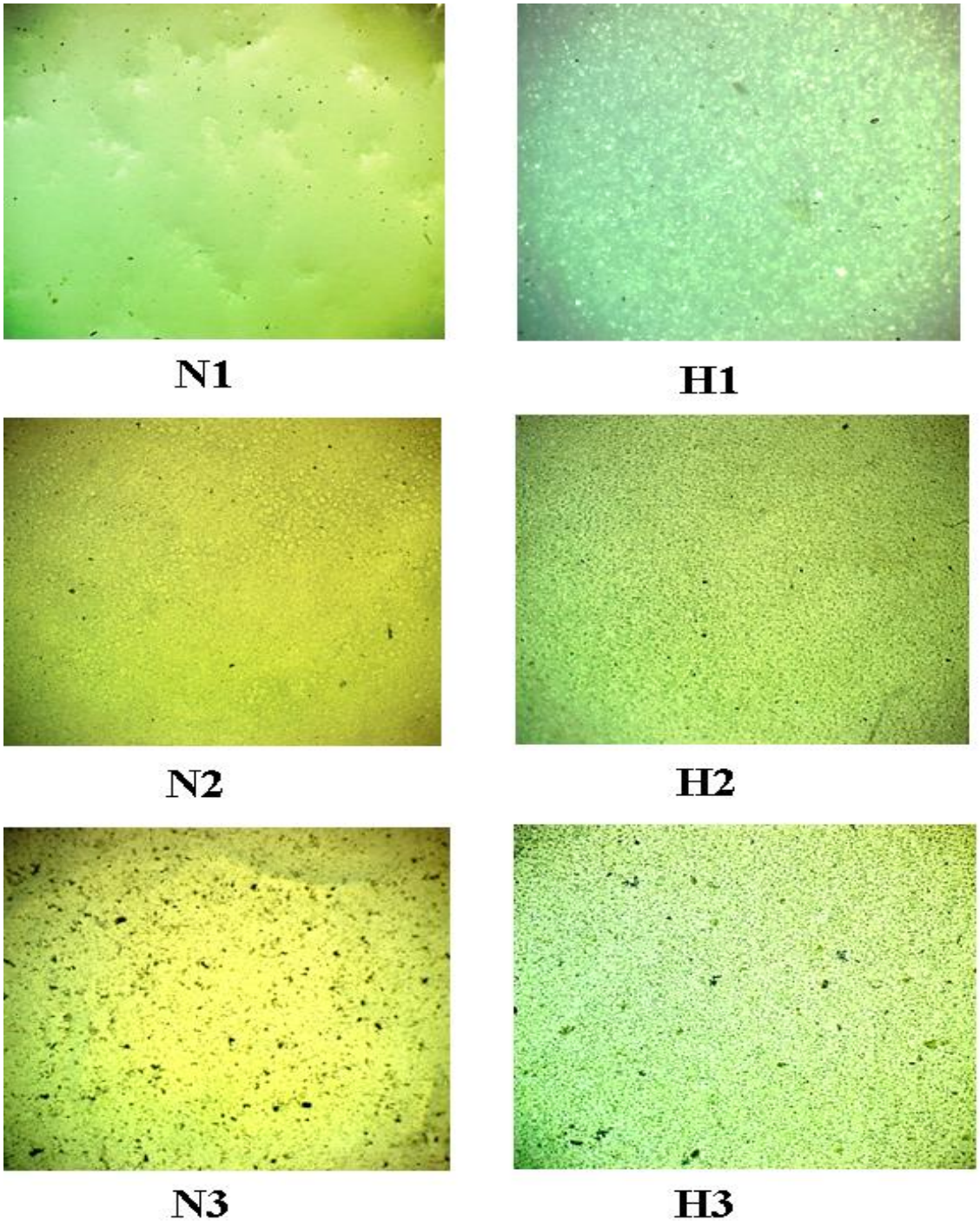


**Figure (4-3). The OM images of N1, N2, N3, H1, H2, and H3**

### 4.2.4 Scanning Electron Microscope Measurements (SEM)

Figure (4-4) represents the SEM images with two magnifications 1 micron and 200 nm of the surface morphology of each sample. The image in

Figures (4 A and B) illustrates the nano-filling in dimensions of 1 micron, and 200 nm, it clarified the composition of the nano-filling as grainy particles, and rough with cavities surface shape. Whereas in Figures (4 C and D), morphology behviour was significantly changed and the most grained partials were covered in addition to filling the cavities and spaces between the filler partials components, the filler-PMMA sample showed tiny cracks on the surface that related to the nature of PMMA as reported by another researcher [118]. These cracks were inhibited and the surface was strongly changed after the contribution of GO nanosheets, as illustrated in Figures (4E and F), as they interacted perfectly as a result of continuous mixing. The pictures in Figures (4 G and H) showed the hybrid filling and the surface topography of the sample. the loaded of PMMA revealed covering of the most particles and fill the gaps between the filler components, in addition, the surface of the samples showed tiny cracks on the surface that related to the nature of PMMA, as is evident in the (I and J). However, the GO strongly contributed created a big difference because GO has many stretching bonds that enable to link the molecules with each other tightly and overcome the surface cracks, this is clear in the pictures (K and L).This change in the morphology of the surface of filler is related to the impact of the long chains of polymer molecules that have covered the most and bonded the filler partials components, in addition to filling the gaps between the filler particle. This shows well working together between the filler particles and polymer, whereas the functional groups of GO give it the ability to form a stronger interfacial interaction to create strong bonds among fillers, polymer molecules, and GO nanosheet, as that strongly presented in the FTIR and XRD results that showed strong new peaks in addition to shifting of other peaks in agreement with another finding [123].

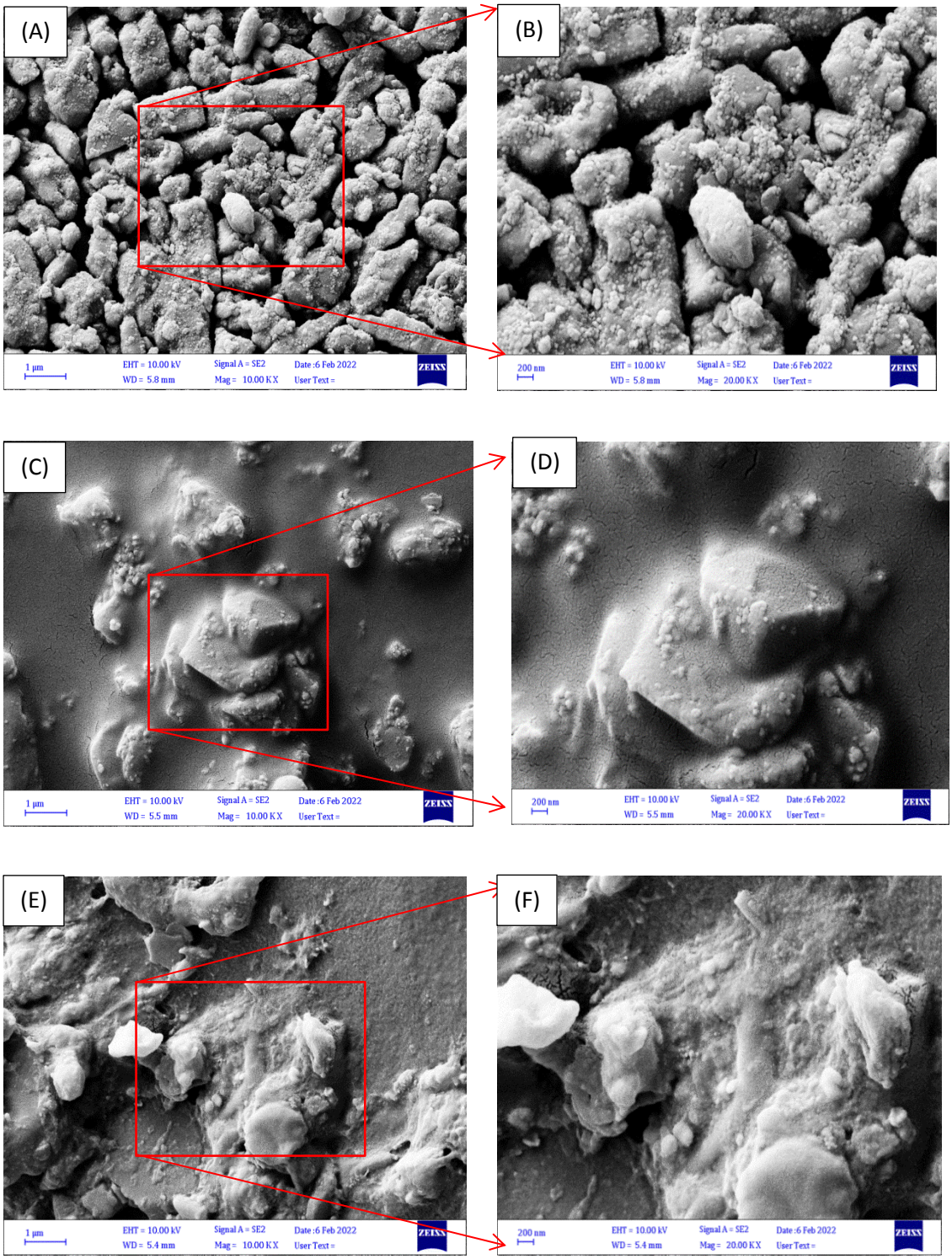
(A)
(B)
(C)
(D)
(E)
(F)

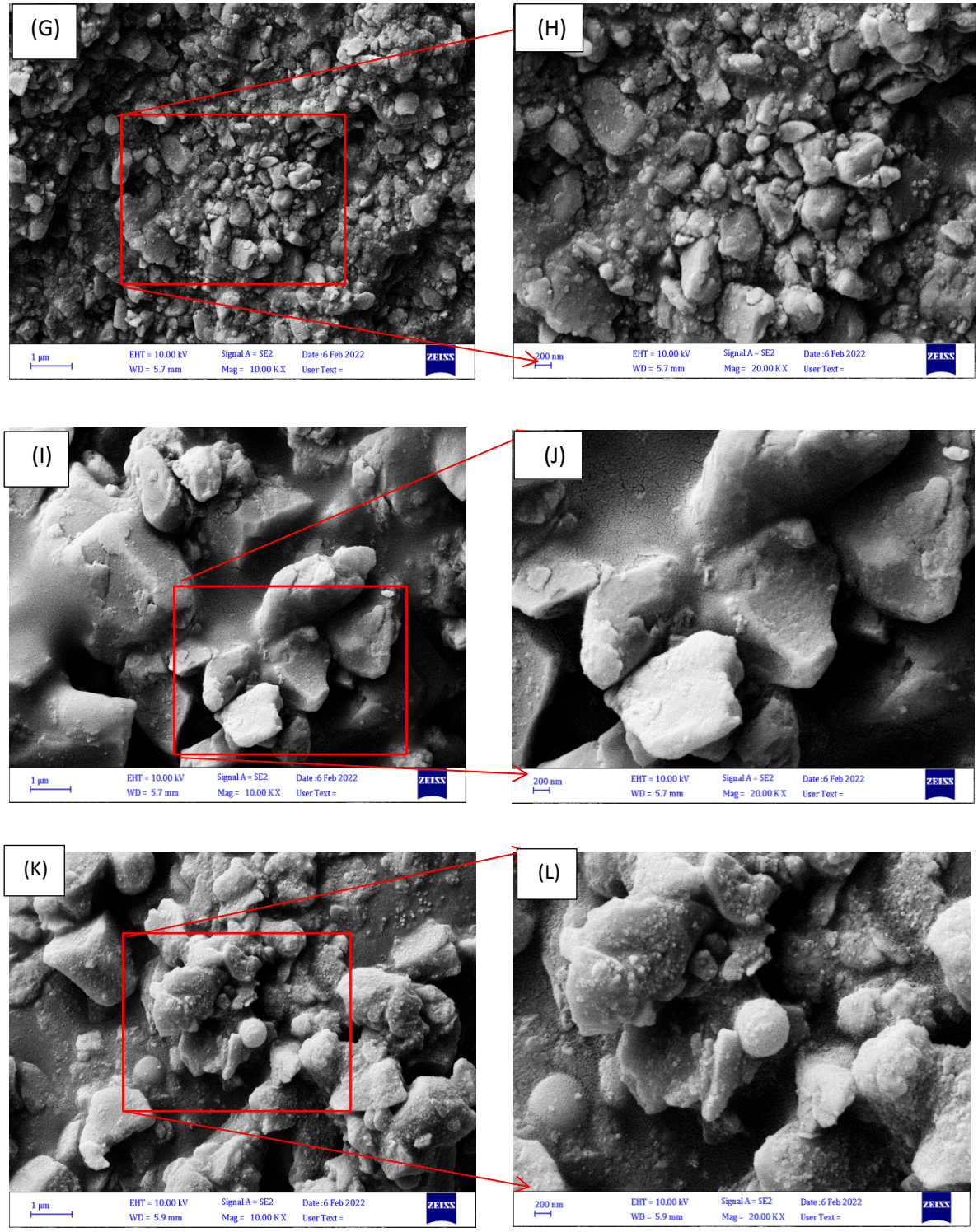


**Figure (4-4)**. SEM images with two magnifications of the surface morphology of the samples.

### 4.3 The Rheological Properties

Some of the rheological properties were calculated as is important to help to understand and calculate the mechanical properties.

#### 4.3.1 Density

In Table (1), the density of the samples was evaluated before and after the addition of the polymer (PMMA) and graphene oxide to the dental fillings. It was noted from the density results of the nanofiller that it has a density higher than the hybrid filler. In addition, the loading of PMMA and graphene oxide exhibited a clear increase in the density of the filling-PMMA matrix, and filling nanocomposites. Where the mass over the volume is the definition as the density, and a linear increase in density is presented when polymer and GO were added to the mixture [134].

**Table (4-1). The sample density.**

| Compounds | Density g. $ml^{-1}$ |
|---|---|
| **N1** | **0.969** |
| **N2** | **1.027** |
| **N3** | **1.119** |
| **H1** | **0.944** |
| **H2** | **1.013** |
| **H3** | **1.096** |

#### 4.3.2 Viscosity

The flow time of the pure dental fillings was measured before and after the loaded of PMMA polymer and GO The finding in Table (2) showed a change in flow time values between the types of filling, and the loading of

PMMA revealed the molecules become larger in the matrix, In addition, the amount of molecules in the polymeric solution rises as a result of an increase in the forces applied that are present between the molecules (big molecules), which obstructs the flow of the solution, while it is being transported through the capillaries viscosity [135]. It is also possible to see this in Table 2, which shows that the flow time rose to 18% of N2, and 20% of H2 with the contribution of PMMA, whereas the contribution of GO significantly improve up to 32% of N3, and 35% of H3, respectively compared with N1 and H1.

These results were obtained as a consequence of the impact of polymer and nanosheets additives, which increased the density and friction forces between the dental filling particles [135]. Viscosity was determined using the relationship 2 which exhibited different viscosity values of each filler. When the polymer was loaded to N2, the viscosity increased by 25%, and when GO was added to N2, the viscosity increased by 53% compared with N1. Adding the polymer in H2 increased the viscosity up to 29%, which was improved up to 57% after the contribution of GO in H3. These results were obtained as a consequence of the action of nanosheets additives and polymer, which increased the density and friction forces between the dental filling particles [136]. Second, while comparing the viscosities of the nano filling with the hybrid filling after loading the polymer and GO, the nano filling results were higher than the viscosities of the hybrid filling, as represented in Figure (4-5).

**Table (4-2). The flow time for the dental filling with nanosheets.**

| Compounds | Solution Flow Time, sec |
|---|---|
| N1 | 65:53 |
| N2 | 77:61 |
| N 3 | 86:82 |
| H1 | 63:98 |
| H2 | 76:09 |
| H3 | 85:87 |

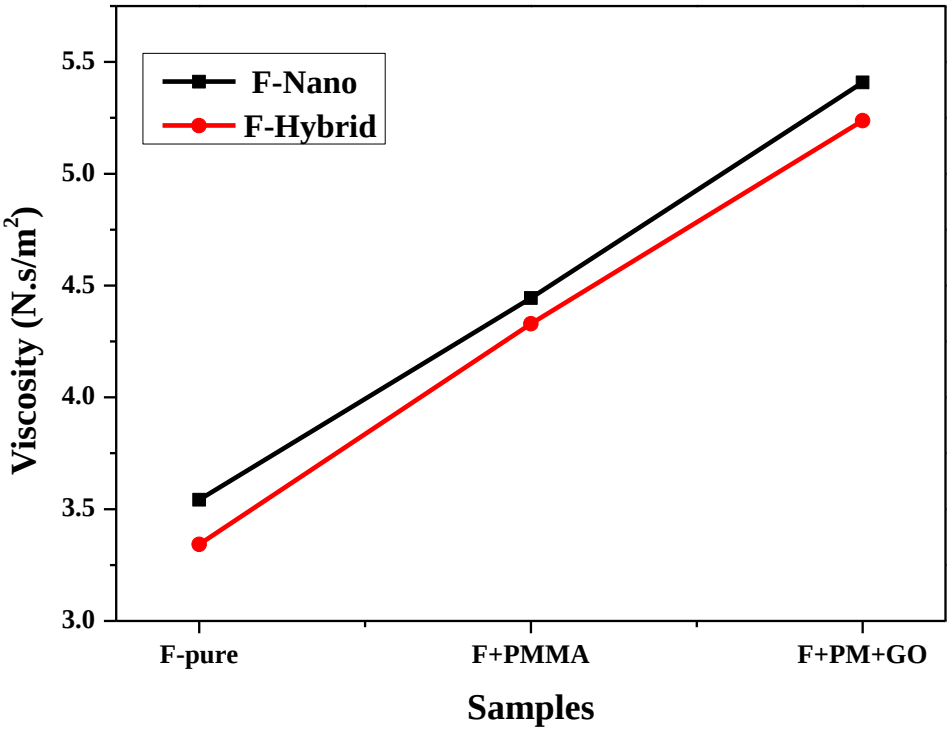


**Figure (4-5). The viscosity for dental filling and their samples.**

## 4.4 Mechanical Properties

### 4.4.1 Ultrasonic Velocity

The outcomes of the measurements of the samples' ultrasonic velocities of the (N1, N2, N3, H1, H2, and H3) at 40 Hz frequency are presented in Figure (4-6) calculated from equation (3). The ultrasound velocity improved after the PMMA loaded up to 12 % of the nano filling and 33 % of the hybrid filling, whereas it was significantly enhanced after the contribution of GO up to 30 % of the nano filling and 51 % of the hybrid filling compared with their fillers, as exhibited in Figure (4-6). Where the incorporation of PMMA and GO resulted in a significant impact and development for the rate of the ultrasound velocity compared to their pure dental filling for both kinds. The ultrasonic velocity of nano-dental filling was revealed to be slightly higher than the ultrasound velocity of hybrid dental filling. Moreover, nanofiller- PMMA/GO (N3) showed better ultrasound velocities up to 30 % than hybrid filler-PMMA/GO dental nanocomposites (H3). This is owing to the large volume of the polymeric chains that come linked to each other, as well as the GO nanosheet, which amplifies the interfacial interaction between the dental fillings in agreement with FTIR results and agreed with other findings [126].

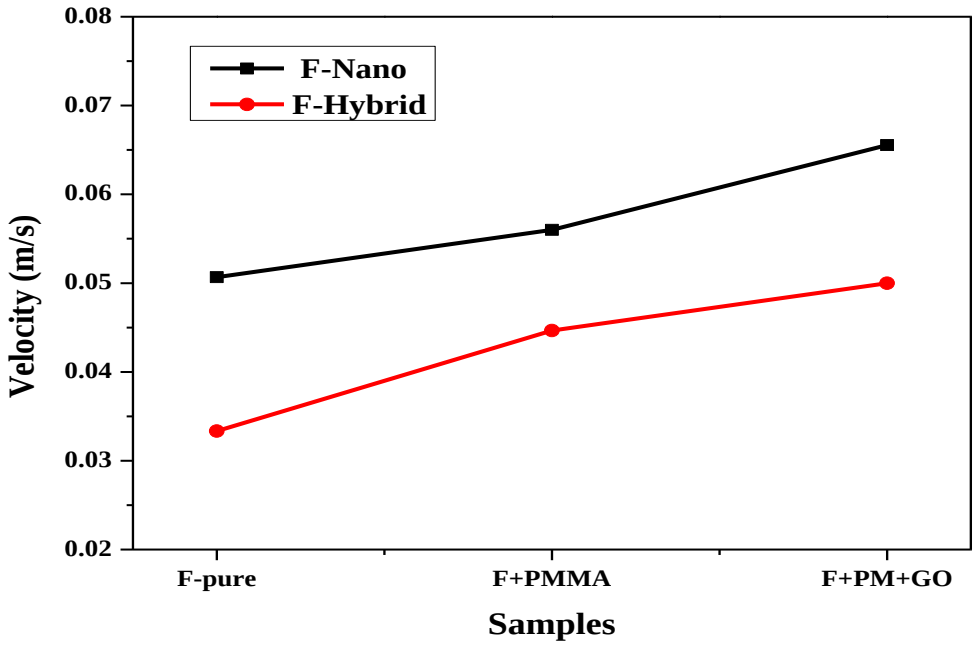


**Figure (4-6). The ultrasound velocity for dental filling and their sample.**

### 4.4.2 The Absorption Coefficient

In Figure (4-7), the ultrasonic absorption coefficient values of all samples were measured by equation (4). Comparing the results for dental filling with the samples containing polymer and GO, it was noted the absorption coefficient increased with the addition of PMMA, meanwhile, it was significantly increased with the incorporation of GO nanosheets. Interestingly, the absorption coefficient of N1 was higher than that of H1. The addition of PMMA in both fillers resulted in an improvement up to 77 % and 200 % for N2 and H2 and following the contribution of GO nanosheets exhibited an excellent enhancement up to 166 % and 325% for both nanocomposites N3, and H3 respectively, compared to their dental filling N1, H1. However, the findings revealed that N3 dental nanocomposites outperformed up to 41% more than H3 dental nanocomposites. Where the absorption coefficient is mostly determined by the content of the additional materials in the dental filler matrix and also

the adjustment of either the structure relaxation that takes place between the molecules of dental filler in the matrix of the dental. The particles and the medium that surrounds them engage in a process of heat exchange and friction, which leads to the attenuation, in addition to the fine dispersion of the GO nanosheets assist in this improvement of the ultrasonic absorption coefficient result [134]. In the fact that ultrasound travels through a medium in the form of compression and dissociation, this location results in a growth in the viscosity of the solution. As a direct consequence of this, the polymer chains that are present in the solution now have a bigger degree of adaptability as a direct outcome of the addition of GO Other researchers' findings are consistent with these results [12,134].

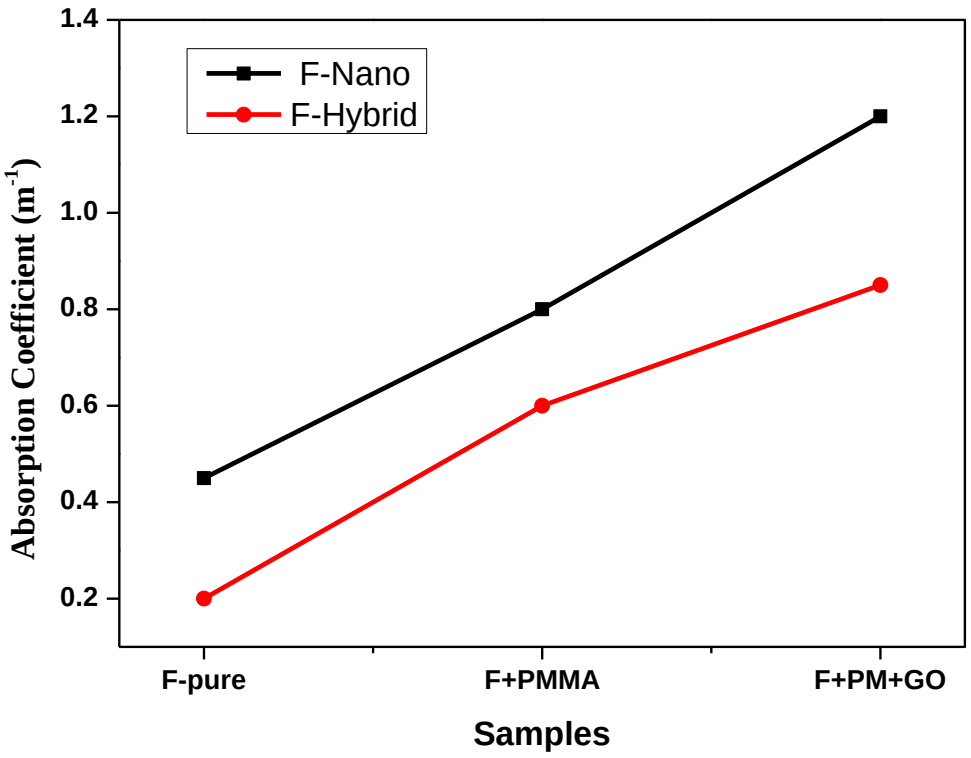


**Figure (4-7). The ultrasound absorption coefficient for dental filling and their samples.**

### 4.4.3 Relaxation Time

Figure (4-8) depicts the relaxation time of N1, N2, N3, H1, H2, and H3 calculated from equation (8). The relaxing time of the F-Nano was lower than that of the F-Hybrid, these results were reduced after the addition of PMMA. Additionally, loading the GO nanosheets presented a significant reduction in the relaxation time of nanocomposites compared with their dental filling pure. This reduction in the results related to the restriction of bonded the PMMA and GO functional group with fillers that resulted in more restricted the molecules of the samples than their original fillers. Also, N2 and N3 performed more restricted than H2 and H3. Because of the disruptions and impacts caused by the addition of the PMMA polymer, the internal friction that exists between the layers became greater as the length of the dental filling chains became greater. This effect was exacerbated by the addition loading ratio of GO As a result, the time required to restore a molecule to its former state rises [137].

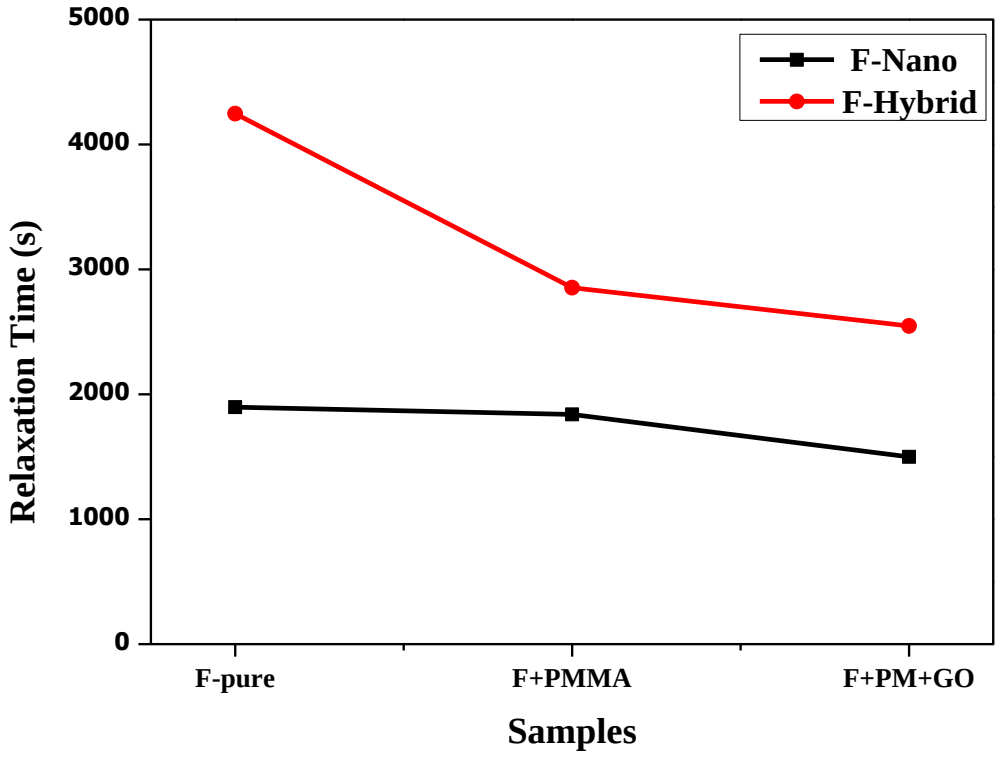


**Figure (4-8). The Relaxation time for dental filling and their samples.**

### 4.4.4 Compressibility

Figure (4-9) depicts the compressibility of a dental filling with polymer and nanocomposites that was calculated from equation (5). The nano-fillers (N1) revealed better resistance compressibility than hybrid-filler (H1). The compressibility results showed a significant effect of the additions of PMMA and GO on the reduction of the ability of the sample to compress. That was reduced up to 15% for N2 and 33% for N3 for nano-fillers nanocomposites respectively, compared with N1, whereas it was reduced up to 29% for H2 and 41% for H3 respectively, compared to H1 nanocomposites. In general, the results showed that the nano filling and their nanocomposites have a better ability to resist compressibility than the hybrid filling and their nanocomposites. The reason for the decrease the compressibility is the properties of the polymer and the bonding strength between molecules and the interfacial spaces, as well as the properties of nanosheets, whose strength reaches 130 MPa and durability up to one terminal and is characterized by having functional groups that help to form bonds with hydrogen, which increases the bonding between the fillings, the polymer, and the nanomaterials, and then helps in distributing the pressure of the loads, and thus the compressibility of the materials decreases. This is in line with the researcher's findings [138].

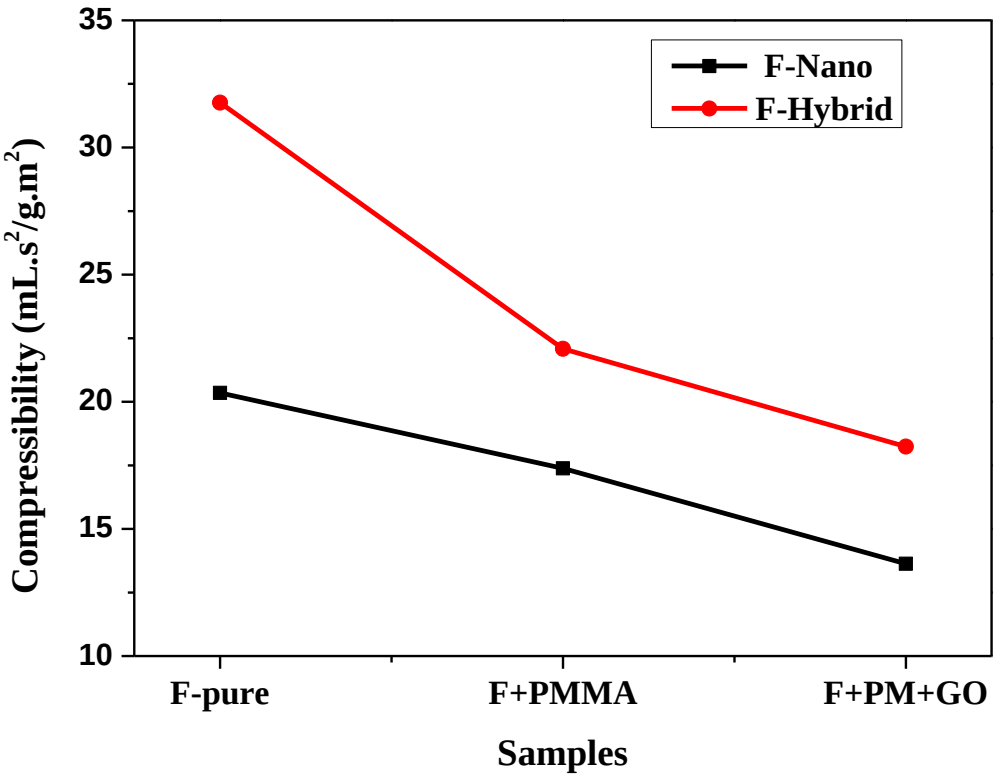


**Figure (4-9). The compressibility of dental filling and their samples.**

### 4.4.5 Bulk Modulus

Figure (4-10) shows the changes in behviour of the bulk modulus of dental fillings with the addition of PMMA and GO nanosheets. The results of the F-Nano presented better results than the F-Hybrid. Additionally, the N2 results showed increasing the elastic modulus value after adding the polymer up to 29% and the ratio significantly enhanced up to 93% with the contribution of GO into N3. Whereas, the elastic modulus of H2 increased by 92% when PMMA was added, whereas it was notable improved up to 160% of the H3 compared with H1. The nanofillers nanocomposites N3 showed better results up to 80% than hybrid-filler nanocomposites H3. This improvement related to the unique mechanical properties of graphene oxide, which has a strength nanosheets with 1 TPa, was inversely proportional to the elasticity modulus of fillers by the formulation of strong

interaction by hydrogen boned among fillers, PMMA, and GO in agreement with another finding[139].

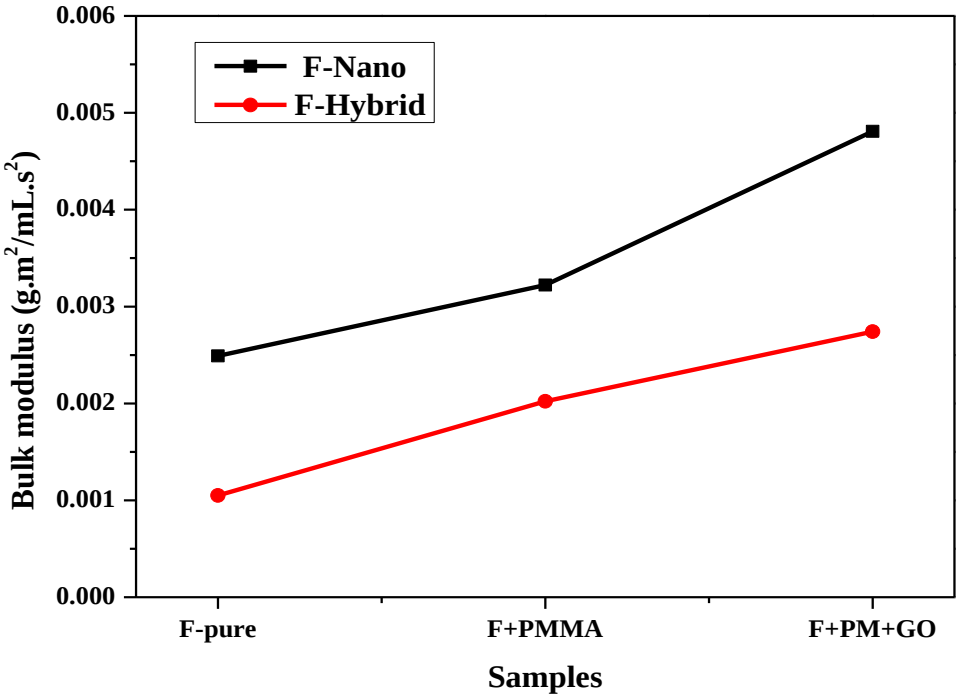


**Figure (4-10). The bulk modulus for dental filling and their samples.**

### 4.4.6 The Specific Acoustic Impedance

Figure (4-11) depicts the acoustic impedance for nano and hybrid filler before and after being reinforced with polymer and GO nanosheets. Figure (4-11) shows the greatest results for the N1 compared with H1 results that significantly improved after being reinforced with polymer and GO The acoustic impedance increased by 17.7 % for N2, and 50 % for N3, whereas it was improved up to 43% for H2 and 70% for H3, due to the contribution of PMMA and GO nanosheets, respectively. Generally, nanofillers nanocomposites N3 showed better results up to 35% than hybrid-filler nanocomposites H3. The acoustic impedance (Z) of nanocomposites is calculated by multiplying the density of the material with its acoustic velocity. The measurement of acoustic transmission and reflection at the

interface interaction between two materials with contrasting acoustic impedances, as shown in equation (9). This behavior is comparable and agreed with the researcher's finding [140].

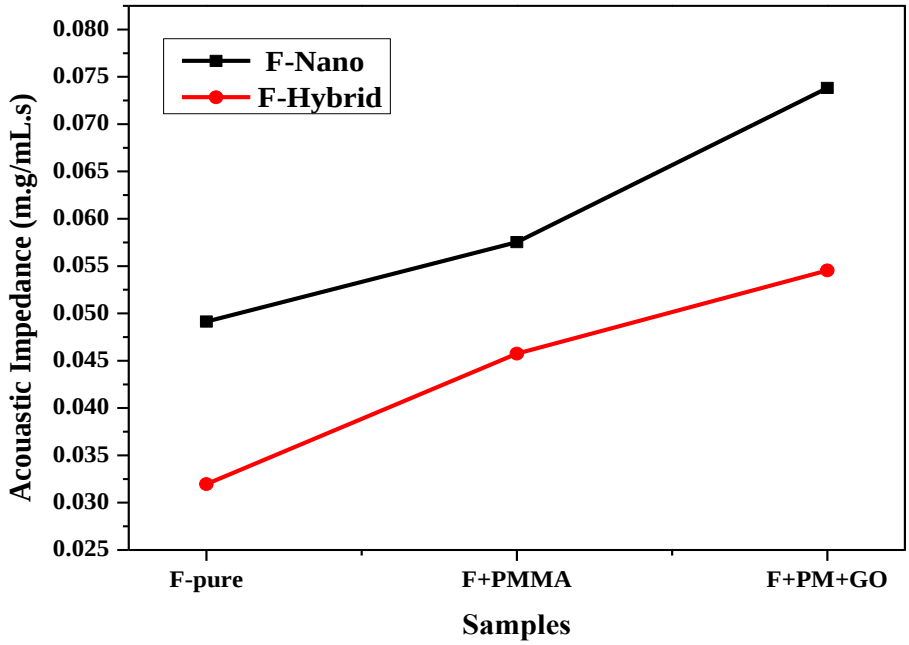


**Figure (4-11). The acoustic impedance for dental filling and their samples.**

### 4.4.7 Relaxation Amplitude

Figure (4-12) demonstrates increasing the load ratios of polymers and nanosheets resulted in an improvement in the relaxation amplitude. According to the findings, N1 dental had a higher relaxation amplitude up to 55% than H1, and the results were significantly improved after the loaded of PMMA up to 77% for N2 and 166% when GO was added to the N3 in compassion with N1, whereas H2 improved up to 250% after the PMMA was loaded, then significantly enhanced up to 375 % of H3 compared to their dental filling H1. However, N3 showed higher relaxation amplitude results up to 25% than H3. For this reason, the moment of inertia of the bigger filling molecules is lowered, causing the excited particles to

be displaced until they become tiny [141]. The relaxation amplitude behaved in the same way as the absorption coefficient at a constant frequency, as the absorption coefficient increased, so did the relaxation amplitude.

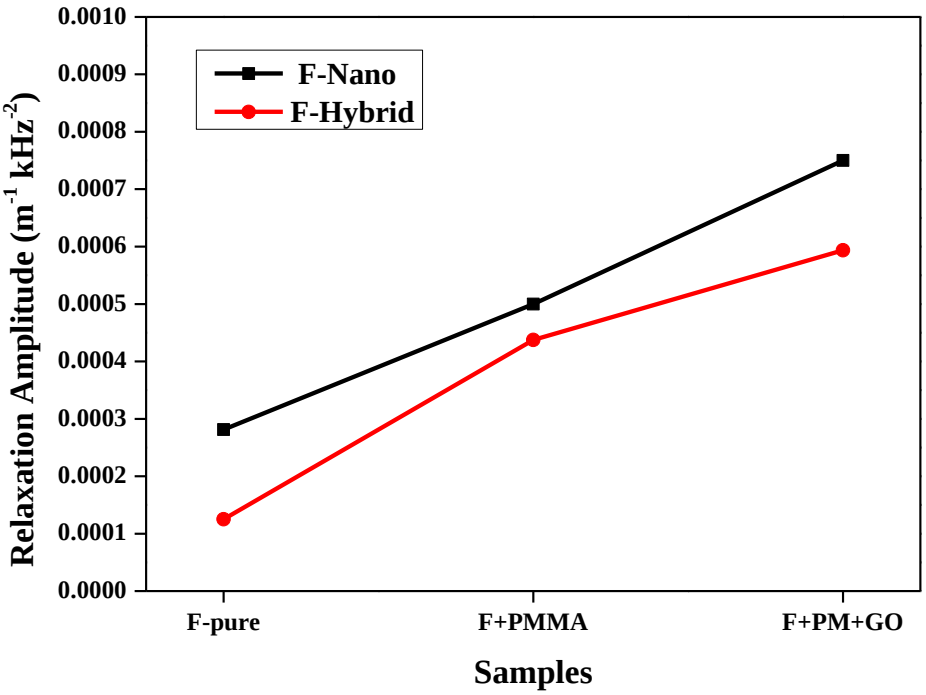


**Figure (4-12). The Relaxation Amplitude for dental filling and their samples.**

## 4.5 The biological properties

### 4.5.1 Antibacterial Activity

The chemical molecule that can destroy harmful germs is what it means by the term "antimicrobial agent [86]. Filler particles in resin composite materials can be modified to include an antibacterial component [87]or the resin mixture [88].

In Figure (4-13), the result showed the effectiveness of samples against E. faecalis and E. Staph bacterial. The nano dental filling (N1) showed resistance to bacteria with a zone of inhibition of 21 mm diameter against Enterococcus faecalis and 11.5 mm against E. Staph, whereas it slightly increased up to 22 and 14 mm respectively, after the addition of PMMA in N2. The contribution of GO in N3 produced significant improvement in the zone of inhibition of the E. faecalis bacteria with a diameter of 25 mm, meanwhile, it was 16.8 mm against E.Staph, as shown in Table 4.

The hybrid dental filling (H1) showed resistance to bacteria and the zone of inhibition diameter was revealed 13.5 mm against the E. Faecalis and 13.8 mm against the E. Staph. The lading of PMMA in H2 produced improving in the zone of inhibition diameter from 13.5 mm to 16 mm against E. Faecalis and from 13.8 mm to 15.3 mm against E. Staph. Whereas, the GO exhibited effectiveness of H3 compared with H1 that significantly improved the zone of inhibition with a diameter of approximately up to 18.5 mm against E. Faecalis and 16.4 mm against E.staph as exposed in Table 4.

Where the nano/hybrid dental fillings have resistance to bacteria. When the polymer was added, there was a slight increase in this resistance, but when nanosheets (GO) were added, there was a clear increase in the killing area.

The fact that cell trapping could be an additional possible mechanism for the antimicrobial activities of GO Upon coming into touch with the bacterial cells, the GO sheets may become able to entrap them. GO able to kill the imprisoned bacteria will get cut off beginning the exterior microenvironment, and their availability of nutrition elements would be limited which will prevent their growth. In this context, the size of the GO may have a considerable effect on cell encapsulation [99]. Additionally, it is reasonable to believe that GO nanosheets can kill bacteria by entrapping them and cutting them with their edges [25].

The SEM images show the cavities in N1 and H1 that assist to grow the bacteria, which produce acid and dissolve the hard parts of the teeth cementum, dentin, and enamel and caused the tooth decay [82]. Moreover, the food or sugar listed on the tooth's surface is associated with to growth of these bacteria to generate acid [83]. Whereas, according to the SEM in N2, N3, H2, and H3, these cavities in samples were filled and inhibited by PMMA and GO which strongly impact the growth of the bacterial and reduced their activity, which strongly the interaction presented in the FTIR and these results support the antibacterial findings.

Generally, nanofillers dental samples showed a better ability to kill the bacteria and a bigger zone of inhibition diameter of antibacterial, whereas N3 showed a better result in the zone of inhibition diameter of both bacteria compared with all samples.

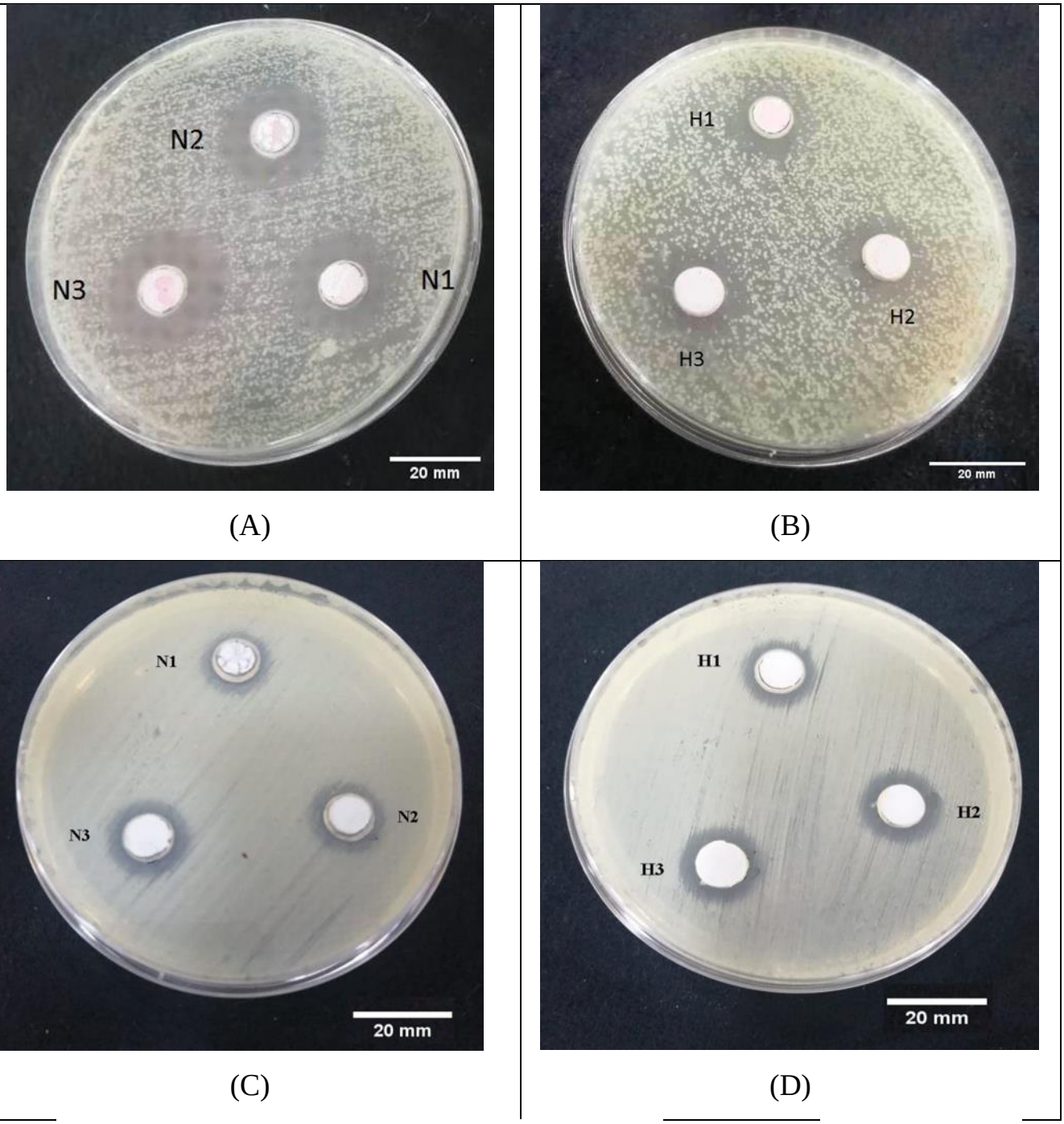


**Figure (4-13). In Vitro-antibacterial activity of dental filler samples against (A and B) Enterococcus faecalis and (C and D) E. Staph.**

**Table (4-4). zone of inhibition diameter of antibacterial generated dental filler samples.**

| Bacterial Isolates | Enterococcus faecalis | E.staph |
|---|---|---|
| Samples ID | Area(mm) | Area(mm) |
| N1 | 21 | 11.5 |
| N2 | 22 | 14 |
| N3 | 25 | 16.8 |
| H1 | 13.5 | 13.8 |
| H2 | 16 | 15.3 |
| H3 | 18.5 | 16.4 |

### 4.6 Conclusions

In this thesis,

1. The method was successfully prepared for the nano/hybrid filling-PMMA/GO dental nanocomposite fillers.
2. The FTIR demonstrated the distinctions between the functional groups of each component. Also, FTIR shows a strong impact and good interfacial interaction between the fillers and the reinforcement materials (PMMA and GO nanosheets).
3. The XRD showed a change in the crystalline behavior of fillers as the impact of both PMMA and GO
4. The optical microscopy images revealed a homogeneous sample and a fine dispersion of GO, which provided improvements in the morphology properties as significantly confirmed by SEM images.
5. The results showed the important impact of PMMA and GO nanosheets on the density, viscosity, and mechanical properties of nano and hybrid-dental nanocomposite fillers compared with the original fillers.
6. This is evident in the bulk ultrasound velocity values of 93% for the nano filling and 160% for the hybrid filling, modulus, the ultrasound absorption coefficient enhancement up to 166% and 325% for both nanocomposites N3 and H3, and others, where their values increased with the addition of PMMA and increased even more when GO was added to the filler matrix.
7. Generally, nanofillers presented better results than hybrid fillers.
8. These results bring significant attention to promising new modified fillers in this study that could be cheap, and stronger with the longest lifetime than the original fillers, which could be easily used and changed in the future.

9. Generally, nanofillers dental samples showed a better ability to kill the bacteria, where N3 the zone of inhibition diameter increased 25% from 21 to 25 mm of Enterococcus faecalis and 46% from 11.5 to 16.5 mm of E. Staph.

## 4.7 Future Work

1. Study the optical properties of prepared dental filling after reinforced with PMMA and GO nanosheets.
2. Explored ageing and the thermal properties of prepared dental filling after reinforced with PMMA and GO nanosheets.
3. Examined the effect of other of several different polymers on the structure, morphology and properties of dental fillers properties.
4. Discovered the effect of different loading ratios of GO nanosheets on the structure and properties of dental fillers.
5. Considered different graphene derivatives such as RGO to prepare the dental filling with other polymers or resin.
6. Investigated the effect of GO nanosheets on other properties grow moth bacteria activity.
7. Investigated the impact of light curing on the mechanical and thermal properties of dental filler.

# Reference

# ***Reference***

## The Reference


[1] Z. Ge, L. Yang, F. Xiao, Y. Wu, T. Yu, J. Chen, J. Lin, Y. Zhang, Graphene Family Nanomaterials: Properties and Potential Applications in Dentistry, Int. J. Biomater. 2018 (2018). https://doi.org/10.1155/2018/1539678.

[2] M. Atai, M. Nekoomanesh, S.A. Hashemi, S. Amani, Physical and mechanical properties of an experimental dental composite based on a new monomer, (2004) 663–668. https://doi.org/10.1016/j.dental.2003.08.008.

[3] V. Miletic, Dental Composite Materials for Direct Restorations, Springer International Publishing, Cham, 2018. https://doi.org/10.1007/978-3-319-60961-4.

[4] K.R. St. John, Biocompatibility of Dental Materials, Dent. Clin. North Am. 51 (2007) 747–760. https://doi.org/10.1016/j.cden.2007.03.003.

[5] M.F. Şuhani, G. Băciuţ, M. Băciuţ, R. Şuhani, S. Bran, Current perspectives regarding the application and incorporation of silver nanoparticles into dental biomaterials, Clujul Med. 0 (2018) 274–279. https://doi.org/10.15386/cjmed-935.

[6] Z. Yingchao, G. Haihuan, F. Dan, F. Tengjiaozi, C. Danfeng, S. Zuosen, Z. Song, C. Zhanchen, New strategy for overcoming microleakage: An elastic layer for dental caries restoration, J. Mater. Chem. B. 3 (2015) 4401–4405. https://doi.org/10.1039/C5TB00432B.

[7] X. Xu, L. He, B. Zhu, J. Li, J. Li, Advances in polymeric materials for dental applications, Polym. Chem. 8 (2017) 807–823. https://doi.org/10.1039/C6PY01957A.

[8] A.R. Torabi, S. Shahbaz, S. Cicero, M.R. Ayatollahi, Fracture testing and estimation of critical loads in a PMMA-based dental material

# ***Reference***

with nonlinear behavior in the presence of notches, Theor. Appl. Fract. Mech. 118 (2022) 103282. https://doi.org/10.1016/J.TAFMEC.2022.103282.

[9] K.D. Jandt, D.C. Watts, Nanotechnology in dentistry: Present and future perspectives on dental nanomaterials, Dent. Mater. 36 (2020) 1365–1378. https://doi.org/10.1016/J.DENTAL.2020.08.006.

[10] G.C. Padovani, V.P. Feitosa, S. Sauro, F.R. Tay, G. Durán, A.J. Paula, N. Durán, Advances in Dental Materials through Nanotechnology: Facts, Perspectives and Toxicological Aspects, Trends Biotechnol. 33 (2015) 621–636. https://doi.org/10.1016/j.tibtech.2015.09.005.

[11] M.I. Katsnelson, K.S. Novoselov, Graphene: New bridge between condensed matter physics and quantum electrodynamics, Solid State Commun. 143 (2007) 3–13. https://doi.org/10.1016/J.SSC.2007.02.043.

[12] A.I. Abdelamir, E. Al-Bermany, F.S. Hashim, Important factors affecting the microstructure and mechanical properties of PEG/GO-based nanographene composites fabricated applying assembly-acoustic method, in: AIP Conf. Proc., 2020: p. 020110. https://doi.org/10.1063/5.0000175.

[13] A. Radhi, D. Mohamad, F.S. Abdul Rahman, A.M. Abdullah, H. Hasan, Mechanism and factors influence of graphene-based nanomaterials antimicrobial activities and application in dentistry, J. Mater. Res. Technol. 11 (2021) 1290–1307. https://doi.org/10.1016/J.JMRT.2021.01.093.

[14] S. Liu, T.H. Zeng, M. Hofmann, E. Burcombe, J. Wei, R. Jiang, J. Kong, Y. Chen, Antibacterial activity of graphite, graphite oxide, graphene oxide, and reduced graphene oxide: Membrane and oxidative stress, ACS Nano. 5 (2011) 6971–6980.

# ***Reference***

https://doi.org/10.1021/nn202451x.

[15] D. Olteanu, A. Filip, C. Socaci, A.R. Biris, X. Filip, M. Coros, M.C. Rosu, F. Pogacean, C. Alb, I. Baldea, P. Bolfa, S. Pruneanu, Cytotoxicity assessment of graphene-based nanomaterials on human dental follicle stem cells, Colloids Surfaces B Biointerfaces. 136 (2015) 791–798. https://doi.org/10.1016/j.colsurfb.2015.10.023.

[16] R. Elashnikov, O. Lyutakov, P. Ulbrich, V. Svorcik, Light-activated polymethylmethacrylate nanofibers with antibacterial activity, Mater. Sci. Eng. C. 64 (2016) 229–235. https://doi.org/10.1016/j.msec.2016.03.047.

[17] J. Wen, F. Jiang, C.-K. Yeh, Y. Sun, Controlling fungal biofilms with functional drug delivery denture biomaterials, Colloids Surfaces B Biointerfaces. 140 (2016) 19–27. https://doi.org/10.1016/j.colsurfb.2015.12.028.

[18] R. Srivastava, J. Wolska, J. Walkowiak-Kulikowska, H. Koroniak, Y. Sun, Fluorinated bis-GMA as potential monomers for dental restorative composite materials, Eur. Polym. J. 90 (2017) 334–343. https://doi.org/10.1016/j.eurpolymj.2017.03.027.

[19] H. Xie, T. Cao, F.J. Rodríguez-Lozano, E.K. Luong-Van, V. Rosa, Graphene for the development of the next-generation of biocomposites for dental and medical applications, Dent. Mater. 33 (2017) 765–774. https://doi.org/10.1016/j.dental.2017.04.008.

[20] A.O. Alhareb, H.M. Akil, Z.A. Ahmad, Impact strength, fracture toughness and hardness improvement of PMMA denture base through addition of nitrile rubber/ceramic fillers, Saudi J. Dent. Res. 8 (2017) 26–34. https://doi.org/10.1016/j.sjdr.2016.04.004.

[21] S. Malik, F.M. Ruddock, A.H. Dowling, K. Byrne, W. Schmitt, I. Khalakhan, Y. Nemoto, H. Guo, L.K. Shrestha, K. Ariga, J.P. Hill, Graphene composites with dental and biomedical applicability,

# ***Reference***

Beilstein J. Nanotechnol. 9 (2018) 801–808. https://doi.org/10.3762/bjnano.9.73.

[22] M. Tahriri, M. Del Monico, A. Moghanian, M. Tavakkoli Yaraki, R. Torres, A. Yadegari, L. Tayebi, Graphene and its derivatives: Opportunities and challenges in dentistry, Mater. Sci. Eng. C. 102 (2019) 171–185. https://doi.org/10.1016/j.msec.2019.04.051.

[23] C. Bacali, I. Baldea, M. Moldovan, R. Carpa, D.E. Olteanu, G.A. Filip, V. Nastase, L. Lascu, M. Badea, M. Constantiniuc, F. Badea, Flexural strength, biocompatibility, and antimicrobial activity of a polymethyl methacrylate denture resin enhanced with graphene and silver nanoparticles, Clin. Oral Investig. 24 (2020) 2713–2725. https://doi.org/10.1007/s00784-019-03133-2.

[24] K. Ioannidis, S. Niazi, P. Mylonas, F. Mannocci, S. Deb, The synthesis of nano silver-graphene oxide system and its efficacy against endodontic biofilms using a novel tooth model, Dent. Mater. 35 (2019) 1614–1629. https://doi.org/10.1016/j.dental.2019.08.105.

[25] M.T.H. Aunkor, T. Raihan, S.H. Prodhan, H.S.C. Metselaar, S.U.F. Malik, A.K. Azad, Antibacterial activity of graphene oxide nanosheet against multidrug resistant superbugs isolated from infected patients, R. Soc. Open Sci. 7 (2020) 200640. https://doi.org/10.1098/rsos.200640.

[26] D. Ali Hameed, N. Ameer, Nano Silica and Nano Graphene Used in Dental Fillers: The Relation Between the Mechanical and Topography Properties, Res. J. Med. Sci. 14 (2020) 20–25. https://doi.org/10.36478/rjmsci.2020.20.25.

[27] C. Bacali, R. Carpa, S. Buduru, M.L. Moldovan, I. Baldea, A. Constantin, M. Moldovan, D. Prodan, L.M. Dascalu (Rusu), O. Lucaciu, F. Catoi, M. Constantiniuc, M. Badea, Association of Graphene Silver Polymethyl Methacrylate (PMMA) with

# ***Reference***

Photodynamic Therapy for Inactivation of Halitosis Responsible Bacteria in Denture Wearers, Nanomaterials. 11 (2021) 1643. https://doi.org/10.3390/nano11071643.

[28] P.R. Lloret, K.M. Rode, M.L. Turbino, Dentine bond strength of a composite resin polymerized with conventional light and argon laser, Braz. Oral Res. 18 (2004) 271–275. https://doi.org/10.1590/S1806-83242004000300017.

[29] A. Lindberg, Resin composites: sandwich restorations and curing techniques, (2005). https://doi.org/https://www.diva-portal.org/smash/record.jsf?pid=diva2%3A143655.

[30] N. Kramer, U. Lohbauer, F. Garcia-Godoy, R. Frankenberger, Light curing of resin-based composites in the LED era., Am. J. Dent. 21 (2008) 135. https://europepmc.org/article/med/18686762.

[31] R. Van Noort, M. Barbour, Introduction to Dental Materials-E-Book, Elsevier Health Sciences, 2014.

[32] N.A. Salih, Comparing Between Two Lights Curing of Dental Restorative (Laser and Halogen) by Using Physical Parameters, (n.d.). Comparing Between Two Lights Curing of Dental Restorative (Laser and Halogen) by Using Physical Parameters.

[33] A. Hervás García, M. Lozano, J. Cabanes Vila, A. Barjau Escribano, P. Fos Galve, Composite resins: a review of the materials and clinical indications, (2006). http://hdl.handle.net/10550/63556.

[34] H.M. Ridha, The effect of using variable curing light types and intensities on the parameters of a mathematical model that predicts the depth of cure of light-activated dental composites, (2009). https://doi.org/http://dx.doi.org/10.7912/C2/1566.

[35] M.S. Spiller, Dental composites: a comprehensive review, Acad. Dent. Learn. OSHA Training, LLC. 23 (2012) 1–36. https://dentallearning.org/course/Composites/Dental_Composites.pdf.

# ***Reference***


[36] S.J. Marshall, G.W. Marshall, Dental Amalgam: the Materials, Adv. Dent. Res. 6 (1992) 94–99. https://doi.org/10.1177/08959374920060012401.

[37] D. Taifour, J.E. Frencken, N. Beiruti, M.A. van ‘t Hof, G.J. Truin, Effectiveness of Glass-Ionomer (ART) and Amalgam Restorations in the Deciduous Dentition: Results after 3 Years, Caries Res. 36 (2002) 437–444. https://doi.org/10.1159/000066531.

[38] N. Thongbai-on, D. Banomyong, Flexural strengths and porosities of coated or uncoated, high powder-liquid and resin-modified glass ionomer cements, J. Dent. Sci. 15 (2020) 433–436. https://doi.org/10.1016/j.jds.2020.02.004.

[39] J.A. Donaldson, The use of gold in dentistry, Gold Bull. 13 (1980) 117–124. https://doi.org/10.1007/BF03216551.

[40] B. Henriques, D. Soares, F.S. Silva, Microstructure, hardness, corrosion resistance and porcelain shear bond strength comparison between cast and hot pressed CoCrMo alloy for metal–ceramic dental restorations, J. Mech. Behav. Biomed. Mater. 12 (2012) 83–92. https://doi.org/10.1016/j.jmbbm.2012.03.015.

[41] N. Akbarianrad, F. Mohammadian, M. Alhuyi Nazari, B. Rahbani Nobar, Applications of nanotechnology in endodontic: A Review, Nanomedicine J. 5 (2018) 121–126. https://doi.org/10.22038/NMJ.2018.005.0001.

[42] E.G. Mota, K. Subramani, Nanotechnology in operative dentistry: A perspective approach of history, mechanical behavior, and clinical application, Emerg. Nanotechnologies Dent. Second Ed. (2018) 59–82. https://doi.org/10.1016/B978-0-12-812291-4.00004-2.

[43] B. Bhushan, Introduction to Nanotechnology, in: Springer Handb. Nanotechnol., Springer, 2017: pp. 1–19. https://doi.org/10.1007/978-3-662-54357-3_1.

# ***Reference***


[44] A. Nasir, Nanodermatology: a glimpse of caution just beyond the horizon–part II, Ski. Ther. Lett. 15 (2010). https://europepmc.org/article/med/20945053.

[45] A. Roguska, M. Pisarek, M. Andrzejczuk, M. Lewandowska, Synthesis and characterization of ZnO and Ag nanoparticle-loaded TiO2 nanotube composite layers intended for antibacterial coatings, Thin Solid Films. 553 (2014) 173–178. https://doi.org/10.1016/j.tsf.2013.11.057.

[46] S.S. Sasalawad, N.N. Sathyajith, K.K. Shashibhushan, P. Poornima, S.M. Hugar, N.M. Roshan, "Nanodentistry"-The Next Big Thing Is Small, Int. J. Contemp. Dent. Med. Rev. 2014 (2014). https://core.ac.uk/download/pdf/228420975.pdf.

[47] G.C. Padovani, V.P. Feitosa, S. Sauro, F.R. Tay, G. Durán, A.J. Paula, N. Durán, Advances in Dental Materials through Nanotechnology: Facts, Perspectives and Toxicological Aspects, Trends Biotechnol. 33 (2015) 621–636. https://doi.org/10.1016/J.TIBTECH.2015.09.005.

[48] L. Kashinath, R. Senthil Kumar, Y. Hayakawa, G. Ravi, Synthesis &Structural Study on Graphene Nano Particles, Int. J. Sci. Eng. Appl. 7560 (2013) 8–12. https://doi.org/10.7753/ijseancrtam.1003.

[49] R.J. Young, M. Liu, I.A. Kinloch, S. Li, X. Zhao, C. Vallés, D.G. Papageorgiou, The mechanics of reinforcement of polymers by graphene nanoplatelets, Compos. Sci. Technol. 154 (2018) 110–116. https://doi.org/10.1016/j.compscitech.2017.11.007.

[50] Q. Wu, D. jian Xie, Y. du Zhang, Z. min Jia, H. zhao Zhang, Mechanical properties and simulation of nanographene/polyvinylidene fluoride composite films, Compos. Part B Eng. 156 (2019) 148–155. https://doi.org/10.1016/j.compositesb.2018.08.061.

# ***Reference***


[51] D. Olteanu, A. Filip, C. Socaci, A.R. Biris, X. Filip, M. Coros, M.C. Rosu, F. Pogacean, C. Alb, I. Baldea, P. Bolfa, S. Pruneanu, Cytotoxicity assessment of graphene-based nanomaterials on human dental follicle stem cells, Colloids Surfaces B Biointerfaces. 136 (2015) 791–798. https://doi.org/10.1016/j.colsurfb.2015.10.023.

[52] N. Dubey, S.S. Rajan, Y.D. Bello, K.S. Min, V. Rosa, Graphene nanosheets to improve physico-mechanical properties of bioactive calcium silicate cements, Materials (Basel). 10 (2017) 1–12. https://doi.org/10.3390/ma10060606.

[53] N.V. Tarasenko, A.V. Butsen, E.A. Nevar, Laser-induced modification of metal nanoparticles formed by laser ablation technique in liquids, Appl. Surf. Sci. 247 (2005) 418–422. https://doi.org/10.1016/j.apsusc.2005.01.093.

[54] D. Dorranian, Z. Abedini, A. Hojabri, M. Ghoranneviss, Effects of Oxygen RF Plasma on Properties of Poly Methyl Methacrylate Polymer, Iran. Phys. J. 2 (2008) 17–21. https://www.sid.ir/FileServer/JE/134220080104.

[55] A. Castañeda-Ovando, M. de L. Pacheco-Hernández, M.E. Páez-Hernández, J.A. Rodríguez, C.A. Galán-Vidal, Chemical studies of anthocyanins: A review, Food Chem. 113 (2009) 859–871. https://doi.org/10.1016/j.foodchem.2008.09.001.

[56] J.H. Nahida, Spectrophotometric analysis for the UV-irradiated (PMMA), Int. J. Basic Appl. Sci. 12 (2012) 58–67.

[57] J.H. Lee, J.K. Jo, D.A. Kim, K.D. Patel, H.W. Kim, H.H. Lee, Nano-graphene oxide incorporated into PMMA resin to prevent microbial adhesion, Dent. Mater. 34 (2018) e63–e72. https://doi.org/10.1016/j.dental.2018.01.019.

[58] F.W. Billmeyer, F.W. Billmeyer, Textbook of polymer science, Wiley New York, 1984.

# ***Reference***


[59] X.L. Ji, J.K. Jing, W. Jiang, B.Z. Jiang, Tensile modulus of polymer nanocomposites, Polym. Eng. Sci. 42 (2002) 983–993. https://doi.org/10.1002/pen.11007.

[60] R.M. Jones, Mechanics of composite materials, CRC press, 1998.

[61] T. BritanniAca, Editors of Encyclopaedia, Argon. Encycl. Br. (2020).

[62] H. Baharvand, M.E. Zeynali, A. Rabii, H. Baharvand, Synthesis of partially hydrolyzed polyacrylamide and investigation of solution properties (Viscosity Behaviour), Iran. Polym. J. 13 (2004) 479–484. https://www.sid.ir/en/Journal/ViewPaper.aspx?ID=12672.

[63] A. Białous, M. Gazda, G. Śliwiński, Structure and optical properties of TiO2 thin films prepared by pulsed laser deposition, 8770 (2015) 877008. https://doi.org/10.1117/12.2013426.

[64] A.S. Dukhin, P.J. Goetz, New developments in acoustic and electroacoustic spectroscopy for characterizing concentrated dispersions, Colloids Surfaces A Physicochem. Eng. Asp. 192 (2001) 267–306. https://doi.org/10.1016/S0927-7757(01)00730-0.

[65] W.R. Hendee, E.R. Ritenour, Medical Imaging Physics, Fourth, 2002. https://doi.org/10.1118/1.1563664.

[66] P.A.A. Mahaboob, , " Ultrasonic Studies On Molecular Interactions In Certain Binary And Ternary Systems", Ph.D. Thesis, University of Madras., (2006).

[67] R. William, Medical Imaging Physics, (2002).

[68] D. Gasni, Ultrasonic Reflection for Measurement of Oil Film Thickness and Contact between Dissimilar Materials, (2012).

[69] T. Hornowski, A. Józefczak, A. Skumiel, M. Łabowski, Effect of Poly(Ethylene Glycol) Coating on the Acoustic Properties of Biocompatible Magnetic Fluid, Int. J. Thermophys. 31 (2010) 70–76. https://doi.org/10.1007/s10765-009-0619-x.

[70] A.K.J. Al-Bermany, A Study of the Physical Properties of some

# ***Reference***

Cellulose Derivative Polymers, Al-Mustansiryah Univ. Ph. D. Thesis. (1995).

[71] R. Martinez, L. Leija, A. Vera, Ultrasonic attenuation in pure water: Comparison between through-transmission and pulse-echo techniques, in: 2010 Pan Am. Heal. Care Exch., IEEE, 2010: pp. 81–84. https://doi.org/10.1109/PAHCE.2010.5474593.

[72] D. Ubagaramary, P. Neeraja, Ultrasonic study of molecular interaction in Binary liquid mixture at 308 K, J. Appl. Chem. 2 (2012) 1–19.

[73] P. Paul Divakar, B. V. Rao, K. Samatha, Study of molecular interactions in binary liquid mixtures by acoustical method at 303K, E-Journal Chem. 9 (2012) 1332–1335. https://doi.org/10.1155/2012/681241.

[74] J.H. Ibrahim, Effect Of Pbo On The Some Physical Properties Of Compounding Rubber, 4 (2013) 58–65. http://www.savap.org.pk/journals/ARInt./Vol.4(2)/2013(4.2-05).pdf.

[75] G.J. Moridis, D.A. McVay, D.L. Reddell, T.A. Blasingame, The Laplace Transform Finite Difference (LTFD) Numerical Method for the Simulation of Compressible Liquid Flow in Reservoirs, SPE Adv. Technol. Ser. 2 (1994) 122–131. https://doi.org/10.2118/22888-PA.

[76] A. - Kareem Al - Bermany, B. Yahya Kadem, R. Mizher Obiad, L.F. Nasser, A. Kareem Al - Bermany, B. Yahya Kadem, R. Mizher Obiad, L.F. Nasser, Study of some mechanical and rheological properties of PVA / FeCl 3 by ultrasonic, Int. J. Adv. Sci. Tech. Res. Issue 1. 2 (2011) 222–231.

[77] I. Lawson, K.A. Danso, H.C. Odoi, C.A. Adjei, F.K. Quashie, I.I. Mumuni, I.S. Ibrahim, Non-destructive evaluation of concrete using ultrasonic pulse velocity, Res. J. Appl. Sci. Eng. Technol. 3 (2011) 499–504.

# ***Reference***


[78] L. Giachetti, D. Scaminaci Russo, C. Bambi, R. Grandini, A review of polymerization shrinkage stress: current techniques for posterior direct resin restorations, J Contemp Dent Pr. 7 (2006) 79–88.

[79] M. Kilian, I.L.C. Chapple, M. Hannig, P.D. Marsh, V. Meuric, A.M.L. Pedersen, M.S. Tonetti, W.G. Wade, E. Zaura, The oral microbiome–an update for oral healthcare professionals, Br. Dent. J. 221 (2016) 657–666.

[80] S.F. Kane, The effects of oral health on systemic health, Gen Dent. 65 (2017) 30–34.

[81] A.R. Yadav, S.K. Mohite, C.S. Magdum, Preparation and evaluation of antibacterial herbal mouthwash against oral pathogens, Asian J. Res. Pharm. Sci. 10 (2020).

[82] K.H. Metwalli, S.A. Khan, B.P. Krom, M.A. Jabra-Rizk, Streptococcus mutans, Candida albicans, and the human mouth: a sticky situation, PLoS Pathog. 9 (2013) e1003616.

[83] M. Nayak, Effect of Modern (Junk) Food in Dental Caries., Indian J. Forensic Med. Toxicol. 14 (2020).

[84] V. Kassardjian, M. Andiappan, N.H.J. Creugers, D. Bartlett, A systematic review of interventions after restoring the occluding surfaces of anterior and posterior teeth that are affected by tooth wear with filled resin composites, J. Dent. 99 (2020) 103388.

[85] N. Beyth, S. Farah, A.J. Domb, E.I. Weiss, Antibacterial dental resin composites, React. Funct. Polym. 75 (2014) 81–88.

[86] E.-R. Kenawy, S.A. Khattab, M.M. Azaam, Synthesis and Antibacterial Activity of Schiff base Compounds Based on Poloxamine, Delta J. Sci. 40 (2019) 69–77.

[87] N.L.S. Vásquez, Control de la placa dental en pacientes con ortodoncia. Una revisión de la literatura, Rev. KIRU. 16 (2019).

[88] W. Zhou, X. Peng, X. Zhou, M.D. Weir, M.A.S. Melo, F.R. Tay, S.

# ***Reference***

Imazato, T.W. Oates, L. Cheng, H.H.K. Xu, In vitro evaluation of composite containing DMAHDM and calcium phosphate nanoparticles on recurrent caries inhibition at bovine enamel-restoration margins, Dent. Mater. 36 (2020) 1343–1355.

[89] S.M.J. Shiadeh, A. Pormohammad, A. Hashemi, P. Lak, Global prevalence of antibiotic resistance in blood-isolated Enterococcus faecalis and Enterococcus faecium: a systematic review and meta-analysis, Infect. Drug Resist. 12 (2019) 2713.

[90] G. Abdurrahmanm, B.M. Bröker, Staphylococcus aureus and Its Proteins, in: Chronic Rhinosinusitis, Springer, 2022: pp. 121–131.

[91] O. Akhavan, E. Ghaderi, Toxicity of Graphene and Graphene Oxide Nanowalls Against Bacteria, ACS Nano. 4 (2010) 5731–5736. https://doi.org/10.1021/nn101390x.

[92] A. Anand, B. Unnikrishnan, S.C. Wei, C.P. Chou, L.Z. Zhang, C.C. Huang, Graphene oxide and carbon dots as broad-spectrum antimicrobial agents-a minireview, Nanoscale Horizons. 4 (2019) 117–137. https://doi.org/10.1039/C8NH00174J.

[93] Y. Tu, M. Lv, P. Xiu, T. Huynh, M. Zhang, M. Castelli, Z. Liu, Q. Huang, C. Fan, H. Fang, R. Zhou, Destructive extraction of phospholipids from Escherichia coli membranes by graphene nanosheets, Nat. Nanotechnol. 8 (2013) 594–601. https://doi.org/10.1038/nnano.2013.125.

[94] S. Gurunathan, J. Woong Han, A. Abdal Daye, V. Eppakayala, J.-H. Kim, Oxidative stress-mediated antibacterial activity of graphene oxide and reduced graphene oxide in Pseudomonas aeruginosa, Int. J. Nanomedicine. 7 (2012) 5901. https://doi.org/10.2147/IJN.S37397.

[95] J. Wang, Y. Wei, X. Shi, H. Gao, Cellular entry of graphene nanosheets: the role of thickness, oxidation and surface adsorption, RSC Adv. 3 (2013) 15776. https://doi.org/10.1039/c3ra40392k.

# ***Reference***


[96] W. Hu, C. Peng, W. Luo, M. Lv, X. Li, D. Li, Q. Huang, C. Fan, Graphene-based antibacterial paper, ACS Nano. 4 (2010) 4317–4323.

[97] X. Wu, S. Tan, Y. Xing, Q. Pu, M. Wu, J.X. Zhao, Graphene Oxide as an Efficient Antimicrobial Nanomaterial for Eradicating Multi-Drug Resistant Bacteria in Vitro and in Vivo, (2017).

[98] J. He, X. Zhu, Z. Qi, C. Wang, X. Mao, C. Zhu, Z. He, M. Li, Z. Tang, Killing dental pathogens using antibacterial graphene oxide, ACS Appl. Mater. Interfaces. 7 (2015) 5605–5611. https://doi.org/10.1021/acsami.5b01069.

[99] S. Liu, M. Hu, T.H. Zeng, R. Wu, R. Jiang, J. Wei, L. Wang, J. Kong, Y. Chen, Lateral Dimension-Dependent Antibacterial Activity of Graphene Oxide Sheets, Langmuir. 28 (2012) 12364–12372. https://doi.org/10.1021/la3023908.

[100] F. Perreault, A.F. de Faria, S. Nejati, M. Elimelech, Antimicrobial Properties of Graphene Oxide Nanosheets: Why Size Matters, ACS Nano. 9 (2015) 7226–7236. https://doi.org/10.1021/acsnano.5b02067.

[101] F. Zou, H. Zhou, D.Y. Jeong, J. Kwon, S.U. Eom, T.J. Park, S.W. Hong, J. Lee, Wrinkled Surface-Mediated Antibacterial Activity of Graphene Oxide Nanosheets, ACS Appl. Mater. Interfaces. 9 (2017) 1343–1351. https://doi.org/10.1021/acsami.6b15085.

[102] Z. Wang, D. Tonderys, S.E. Leggett, E.K. Williams, M.T. Kiani, R. Spitz Steinberg, Y. Qiu, I.Y. Wong, R.H. Hurt, Wrinkled, wavelength-tunable graphene-based surface topographies for directing cell alignment and morphology, Carbon N. Y. 97 (2016) 14–24. https://doi.org/10.1016/j.carbon.2015.03.040.

[103] V. Palmieri, F. Bugli, M.C. Lauriola, M. Cacaci, R. Torelli, G. Ciasca, C. Conti, M. Sanguinetti, M. Papi, M. De Spirito, Bacteria Meet Graphene: Modulation of Graphene Oxide Nanosheet Interaction with Human Pathogens for Effective Antimicrobial

# ***Reference***

Therapy, ACS Biomater. Sci. Eng. 3 (2017) 619–627. https://doi.org/10.1021/acsbiomaterials.6b00812.

[104] F.T. Infrared, A. Ftir, What is FTEM ?, Aust. Orienteer. (2013) 28–29.

[105] S.-N. Wang, F.-D. Zhang, A.-M. Huang, Q. Zhou, Distinction of four Dalbergia species by FTIR, 2nd derivative IR, and 2D-IR spectroscopy of their ethanol-benzene extractives, Holzforschung. 70 (2016) 503–510. https://doi.org/10.1515/hf-2015-0125.

[106] W.S. Lau, Infrared characterization for microelectronics, World scientific, 1999.

[107] K. Zhang, L.L. Zhang, X.S. Zhao, J. Wu, Graphene/Polyaniline Nanofiber Composites as Supercapacitor Electrodes, Chem. Mater. 22 (2010) 1392–1401. https://doi.org/10.1021/cm902876u.

[108] J.D. Wuest, A. Rochefort, Strong adsorption of aminotriazines on graphene, Chem. Commun. 46 (2010) 2923. https://doi.org/10.1039/b926286e.

[109] Y. Xu, Z. Lin, X. Huang, Y. Wang, Y. Huang, X. Duan, Functionalized Graphene Hydrogel-Based High-Performance Supercapacitors, Adv. Mater. 25 (2013) 5779–5784. https://doi.org/10.1002/adma.201301928.

[110] Y. Lu, Y. Huang, F. Zhang, L. Zhang, X. Yang, T. Zhang, K. Leng, M. Zhang, Y. Chen, Functionalized graphene oxide based on p-phenylenediamine as spacers and nitrogen dopants for high performance supercapacitors, Chinese Sci. Bull. 59 (2014) 1809–1815. https://doi.org/https://doi.org/10.1007/s11434-014-0297-3.

[111] Y. Cui, Q.-Y. Cheng, H. Wu, Z. Wei, B.-H. Han, Graphene oxide-based benzimidazole-crosslinked networks for high-performance supercapacitors, Nanoscale. 5 (2013) 8367. https://doi.org/10.1039/c3nr01480k.

# ***Reference***


[112] D.C. Giancoli, Physics for scientists & engineers with modern physics, Pearson Education, 2008.

[113] M. Qiu, Y. Zhang, B. Wen, Facile synthesis of polyaniline nanostructures with effective electromagnetic interference shielding performance, J. Mater. Sci. Mater. Electron. 29 (2018) 10437–10444. https://doi.org/10.1007/s10854-018-9100-6.

[114] A. Khursheed, Scanning electron microscope optics and spectrometers, World scientific, 2010. https://doi.org/10.1142/7094.

[115] S. Naureen, Top-down Fabrication Technologies for High Quality III-V Nanostructures Top-down Fabrication Technologies for High Quality III-V Nanostructures Shagufta Naureen Doctoral Thesis Stockholm , Sweden 2013 Division of Semiconductor Materials School of Informat, (2014). https://doi.org/10.13140/2.1.4209.9841.

[116] A. Di Gianfrancesco, Technologies for chemical analyses, microstructural and inspection investigations, Elsevier Ltd, 2017. https://doi.org/10.1016/B978-0-08-100552-1.00008-7.

[117] W. Hummers, R. Offeman, Preparation of Graphitic Oxide, J. Am. Chem. Soc. 80 (1958) 1339.

[118] E. Al-Bermany, B. Chen, Preparation and characterisation of poly(ethylene glycol)-adsorbed graphene oxide nanosheets, Polym. Int. 70 (2021) 341–351. https://doi.org/10.1002/pi.6140.

[119] A.I. Omoregie, L.H. Ngu, D. Ek, L. Ong, P.M. Nissom, Author ' s Accepted Manuscript, Biocatal. Agric. Biotechnol. (2018). https://doi.org/10.1016/j.bcab.2018.11.030.

[120] J. Intra, C. Sarto, S. Mazzola, C. Fania, N. Tiberti, P. Brambilla, In Vitro Activity of Antifungal Drugs Against Trichophyton rubrum and Trichophyton mentagrophytes spp. by E-Test Method and Non-supplemented Mueller–Hinton Agar Plates, Mycopathologia. 184 (2019) 517–523. https://doi.org/10.1007/s11046-019-00360-9.

# ***Reference***


[121] J.Y. Kwon, S.Y. Lee, P. Koedrith, J.Y. Lee, K.-M. Kim, J.-M. Oh, S.I. Yang, M.-K. Kim, J.K. Lee, J. Jeong, E.H. Maeng, B.J. Lee, Y.R. Seo, Lack of genotoxic potential of ZnO nanoparticles in in vitro and in vivo tests, Mutat. Res. Toxicol. Environ. Mutagen. 761 (2014) 1–9. https://doi.org/10.1016/j.mrgentox.2014.01.005.

[122] T.C. Goh, M.Y. Bajuri, S. C. Nadarajah, A.H. Abdul Rashid, S. Baharuddin, K.S. Zamri, Clinical and bacteriological profile of diabetic foot infections in a tertiary care, J. Foot Ankle Res. 13 (2020) 36. https://doi.org/10.1186/s13047-020-00406-y.

[123] M.A. Kadhim, E. Al-Bermany, New fabricated PMMA-PVA/graphene oxide nanocomposites: Structure, optical properties and application, J. Compos. Mater. 50 (2021) 2793–2806. https://doi.org/DOI: 10.1177/0021998321995912.

[124] J. Yang, X. Yan, M. Wu, F. Chen, Z. Fei, M. Zhong, Self-assembly between graphene sheets and cationic poly(methyl methacrylate) (PMMA) particles: preparation and characterization of PMMA/graphene composites, J. Nanoparticle Res. 14 (2012) 717. https://doi.org/10.1007/s11051-011-0717-0.

[125] C. Rameshkumar, S. Sarojini, K. Naresh, R. Subalakshmi, Preparation and Characterization of Pristine PMMA and PVDF Thin Film using Solution Casting Process for Optoelectronic Devices, J. Surf. Sci. Technol. 33 (2017) 12. https://doi.org/10.18311/jsst/2017/6215.

[126] N.R. Aldulaimi, E. Al-Bermany, New Fabricated UHMWPEO-PVA Hybrid Nanocomposites Reinforced by GO Nanosheets: Structure and DC Electrical Behaviour, J. Phys. Conf. Ser. 1973 (2021) 012164. https://doi.org/10.1088/1742-6596/1973/1/012164.

[127] C. Wang, L. Feng, H. Yang, G. Xin, W. Li, J. Zheng, W. Tian, X. Li, Graphene oxide stabilized polyethylene glycol for heat storage, Phys.

# ***Reference***

Chem. Chem. Phys. 14 (2012) 13233. https://doi.org/10.1039/c2cp41988b.

[128] M. Alamgir, G.C. Nayak, A. Mallick, S.K. Tiwari, S. Mondal, M. Gupta, Processing of PMMA nanocomposites containing biocompatible GO and TiO 2 nanoparticles, Mater. Manuf. Process. 33 (2018) 1291–1298. https://doi.org/10.1080/10426914.2018.1424996.

[129] D. Febriantini, A.H. Cahyana, R.T. Yunarti, A microwave assisted, Fe 3 O 4 /Camphor-catalysed threecomponent synthesis of 2-amino-4H -chromenes and their antibacterial and antioxidant activity, IOP Conf. Ser. Mater. Sci. Eng. 509 (2019) 012036. https://doi.org/10.1088/1757-899X/509/1/012036.

[130] H.N. Kim, S.K. Lee, Effect of particle size on phase transitions in metastable alumina nanoparticles: A view from high-resolution solid-state 27Al NMR study, Am. Mineral. 98 (2013) 1198–1210. https://doi.org/10.2138/am.2013.4364.

[131] Y. Fu, W. Xiong, J. Wang, J. Li, T. Mei, X. Wang, Polyethylene Glycol Based Graphene Aerogel Confined Phase Change Materials with High Thermal Stability, J. Nanosci. Nanotechnol. 18 (2018) 3341–3347. https://doi.org/10.1166/jnn.2018.14635.

[132] C. Karunakaran, P. Anilkumar, P. Gomathisankar, Photoproduction of iodine with nanoparticulate semiconductors and insulators, Chem. Cent. J. 5 (2011) 31. https://doi.org/10.1186/1752-153X-5-31.

[133] A.A. Mohammed, Z.T. Khodair, A.A. Khadom, Preparation and investigation of the structural properties of α-Al2O3 nanoparticles using the sol-gel method, Chem. Data Collect. 29 (2020) 100531. https://doi.org/10.1016/j.cdc.2020.100531.

[134] A.K. Al-shammari, E. Al-Bermany, New Fabricated (PAA-PVA/GO) and (PAAm-PVA/GO) Nanocomposites: Functional Groups and

# ***Reference***

Graphene Nanosheets effect on the Morphology and Mechanical Properties, J. Phys. Conf. Ser. 1973 (2021) 012165. https://doi.org/10.1088/1742-6596/1973/1/012165.

[135] V. Bertola, Dynamic wetting of dilute polymer solutions: The case of impacting droplets, Adv. Colloid Interface Sci. 193–194 (2013) 1–11. https://doi.org/10.1016/j.cis.2013.03.001.

[136] V.Y. Rudyak, S.L. Krasnolutskii, Dependence of the viscosity of nanofluids on nanoparticle size and material, Phys. Lett. A. 378 (2014) 1845–1849. https://doi.org/10.1016/j.physleta.2014.04.060.

[137] V. Samulionis, Š. Svirskas, J. Banys, A. Sánchez-Ferrer, S.J. Chin, T. McNally, Ultrasonic properties of composites of polymers and inorganic nanoparticles, Phys. Status Solidi. 210 (2013) 2348–2352. https://doi.org/10.1002/pssa.201329294.

[138] W.R. Azzam, Behavior of modified clay microstructure using polymer nanocomposites technique, Alexandria Eng. J. 53 (2014) 143–150. https://doi.org/10.1016/j.aej.2013.11.010.

[139] G.A. Evingür, Ö. Pekcan, Mechanical properties of graphene oxide–polyacrylamide composites before and after swelling in water, Polym. Bull. 75 (2018) 1431–1439. https://doi.org/10.1007/s00289-017-2101-4.

[140] C. Lee, X. Wei, J.W. Kysar, J. Hone, Measurement of the Elastic Properties and Intrinsic Strength of Monolayer Graphene, Science (80-. ). 321 (2008) 385–388. https://doi.org/10.1126/science.1157996.

[141] S.H. Al-Nesrawya, M.J. Mohseenb, E. Al-Bermany, Reinforcement the Mechanical Properties of (NR50/SBRs50/OSP) Composites with Oyster Shell Powder and Carbon Black, IOP Conf. Ser. Mater. Sci. Eng. 871 (2020) 012060. https://doi.org/10.1088/1757-899X/871/1/012060.

# الخلاصة


المتراكبات النانوية المكونة من الجرافين-البوليمر تؤثر بشكل كبير على خصائص حشوات الأسنان و فعاليتها ضد البكتيريا. تم استخدام أوكسيد الجرافين النانوي (GO) المحضر والبولي (ميثيل ميثاكريلات) (PMMA) لتحسين و تعزيز نوعين من حشوات الأسنان التجارية الهجينة و النانوية. تهدف هذه الدراسة إلى تعزيز خصائص حشوات الأسنان التجارية وتحسين نشاطها المضاد للبكتيريا باستخدام اوكسيد الجرافين النانوية و البولي (ميثيل ميثاكريلات).

تم تقسيم الرسالة إلى أربعة فصول ، قدم الفصل الأول المقدمة ومراجعات الأدبيات وأهداف الدراسة ، بينما قدم الفصل الثاني مقدمة موجزة عن تركيبات حشوات الأسنان والمفاهيم الفيزيائية والحسابات ، بينما تناول الفصل الثالث القسم التجريبي وتوصيفات الاجهزة و الادوات المستخدمة. عرض الفصل الرابع النتائج والمناقشات والتطبيقات ، وكذلك اهم الاستنتاجات والأعمال المستقبلية.

تم تطبيق طريقة مطورة من خلط و صب للمحلول المصوتن لتصنيع المركبات النانوية الجديدة من حشوات اسنان مدعمة بالجرافين والبوليمر. تم فحص الخواص التركيبية والريولوجية والميكانيكية و مقاومتها للبكتريا لحشوة الاسنان بعد اضافة كلا من البوليمر و من ثم اوكسيد الكرافين النانوي. أظهر تحويل فورييه بالأشعة تحت الحمراء (FTIR) تفاعلًا جديدا بين الحشوات والمواد المضافة. ووضح تحليل حيود الأشعة السينية (XRD) عن تغيير كبير في السلوك البلوري. بينما أظهر المجهر البصري (OM) و صور المجهر الإلكتروني (FESEM) تغيرًا كبيرًا في سطح و تبوغرافية العينات مع ذوبان و ترابط متجانس للبوليمر وتوزيع جيد للمواد النانوية في الحشوات.

تم قياس بعض الخصائص الريولوجية مثل الكثافة و اللزوجة التي تحسنت بشكل ملحوظ بعد إضافة البوليمر وكذلك عند أضافة GO حيث زادت بمقدار 57٪ مقارنة مع الحشوات المايكروية و النانوية. كما اظهرت دراسة

الخـــواص الميكانيكيـــة للموجـــات فـــوق الصـــوتية مثـــل ســـرعة الموجـــات فـــوق الصـــوتية ومعامـــل الامتصـــاص وقابليـــة الانضـــغاط ومعامـــل يونـــك وغيرهـــا مـــن الخـــواص الميكانيكيـــة تحســـن بشـــكل ملحـــوظ بعـــد مســـاهمة البـــوليمر و اوكســـيد الكـــرافين النـــانوي وصـــلت إلـــى 325 ٪ مـــن معامـــل الامتصـــاص بالموجـــات فـــوق الصـــوتية بالمقارنة مع حشوات الاسنان المايكروية او النانوية.

تـــم اختبـــار قابليـــة النمـــاذج المحضـــرة مـــن حشـــوات الاســـنان المعـــززة بـــالبوليمر و اوكســـيد الكـــرافين النـــانوي ضـــد نوعـــان مـــن انـــواع مـــن البكتريـــا ( Enterococcus faecalis and E. stap) وبينـت النتـائج زيـادة طفيفـة فـي قطـر منطقـة القتـل بعـد اضـــافة البـــوليمر لكـــن المســـاهمة الاكبـــر بعـــد اضـــافة الصـــفائح النانويـــة (GO) حيـــث زادت مســـاحة القتـــل بنســـبة تصـــل إلـــى 46٪ . بشـــكل عـــام قـــدمت حشـــوات النـــانو المشـــوبة بـــالبوليمر و اوكســـيد الغـــرافين النـــانوي تحســـن افضـــل بالمقارنـــه مـــع حشـــوات المايكريويـــة الهجينـــة فـــي كـــلا مـــن الخصـــائص و اظهـــرت مقاومـــه افضـــل ضد البكتريا التي تعيش في الفم و على الانسجة الحيوية.

جمهورية العراق
وزارة التعليم العالي والبحث العلـمي
جامعة بابل - كلية التربية للعلوم الصرفة
قســـم الفـيزياء

# كفاءة المتراكبات الهجينة - النانوية للكرافين في تطبيقات حشوات الاسنان

رسالة مقدمة

إلى مجلس كلية التربية للعلوم الصرفة في جامعة بابل وهي جزء من متطلبات

نيل درجة الماجستير في التربية / الفيزياء

من الطالب

**مهند عبد السلام حسين موسى**

بكالـوريوس في الفيزياء

جامعة بغداد 2010 م

دبلوم عالي في فيزياء المواد وتطبيقاتها

جامعة بابل 2017

بإشراف

**أ.د. إحسان ضياء جواد البيرماني**

**1444 هـ** **2022 م**